

RAID Organizations for Improved Reliability and Performance: A Not Entirely Unbiased Tutorial

Alexander Thomasian*

Abstract

This is a followup to the 1994 tutorial by Berkeley RAID researchers whose 1988 RAID paper foresaw a revolutionary change in storage industry based on advances in magnetic disk technology, i.e., replacement of large capacity expensive disks with arrays of small capacity inexpensive disks. NAND flash SSDs which use less power, incur very low latency, provide high bandwidth, and are more reliable than HDDs are expected to replace HDDs as their prices drop. Replication in the form of mirrored disks and erasure coding via parity and Reed-Solomon codes are two methods to achieve higher reliability through redundancy in disk arrays. RAID(4+k), $k=1,2,\dots$ arrays utilizing k check strips makes them k -disk-failure-tolerant with maximum distance separable coding with minimum redundancy. Clustered RAID, local recovery codes, partial MDS, and multilevel RAID are proposals to improve RAID reliability and performance. We discuss RAID5 performance and reliability analysis in conjunction with HDDs w/o and with latent sector errors - LSEs, which can be dealt with by intradisk redundancy and disk scrubbing, the latter enhanced with machine learning algorithms. Undetected disk errors causing silent data corruption are propagated by rebuild. We utilize the M/G/1 queueing model for RAID5 performance evaluation, present approximations for fork/join response time in degraded mode analysis, and the vacationing server model for rebuild analysis. Methods and tools for reliability evaluation with Markov chain modeling and simulation are discussed. Queueing and reliability analysis are based on probability theory and stochastic processes so that the two topics can be studied together. Their application is presented here in the context of RAID arrays in a tutorial manner.

Categories and Subject Descriptors: B.4.2 [Input/Output and Data Communications]: Input/Output Devices; B.4.5 [Input/Output and Data Communications]: Reliability, Testing, and Fault-Tolerance; D.4.2 [Operating Systems]: Storage Management; E.4 [Data]: Coding and Information Theory.

TABLE OF CONTENTS ¹

1. Introduction.
2. Limiting storage utilization to meet performance goals.
 - 2.1. Disk scheduling policies.
 - 2.2. Data compression, compaction and deduplication.
 - 2.3. Dealing with high tail latency.

*Thomasian & Associates, Pleasantville, NY, alexthomasian@gmail.com

¹Sections indicated by asterisks require knowledge of queueing theory and stochastic processes and can be skipped without loss in continuity.

3. RAID classification and proposal to eliminate large disks.
4. Maximum distance separable RAID(4+K) arrays.
 - 4.1. Rotated Diagonal Parity - RDP coded arrays.
 - 4.2. X-code 2DFT array with diagonal parities.
 - 4.3. Partial MDS code.
 - 4.4. Disk adaptive redundancy scheme.
5. Multidimensional coding for higher reliability.
 - 5.1. Grid files.
 - 5.2. REliable Storage at Exabyte Scale - RESAR.
 - 5.3. 2-d and 3-dimensional parity coding.
6. Local Recoverable Code - LRC.
 - 6.1. A systematic comparison of existing LRC schemes.
 - 6.2. Wide stripe erasure codes.
 - 6.3. Practical design considerations for wide stripe LRCs .
7. Reducing rebuild traffic in distributed RAID.
 - 7.1. Pyramid codes.
 - 7.2. Hadoop Distributed File System - HDFS-Xorbas.
 - 7.3. Hadoop Adaptively-Coded Distributed File System - HACDFS.
8. Copyset Replication for Reduced Data Loss Frequency
 - 8.1. More Efficient Data Storage: Replication to Erasure Coding.
9. Clustered RAID5.
 - 9.1. Balanced Incomplete Block Design - BIBD.
 - 9.2. CRAID implementation based on Thorp shuffle.
 - 9.3. Nearly Random Permutation - NRP.
 - 9.4. Shifted parity group placement.
10. Miscellaneous topics.
 - 10.1. Distributed sparing in RAID5.
 - 10.2. Permanent Customer Model - PCM for RAID5 rebuild.
 - 10.3. Rebuild processing in Heterogeneous Disk Arrays - HDAs.
 - 10.4. Optimal single disk rebuild in EVENODD, RDP, X-code.
11. RAID performance evaluation.
- 12*. RAID performance analysis with M/G/1 queueing model.
 - 12.1*. Components of disk service time w/o and with ZBR.
 - 12.2*. Seek distance distribution without and with ZBR.
- 13*. RAID5 performance analysis in normal mode.
- 14*. Fork/Join response time analysis for degraded mode.
15. Rebuild Processing in RAID5.
- 16*. Analysis of rebuild processing with Vacationing Server Model - VSM.
- 17*. M/G/1 VSM analysis with multiple vacations of two types.
- 18*. An alternative method to estimate rebuild time.
19. RAID5 reliability analysis.
 - 19.1*. RAID5/6 reliability analysis with unrecoverable errors.
20. Disk scrubbing and Intra-Disk Redundancy to deal with Latent Sector Errors - LSEs.
 - 20.1. Schemes to implement IDR.
21. IDR's effect on disk performance.
 - 21.1. Comparison of disk scrubbing and IDR with IPC.

- 22. Combining scrubbing with SMART and Machine Learning.
- 23. Undetected Disk Errors - UDE and Silent Data Corruption - SDC.
- 24. Mirrored and Hybrid Disk Arrays Description and Reliability Comparison.
 - 24.1. Shortcut Method to Compare the Reliability of Mirrored Disks and RAID(4+k).
- 25. Reliability analysis of multilevel RAID arrays.
 - 25.1. Mirrored RAID5 - RAID1/5 reliability analysis.
 - 25.2. RAID5 with mirrored disks - RAID5/1.
 - 25.3. Shortcut reliability analysis to compare RAID1/5 and RAID5/1.
 - 25.4. AutoRAID hierarchical array.
- 26. Discrete-event simulation for reliability evaluation.
 - 26.1. Simulation study of a digital archive.
 - 26.2. Simulation of hierarchical RAID reliability.
 - 26.3. Proteus open-source simulator.
 - 26.4. CQSIM_R Tool Developed at AT&T.
 - 26.5. SIMedc simulator for erasure coded data centers.
- 27. Reliability modeling tools.
 - 27.1. Automated Reliability Interactive Estimation System - ARIES Project at ARIES.
 - 27.2. System AVailability Estimator - SAVE Project at IBM Research.
 - 27.3. Symbolic Hierarchical Automated Reliability and Performance Evaluator - SHARPE.
- 28. Research at IBM Zurich Research Lab.
 - 28.1. System reliability metrics.
 - 28.2. Clustered versus declustered data placements.
 - 28.3. Performance analysis of a tape library system at ZRL.
- 29. Flash Solid-State Drives - SSDs.
 - 29.1 Write-Once Memory - WOM codes to enhance SSD lifetimes.
 - 29.2. Predictable microsecond level support for flash.
 - 29.3. Differential RAID for SSDs.
 - 29.4. Fast Array of Wimpy Nodes - FAWN.
 - 29.5. Distributed DRAM-based storage - RAMCloud.
- 30. Conclusions.
- Appendix I. Transient analysis of state probabilities in Markov chains.
- Appendix II. The mathematics behind SHARPE reliability modeling package.
- Abbreviations.
- Bibliography.

1 Introduction

The tutorial is intended for computer science and engineering students and IT professionals interested in storage system organization, performance and reliability evaluation. It is a followup to Chen et al. 1994 [32], Thomasian and Blaum 2009 [214], and an extension of Thomasian 2021 [224]. The title derives from the fact that this is a rapidly growing field and some topics remain uncovered.

Reliability analysis of storage systems initially dealt with disk failures at a course granularity, whole *Hard Disk Drives - HDDs* failures. More complex analysis was introduced to take into account the effect of disk scrubbing and *IntraDisk Redundancy - IDR* to deal with *Latent Sector*

Errors - LSEs in HDDs.

We discuss the queueing analysis of RAID arrays based on HDDs, where performance is more of an issue than NAND SSDs invented at Toshiba in 1989, which provides a high throughput, low latencies, and higher reliability than HDDs.

Some sections require exposure to probability theory and stochastic processes, e.g., Kobayashi et al. 2014 [120], Trivedi 2002 [228] with heavy reliability modeling coverage, and elementary queueing theory, e.g., Kleinrock 1975/76 [118, 119], Coding theory applicable to RAID design are presented in MacWilliams and Sloane 1977 [134], Fujiwara 2006 [62], and short tutorial with good references Blaum 2009 [20].

There are chapters dedicated to storage systems in textbooks on computer architecture, e.g., Hennessey and Patterson 2019 [83], operating systems, e.g., Arpaci-Dusseau 2018 [13], databases, e.g., Ramakrishnan and Gehrke 2002 [171], which can be complemented by Thomasian 2021 [224]. Cache, DRAM, Disk are discussed in Jacob, Ng and Wang 2008[104]. A book on NAND flash memories is Micheloni et al. 2010 [146], whose reading requires electrical engineering background. We have provided url's of web pages on novel developments in the field and some technical topics covered by wikipedia.

Table of contents lists topics covered in the paper. We start the discussion with a simple queueing analysis of disks.

2 Limiting Storage Utilization to Meet Performance Goals

Due to exponential growth of data projected to reach 175 zettabytes - ZB= 10^{21} B) by 2025 and the main role HDDs play in storing data.

<https://www.networkworld.com/article/3325397/>

In spite of multiterabyte capacity disks their storage cannot be fully utilized due to overload in providing access to randomly placed data blocks. This is especially true for *Online Transaction Processing - OLTP* applications where the transfer time for small 4 or 8KB data blocks tends to be negligible, but there is the unproductive positioning time, which is the sum of two components:

Seek time Moving the *Read/Write - R/W* head attached to the disk arm to the target track.

Rotational latency The time for the data on the rotating track to reach the R/W head.

HDDs are classified according to their use: *Personal Storage - PS* versus *Enterprise Storage - ES*, their interface: *Advanced Technology Attachment - ATA* versus *Small Computer System Interface - SCSI* Anderson et al. 2003 [8]. *Serial ATA - SATA* is replacing disks with parallel ATA. SATA and SCSI vary according to their bandwidth and access latency. Less expensive SATA 7200 *Rotations Per Minute - RPM* disks are mainly used in data centers.

Bandwidth is especially important in HDDs accessed by *OnLine Transaction Processing - OLTP* workloads, where accesses to small randomly placed disk blocks with high positioning time, but negligible transfer time. More expensive ES drives provide faster seek time via more expensive circuitry than PS drives. Rotational latency is reduced by adopting SCSI 10K or 15K RPM disks with 3 and 2 ms mean latencies, but also faster seek times. Such a workload was observed by analyzing I/O traces Ramakrishnan et al. 1992 [170]. Such insights were used in specifying database benchmarks by the *Transaction Processing Council - TPC*.

<https://www.tpc.org>.

The use of few tracks allows lower seek times due to short stroking. This is accomplished by just utilizing higher capacity outer disk cylinders, which is due to *Zoned Bit Recording - ZBR* Jacob et al. 2008 [104]. Zoning maintains almost the same linear recording density across disk tracks, so that outer tracks have a higher capacity than inner tracks by a factor of 1.7.

That block transfer time is negligible with respect to rotational latency, which is one half of disk rotation time or 4.17 msec for 7200 RPM disks, while the number of sectors transferred is less than .1% of sectors on a track.

Rotational latency can be shortened by providing two disk arms which are 180° apart, The same effect can be achieved by storing records twice on opposing sides of each track, but this has the disadvantage of adversely affecting sequential accesses. The two-actuator Seagate HDD from Seagate is discussed in Section 29.

We model disks as single server M/M/1 queues with FCFS scheduling Kleinrock 1975 [118]. Disk requests arrive according to a Poisson process with rate λ and have exponentially distributed service times with mean $\bar{x} = 1/\mu$, where μ is the service rate. Disk utilization is the fraction of time the disk is busy: $\rho = \lambda\bar{x}$ Since $\rho < 1$ the maximum sustainable arrival rate is $\lambda_{max} \leq 1/\bar{x}_{disk}$, e.g., for $\bar{x} = 10$ milliseconds (ms) $\lambda_{max} = 100$ IO Per Second - IOPS

If $\lambda\bar{x} > 1$ then m disks should be provided disks so that $\rho = \lambda\bar{x}/m < 1$. Due to Little's result Kleinrock 1975 [118] ρ is also the mean number of requests in service. The distribution of number of requests in M/M/m queues given below can be used to estimate the probability that a request has to wait.

https://en.wikipedia.org/wiki/M/M/c_queue

In fact we have a different queueing system where a single requests is sent to all $m = 3$ servers and assuming slightly different maen disk service times ($\rho_i = \lambda\bar{x}_i, i = 1, 2, 3$) the probability that a request does not have to wait is: $\prod_{i=1}^3 (1 - \rho^i)$

Replicating data on multiple disks is a costly solution, which is adopted by companies operating hyperscalars. It has the advantage of increased reliability and reduced response time which may be necessitated by *Service Level Agreements - SLAs*. SLA's in *Internet Protocol - IP* networks are discussed in Verma 2000 [231].

https://en.wikipedia.org/wiki/Internet_Protocol

https://en.wikipedia.org/wiki/Service-level_agreement

Consider N heterogeneous disks indexed in nonincreasing speed order with a large number of small files, which can be moved across disks to minimized overall mean disk response time (\bar{R}). The Lagrange multiplier method is applied to response times obtained by the M/G/1 queueing model in Section 13 to determine optimal disk arrival rates in Piepmeier 1975 [162].

https://en.wikipedia.org/wiki/Lagrange_multiplier The optimization yields $\lambda_i \geq 0, 1 \leq i \leq N$

$$\bar{R} = \sum_{i=1}^M \frac{\lambda_i}{\Lambda} R_i, \text{ with } \sum_{i=1}^N \lambda_i = \Lambda \text{ and } \lambda_i = 0, M < i \leq N.$$

Note that only $M < N$ disks have $\lambda_i > 0$ and it is assumed they have adequate capacity to hold the data.

Georgiadis et al. 2004 [64] considered the min-max policy to obtain an allocation $\lambda_i, 1 \leq i \leq M$, which equalizes the mean response times over $M \leq N$ fastest devices. The allocation results in higher utilization for faster disks.

The mean disk access time (R_{disk}) is an important contributor to transaction response times in OLTP. Given its maximum: R_{disk}^{max} the corresponding arrival rate using the M/M/1 queueing system is given as follows:

$$R_{disk} = \frac{\bar{x}_{disk}}{1 - \rho} < R_{disk}^{max} \text{ which implies } \lambda_{max} < \frac{1}{\bar{x}_{disk}} - \frac{1}{R_{disk}^{max}}.$$

If $R_{disk}^{max} = 20$ then $\lambda_{target} = 50$, which is $\lambda_{max}/2$.

The response time distribution in M/M/1 queueing system is exponentially distributed:

$$R(t) = 1 - e^{t/R(\rho)}. \quad (1)$$

The arrival rate (λ_p) to achieve a certain percentile (p) for disk response time is: $R_{disk}^{(p)} = -R(\rho)\ln(1 - p)$, hence:

$$\lambda_p = \frac{1}{\bar{x}_{disk}} + \frac{\ln(1 - p)}{R_{disk}^{(p)}}$$

Note that $\ln(1 - p) < 0$ for $0 \leq p < 1$.

Given the second moments of disk service time both analyses can be repeated more accurately using an M/G/1 queueing model Kleinrock 1975 [118].

2.1 Disk Scheduling Policies

Disk access time can be reduced by adopting judicious disk scheduling policies, such as the *Shortest Seek Time First - SSTF* and SCAN by Denning 1967 [45] and *Shortest Access Time First - SATF* by Jacobson and Wilkes 1991 [105]. Disk scheduling policies are compared via simulation in Worthington et al. 1994 [238], Hsu and Smith 2005 [86], Jacob et al. 2008 [104], and Thomasian 2011 [215]. Reported in the latter is an extension of SATF with lookahead and priorities and an empirical equation for SATF mean disk service versus queue-length (q):

$$\bar{x}_{SATF}(q) = \bar{x}_{FCFS}/q^p \text{ where } p \approx 1/5$$

so that disk service time is halved for $q = 32$. Increase in throughput versus q is given in Table 2 in Anderson et al. 2003 [8] and plotted as Figure 6.2 in Hennessey and Patterson 2019 [83].

Discussed below are some other disk scheduling methods and *Complete Fairness Queueing - CFQ* which provides a fair allocation of the disk I/O bandwidth for all the processes which request an I/O operation.

https://en.wikipedia.org/wiki/I/O_scheduling

<https://www.kernel.org/doc/Documentation/block/cfq-iosched.txt>

There have been several studies to reorganize disk data to improve disk access times. This is done dynamically by the *Automatic Locality Improving Storage - ALIS* tool based on common sequences of disk requests Hsu et al. 2005 [87]. This study reviews earlier articles on this topic, which deal with static data allocation. This discussion is relevant to LSA where performance can be improved by maintaining seek affinity Menon 1995 [143].

Anticipatory arm placement of idle disks is another scheme to reduce disk access time Thomasian and Fu 2006 [208]. In the case of single disks with C cylinders the arm is placed at cylinder $C/2$, while in mirrored disks the arms are placed at $C/4$ and $3C/4$. The mean seek distance for reads in the two cases is $C/2$ and $C/4$, which is otherwise $C/3$ and $C/5$ as discussed in Section 24. The paper considers disks with hot spots (frequently accessed cylinders) and zoning.

HDDs due to their lower cost per GB and high capacities are the preferred medium in large data centers Brewer et al. 2016 [27, 28], where the following metrics are identified: (1) Higher IOPS, (2) Higher capacity, (3) Lower tail latency, which is discussed in Subsection 2.3. (4) Security requirements, and (5) *Total Cost of Ownership - TCO*. Higher bandwidth attainable by NAND Flash SSDs require fewer drives to sustain the same workload. Reliability, performance, and cost are identified as key cloud storage parameters in Huang 2013 [92].

Hyperscalars are data centers with a very large number of disks. The four largest hyperscalar platforms out of twelve largest are — AWS (Amazon Web Services), Google Cloud, Meta, and Microsoft Azure, which represent 78% of capacity in this category and consume 13,177 MegaWatts.

<https://www.datacenterknowledge.com/manage/2023-these-are-world-s-12-largest-hyperscalers>

While SSDs cost more per GB than HDDs they incur lower power consumption, but it is the lower TCO that matters.

https://www.snia.org/sites/default/files/SNIA_TCOALC_Workpaper_Final_0.pdf

Power saving in disks is achievable by different levels of disk powering, such as spindown in laptops to save battery power. With dropping NAND Flash storage costs NAND Flash disks are expected to replace disks in laptops.

<https://www.techradar.com/news/ssd-vs-hdd-which-is-best-for-your-needs>

Massive Array of Idle Disks - MAID save power by powering down the majority of disks in a data center Colarelli and Grunwald 2002 [37]. RAID5 requires at least two disks should be powered up for updates, but *NonVolatile RAM - NVRAM*, which is DRAM powered by *Uninterruptible Power Supply - UPS* is another option to preserve updates without disk spin-up. The MAID proposal led to the Copan startup for archival storage.

<http://www.thic.org/pdf/Jul05/copansys.aguha.050720.pdf> Lower power consumption is attainable by NAND Flash SSDs as discussed in Section 29. Other schemes to save disk power are discussed in Chapter 7 in Thomasian 2021 [224].

Power Usage Effectiveness - PUE, which is the ratio of total power consumption (including cooling plus power conversion) to the power used to run IT equipment is a metric used to determine data center energy efficiency. Variation of PUE over (2008-22) and across different Google sites is as follows.

<https://www.google.com/about/datacenters/efficiency/>

Seagate has announce a 30 TB *Heat Assisted Magnetic Recording - HAMR* HDDs in April 2023.

<https://blocksandfiles.com/2023/04/21/seagate-30tb-hamr/>

While Flash NAND SSDs tended to smaller in capacity than HDDs they may exceed HDDs, as in the case of PureStorage 300 TB flash drives in 2026, which will exceed HDD capacity ten-fold.

<https://blocksandfiles.com/2023/03/01/300tb-flash-drives-coming-from-pure-storage/>

2.2 Data Compression, Compaction and Deduplication

While memory costs at all levels are dropping more efficient storage utilization can be attained by preserving storage capacity by using data deduplication, compaction, and compression. The first two methods are applicable at secondary storage level and the third method has been applied to main memory. Data compression methods such as Huffman, Lempel-Ziv - LZ and

arithmetic encoding are discussed in Sayood 2017 [183]. Compressed data in main memory is decompressed as it is loaded into CPU caches and vice-versa as discussed in Section 2.14 in Thomasian 2021 [224].

Deduplication is a technique to duplicate data at block, page, file level. It has been effectively applied to archival and backup storage to reduce storage costs Data deduplication is discussed in Section 2.15 in Thomasian 2021 [224] and Mohammed and Wang 2021 [130]. A classification of deduplication systems according to Paulo and Pereira 2014 [160] is (1) granularity, (2) locality, (3) timing, (4) indexing, (5) technique, and (6) scope.

https://en.wikipedia.org/wiki/Data_deduplication

Duplication can be checked quickly by applying hash functions such as SHA-2 and in the case of a match a byte-by-byte comparison can be applied.

<https://en.wikipedia.org/wiki/SHA-2>

Data compression is suited to LFS and LSA paradigms, since files are not written in place and this allows their size to vary. Data compaction creates large empty spaces by removing older versions of files and cleanup of defunct objects based on their *Time-to-Live - TTL*. Storage fragmentation is dealt with by continuous garbage collection and data compaction, which is the shifting of the location of stored data to release unused storage for reuse.

A performance study of LFS was reported in McNutt 1994 [139]. A directory indicates the physical location of each logical object and the location of the most recent copy for objects written more than once. A mathematical model of garbage collection shows how collection load relates to the utilization of storage and the amount of update locality present in the pattern of updates. A realistic statistical model of updates, based upon trace data analysis is applied. Alternative policies are examined for determining which areas to target.

Performance of RAID5 and LSA is compared using an approximate analysis in Menon 1995 [143], which is based on the following relationship used to estimate the rate of garbage collection. Given *Average Segment Occupancy - ASO* and lowest *Best Segment Occupancy* we have:

$$ASO = (1 - BSO) / \ln(1 - BSO), \quad \text{e.g., if } ASO=0.6 \text{ then } BSO=0.324.$$

There are two types of write hits: (1) to dirty blocks in *NonVolatile Storage - NVS* caches, (2) to clean pages. Given a request rate K the fraction of request to clean pages is C and the fraction of writes to dirty pages is D .

The reading of segments is attributable to garbage collection and only a fraction BSO of segment writing is attributable to garbage collection and the rest to destage. Let KB be the read miss rate, KC the miss rate due to write hits in clean pages and KD the destage rate due to write misses

The rate at which dirty blocks are created in the NVS caches is $K(C + D)/X$ assuming that X blocks are destaged together. It is argued that segments are written and read at rate $(KC + KD)/(X(1 - BSO)Z)$ where Z is the segment size in tracks. The effect of data compression and seek affinity is investigated in this study and it is observed that LSA outperforms RAID5 in throughput, but offers higher response times.

Menon and Stockmeyer 1998 [144] proposed a new algorithm for choosing segments for garbage collection in LFS and LSA and compared it against a greedy and cost-benefit algorithms via simulation. The basic idea is that segments which have been recently filled by writes should not be considered for garbage collection until they achieve a certain age threshold. This is because as time progresses data in such segments is less likely to be updated, making old segments eligible for garbage collection. The algorithm chooses segments that yield the most free

space. Also given is a method to determine the optimal age-threshold under certain assumptions about the workload.

2.3 Dealing with High Tail Latency

The following discussion is based on Dean and Barroso 2013 [41]. Reasons for high tail latency are:

Shared resources Sharing resources such as CPU cores, processor caches, memory and network bandwidth.

Daemons Periodically scheduled background daemons use only limited resources on average, but generate delays when active.

Global resource sharing Network switches, shared file systems.

Maintenance This includes data reconstruction in distributed file systems, periodic log compaction in storage systems as in the case of LSA. In the case of SSDs there is 100-fold increase in random read accesses for a modest write activity as discussed in Section 29.

Queueing delays Enhances variability.

Increased variability may be due to the following:

CPU's may temporarily overrun their power limits, but throttle to lower temperature but that limits CPU speed.

Powersaving modes to save energy in various devices incurs additional latency when moving from inactive to active modes, Spindown is used in laptops to save battery power, but a delay is incurred until spinup is completed.

The effect of subsecond response times in a timesharing computer system on programmer productivity was observed in Thadhani 1981 [198]. There is the double effect that programmers respond faster when response time is subsecond and this reduces the total time to accomplish a task. The effect of response time on successful conversion in e-commerce is discussed here.

<https://queue-it.com/blog/ecommerce-website-speed-statistics/>

Response time in search engines is reduced by concurrently accessing n replicated copies of a file rather than just a single copy on a single device, which may be temporarily or permanently unavailable. Response time is then the minimum of $n > 1$ exponentially distributed responses times. In the case of homogeneous M/M/1 queues $R_{min} = R/n$.

Distributed *Shortest Processing Time First* - SPTF is a request distribution protocol for decentralized brick storage system with high-speed interconnects. D-SPTF dynamically presented in Lumb and Golding 2004 [132] selects servers to satisfy a request while balancing load, exploiting aggregate cache capacity, and reduces positioning times for cache misses.

IBM Intelligent Bricks project is described by Wilcke et al. [233] is an example of brick storage systems. Each brick is a standalone RAID(4+k), but bricks collaborate in 2006. *Hierarchical RAID* proposal in Subsection 26.2 is conceptually similar, but its reliability analysis led to conflicting conclusions Thomasian 2022 [225].

3 RAID Classification and Proposal to Eliminate Large Disks

Two main categories of RAID redundancy are replication (mirroring) and erasure coding (parity in the simplest case). In the case parity coded RAID3, RAID4, RAID5 described in Chen et al. [32] $N - 1$ surviving disks out of N disks need be accessed to recover a lost block and for RAID(4+k) the number is $N - k + 1$ disks.

Erasures are failures whose location is known and hence a single parity is adequate to recover a lost block by *eXclusive-ORing - XORing* corresponding surviving blocks. *Redundant Array of Independent Memories - RAIM* Meaney et al. 2012 and *Redundant Array of Independent Libraries - RAILS* (tapes) Ford et al. 1998 [58] utilize the RAID5 paradigm.

https://en.wikipedia.org/wiki/Redundant_array_of_independent_memory

<https://blocksandfiles.com/2021/10/08/quantums-exabyte-munching-scale-out-modular-tape-library/>

Hamming codes Fujiwara 200 [62] was adopted by Thinking Machines for the Connection Machine 5 - CM5.

https://en.wikipedia.org/wiki/Hamming_code

https://en.wikipedia.org/wiki/Connection_Machine

With the positions of failed disks known up to two disk failures can be recovered, as also noted in Gibson 1992 [65].

The RAID proposal by Patterson, Gibson, and Katz 1988 [159] advocated replacing expensive, large form-factor disks, reliable disks used in conjunction with IBM mainframes with arrays of inexpensive small form-factor, less reliable disks used by PCs - Personal Computers in 1980s.

Large form-factor *Direct Access Storage Devices - DASD*, using variable block sizes with the *Extended Count Key Data - ECKD* format, which is similar to CKD in layout, but support five additional *Channel Command Words - CCWs*.

https://en.wikipedia.org/wiki/Count_key_data

ECKD is supported by IBM's *Multiple Virtual Storage - MVS* operating system and its descendant z/OS operating system family. In IBM mainframes running MVS the *Disk Array Controller - DAC* emulates CCWs issued to ECKD format disks on *Fixed Block Architecture - FBA* disks with 512 B (byte) and 4096 B disk sectors since 2010.

There is reduction in reliability when expensive, large capacity, more reliable disks are replaced by an array of inexpensive, smaller capacity, less reliable disks. The added component count with less reliable disks was addressed by introducing redundancy so that a RAID5 array with the same capacity as IBM's 3390 drives can be made as reliable, while providing parallel access and consuming less power Gibson 1992 [65]. Power was not a major consideration at the time, but Chapter 7 in Thomasian 2021 [224] is dedicated to this topic.

The *Mean Time TO Failure - MTTF* of small disks was estimated crudely in Gibson 1992 [65] based on the time to return broken disks to manufacturers. The statistical methods in first edition of Lawless 2003 [125] were followed in this study. There have been several studies of disk failures Schroeder and Gibson 2007 [186], Jiang et al. [107], Schroeder et al. 1010 [187], and NAND flash-based SSDs in Schroeder et al. 2017 [188], Maneas et al. 2021 [137].

Striping partitions files into fixed size *Stripe Units - SUs* or strips, which are placed in round-robin manner on successive rows of disks modulo the number of disks N . A striped RAID with no redundancy is classified as RAID0. RAID5 uses striping like RAID0 but dedicates one strip to parity.

$$P_N = D_1 \oplus D_2 \oplus D_3 \dots \oplus P_{N-1}.$$

Parity strips in RAID5 are placed in right to left diagonals to balance the parity update workload. This is referred to left symmetric organization. Various parity placements are considered in Chen et al. 1994 [32], which also reviews studies to determine optimal strip size. Default 128 KB and 256 KB strip sizes are adopted by some operating systems.

<https://ioflood.com/blog/2021/02/04/optimal-raid-stripe-size-and-filesystem-readahead-for-raid-10/>

Fault-tolerance in RAID5 is attained at the cost of extra processing. Given a modified disk block d_{new} , d_{old} , which is not cached is read from disk to compute $d_{diff} = d_{old} \oplus d_{new}$. p_{old} if not cached is read to compute $p_{new} = p_{old} \oplus p_{diff}$. Both d_{new} and p_{new} need to be written to disk eventually. The fact that a single write requires four disk accesses is called the *Small Write Penalty - SWP* in Chen et al. 1994 [32]. In the case of RAID(4 + k), $k \geq 1$ $2(k + 1)$ reads and writes are required to update data and k check blocks.

The purpose of RAID striping was disk load balancing and was ascertained by Ganger et al. 1996 [63]. Parity striping proposed in Gray et al. 1990 [73] preserves the original data layout by adding parities contiguously, preferably at the middle disk cylinders to achieve seek affinity. This is because in early RAID5 arrays with no NVS support, the update of a data block was considered completed only when both the data block and the corresponding parity block were written to disk.

Parity striping has the advantage of obviating accesses to multiple disks when large blocks are accessed and the strip size is small. It has the disadvantage of possibly unbalanced disk loads, known as access skew, which can be dealt with via disk load balancing support. Load balancing can be achieved by *Hierarchical Storage Management - HSM* which moves data horizontally across fast disks to balance loads, but also vertically from faster to slower disks and vice-versa. HSM or tiered storage is discussed here.

<https://www.ibm.com/support/pages/operating-system-disk-balancing-support>

https://en.wikipedia.org/wiki/Hierarchical_storage_management

HP's AuroRAID discussed in Subsection 25.4 moves data from RAID1 to RAID5 arrays and vice-versa.

RAID5 is compared with parity striping in Chen and Towsley 1993 [34]. The analysis does not take into account the fact that strip size should be chosen large enough to satisfy most requests sizes and these are satisfied by multi-disk *Fork/Join - F/J* requests resulting in a significant increase in disk loads and this favors parity striping.

In a RAID5 with parity group size G if $n > G/2$ strips are updated then it may be more efficient to read the remaining $G - n$ strips to compute the parity by XORing them according to the *ReConstruct Write - RCW* method Thomasian 2005 [204], which may be more efficient than a *Read Modify Write - RMW* which leads to SWP. Linux's RAID5 employs likewise a simple majority rule to determine a strategy for writing, i.e., if a majority of pages for a stripe are dirty then *Parity Computation - PC* is chosen, otherwise *Parity Increment - PI* is chosen and is used in degraded mode.

Upon the failure of a single disk in RAID5, say Disk₁, its blocks can be reconstructed on demand as follows:

$$d_1 = d_2 \oplus d_3 \oplus \dots \oplus p_N$$

The RAID5 read load on surviving disks is doubled when a single disk fails.

The load increase in processing read and write requests as a function of the fraction of read requests (f_r) is given in Ng and Mattson 1994 [151]:

$$\text{LoadIncr}(f_r) = \frac{U_{\text{faulty}}}{U_{\text{faultfree}}} = \frac{N}{N-1} + \frac{(N-2)f_R + (N-8)f_W}{(N-1)(f_R + 4f_W)}, \quad (2)$$

e.g., $\text{LoadIncr}(0) = 1.333$ and $\text{LoadIncr}1 = 2$.

Rebuild is the systematic reconstruction of strips of the failed disk on a spare disk. Strip D_1 on Disk_1 is reconstructed in the DAC buffer by reading and XORing $N-1$ corresponding strips, before they are written to a spare disk D'_1 , which replaces Disk_1 .

$$D'_1 = D_2 \oplus D_3 \oplus \dots \oplus P_N.$$

Several schemes to attain higher reliability are proposed by the Berkeley RAID team Hellerstein et al. 1994 [82]. 2-dimensional arrays are analyzed in Newberg and Wolf 1994 [150], but the analysis of Full-2 codes by Lin et al. 2009 [131] took much longer. Simulation was used to investigate the effect of varied frequency of repairs (replacing broken disks) on the MTTDL [82]

Reliability of 2D squares and 3D cube

2-D size n^2 and 3-D size n^3 arrays are considered in Basak and Katz 2015 [17]. There are n disks in each dimension protected by n parity disks with an extra parity disk protecting the parities so that the number of disks for n dimensions is $n^d + d \times (n+1)$, $n = 2, 3$. *Continuous Time Markov Chains - CTMCs* are used to estimate MTTDL. It is obvious that four disk failures constituting a rectangle lead to data loss and the number of cases leading to data loss is $\binom{n}{2}n$. Given there are a series ℓ of such squares the total number of disks is $N = (n^2 + 2n + 2)\ell$. The probability of failure with $i = 3$ and $i = 4$ already failed disks is

$$\alpha_3 = \frac{\binom{N}{2}n\ell}{\binom{N}{4}}, \quad \alpha_4 = \frac{[\binom{N}{2}n(n^2 + 2n - 2) + n^2]\ell}{\binom{N}{5}}$$

The analysis is extended to $\alpha_i = \min(1, (i+2)\alpha_i)$, $i \geq 5$ and 3D cubes with $N_3 = 4^3$ data and 15 parity disks which are compared with 2d square $N_2 = 8^2 = 64$ data and 18 parity disks. The cube RAID provides a superior MTTDL with respect to square RAID6 arrays with the same number of data disks.

4 Maximum Distance Separable RAID(4+K)

RAID(4+k) *Maximum Distance Separable - MDS* erasure-coded arrays uses the capacity of k disks to tolerate k disk failures, which is the minimum redundancy known as the Singleton bound Thomasian and Blaum 2009 [214]. RAID(4+k) kDFT arrays for $k \geq 1$ can be implemented using the RS code and its variations, while more efficient computationally efficient parity codes are known for $k = 2$ and $k = 3$

StorageTek's Iceberg was an early RAID6 product with RS coding, adopting the *Log-Structure Array - LSA* paradigm, which is an extension of the *Log-structured File System - LFS* scheme

Rosenblum and Ousterhout 1992 [179]. LSA accumulates a stripe's worth of data in the DAC cache, before the strips are written out as a full stripe. This allows check strips to be computed on-the-fly. LSA with a single parity was compared to RAID5 in Subsection 2.2. Conceptually LSA is not suitable for databases/OLTP applications with frequent updates to records (relational tuples), since extra processing is required to update the indices of updated records not written in place. StorageTek was acquired by Sun Microsystems, itself acquired by Oracle Corp.

<https://www.oracle.com/it-infrastructure/>

Thin Provisioning - TP provides a method for optimizing utilization of available storage was first used in Iceberg, but has since been adopted by others. TP relies on on-demand allocation of blocks of data versus the traditional method of allocating all the blocks in advance.

https://en.wikipedia.org/wiki/Thin_provisioning 3PAR, an HPE subsidiary, advocates TP using *Dedicate on Write - DoW* rather than *Dedicate on Allocate - DoA* paradigm, to reduce disk space. https://web.archive.org/web/20061118125440/http://www.byteandswitch.com/document.asp?doc_id=35674.

DoA paradigm used by IBM's MVS OS where a user had to specify an initial allocation and increments.

Three 2DFTS are EVENODD by Blaum et al. 2002 [19] X-code by Xu and Bruck [243], and *Rotated Diagonal Parity - RDP* by Corbett et al. [38]. EVENODD has been extended to $k = 3$ most notably the STAR code in Huang and Xu 2005 [89], whose decoding complexity is lower than comparable codes. RDP has also been extended twice to $k = 3$ Thomasian and Blaum [214],

RAID7.3 is an MDS 3DFT, whose coding details are not specified. It is argued that 3DFT is required to deal with additional disk failures in view of long rebuild times with HDDs (see Table 19). Given 12 TB drives 540 TB capacity is achieved by 12 RAID6 arrays each with six disks each or RAID7.3 with data disks and 24 P and Q check disks, but the same MTDL is achieved by 45 data and only 3 check disks.

<https://www.hyperscalers.com/jetstor-raidix-1185mbs-storage-nas-san-record>

While EVENODD, RDP, and X-code are described in Thomasian and Blaum 1992 [214], but the latter two are described in this paper for the sake of self-completeness, since they are discussed in Section 5.1 and Section 10.4.

RM2 is a non-MDS 2DFT parity code where 1-out- m rows are dedicated to check blocks Park 1995 [158]. Blocks in the first $m - 1$ rows each protected by two parities in the m^{th} row, RM2 is described and evaluated in detail in Thomasian et al. 2007 [212]. RM2 was patented at about the same time as EVENODD it lost its importance given that it is not MDS and more complex rebuild for two failed disks.

Coding is applied to m rows at a time, which are referred here as segments. $m - 1$ rows are dedicated to data blocks and the m^{th} row to parity, hence the redundancy level is $p = 1/M$. There are $2(m - 1)$ data blocks associated with each parity block, but each data block is protected by two parities as exemplified by Figure 1 $N = 7$ disks and $M = 3$ rows. Parity strips in the bottom two protect the data strips in top two rows. P_0 protects a PG consisting of four strips: $(D_{0,6}, D_{0,1}, D_{0,4}, D_{0,3})$, with the first two strips in row 1 and the other two strip in rows 2, and P_1 protects $(D_{0,1}, D_{1,2}, D_{1,4}, D_{1,5})$, etc. Note that RM2 is not MDS since $2/7 < p = 1/3$.

Disk0	Disk1	Disk2	Disk3	Disk4	Disk5	Disk6
$D_{2,3}$	$D_{3,4}$	$D_{4,5}$	$D_{5,6}$	$D_{6,0}$	$D_{0,1}$	$D_{1,2}$
$D_{1,4}$	$D_{2,5}$	$D_{3,6}$	$D_{4,0}$	$D_{5,1}$	$D_{6,2}$	$D_{0,3}$
P_0	P_1	P_2	P_3	P_4	P_5	P_6

Figure 1: RM2 data layout with $N = 7$ disks and $M = 3$ rows per segment, with redundancy $p = 1/M = 33.3\%$.

4.1 Rotated Diagonal Parity - RDP Coded Arrays

RDP is an MDS 2DFT code developed ten years after the EVENODD code and was adopted in NetApp's 2DFT array Corbett et al. 2004 [38]. There are $p + 1$ blocks in each row where the first $p - 1$ blocks hold data, the p^{th} block holds a horizontal parity and $p + 1^{st}$ block holds the diagonal parity. The controlling parameter $p > 2$ should be a prime number. When a block is updated the horizontal parity is updated first and is used in updating the corresponding diagonal parity, RDP with $p = 5$ is shown in Figure 2.

Horizontal parity blocks hold the even parity of the data blocks in that row. Diagonal parity blocks hold the even parity of data and row parity blocks in the same diagonal. Horizontal parities on Disk₄ and diagonal parities at Disk₅ are computed as follows A proof that two disk failures can be dealt with is given in the paper.

$$\begin{aligned}
d^{i,4} &= d^{i,0} \oplus d^{i,1} \oplus d^{i,2} \oplus d^{i,3}, i = 0, 3. \\
d_{0,5} &= d_{0,0} \oplus d_{3,2} \oplus d_{2,3} \oplus d_{1,4} \\
d_{1,5} &= d_{0,1} \oplus d_{1,0} \oplus d_{3,3} \oplus d_{2,4} \\
d_{2,5} &= d_{0,2} \oplus d_{1,1} \oplus d_{2,0} \oplus d_{3,4} \\
d_{3,5} &= d_{0,3} \oplus d_{1,2} \oplus d_{2,1} \oplus d_{3,0}
\end{aligned}$$

According to Theorem 2 in Thomasian and Blaum 2009 [214] given an array of n disks $2 - 2/n$ is the minimum number of XORs required to protect against two disk failures. RDP protects $(p - 1)^2$ data blocks using $2p^2 - 6p + 4$ XORs. Setting $n = p - 1$ we have $2n^2 - 2n$ XORs, hence RDP requires $2 - 2/n$ XORs per block.

EVENODD with n data disk each with $n - 1$ data blocks requires $(n - 1)^2$ XORs to compute row parities and $(n - 2)n$ XORs to compute diagonal parities. EVENODD requires a further $n - 1$ XORs to add the parity of a distinguished diagonal to the parity of each of the other $n - 1$ diagonals. $2n^2 - 3n$ XORs are required to encode $n(n - 1)$ blocks or $2 - 1/(n - 1)$ XORs per

Disk ₀	Disk ₁	Disk ₂	Disk ₃	Disk ₄	Disk ₅
$d_{0,0}^0$	$d_{0,1}^1$	$d_{0,2}^2$	$d_{0,3}^3$	$d_{0,4}^4$	$d_{0,5}$
$d_{1,0}^1$	$d_{1,1}^2$	$d_{1,2}^3$	$d_{1,3}^4$	$d_{1,4}^0$	$d_{1,5}$
$d_{2,0}^2$	$d_{2,1}^3$	$d_{2,2}^4$	$d_{2,3}^0$	$d_{2,4}^1$	$d_{2,5}$
$d_{3,0}^3$	$d_{3,1}^4$	$d_{3,2}^0$	$d_{3,3}^1$	$d_{3,4}^2$	$d_{3,5}$

Figure 2: Storage system with RDP code with $p = 5$. The superscripts are the diagonal parity groups on Disk₅. The parity of diagonal 4 is not stored.

Row#	D_0	D_1	D_2	D_3	D_4	D_5	D_6
0	$B_{0,0}^2$	$B_{0,1}^3$	$B_{0,2}^4$	$B_{0,3}^5$	$B_{0,4}^6$	$B_{0,5}^0$	$B_{0,6}^1$
1	$B_{1,0}^3$	$B_{1,1}^4$	$B_{1,2}^5$	$B_{1,3}^6$	$B_{1,4}^0$	$B_{1,5}^1$	$B_{1,6}^2$
2	$B_{2,0}^4$	$B_{2,1}^5$	$B_{2,2}^6$	$B_{2,3}^0$	$B_{2,4}^1$	$B_{2,5}^2$	$B_{2,6}^3$
3	$B_{3,0}^5$	$B_{3,1}^6$	$B_{3,2}^0$	$B_{3,3}^1$	$B_{3,4}^2$	$B_{3,5}^3$	$B_{3,6}^4$
4	$B_{4,0}^6$	$B_{4,1}^0$	$B_{4,2}^1$	$B_{4,3}^2$	$B_{4,4}^3$	$B_{4,5}^4$	$B_{4,6}^5$
5	$B_{5,0}^0$	$B_{5,1}^1$	$B_{5,2}^2$	$B_{5,3}^3$	$B_{5,4}^4$	$B_{5,5}^5$	$B_{5,6}^6$
6							

Row#	D_0	D_1	D_2	D_3	D_4	D_5	D_6
0	$B_{0,0}^5$	$B_{0,1}^6$	$B_{0,2}^0$	$B_{0,3}^1$	$B_{0,4}^2$	$B_{0,5}^3$	$B_{0,6}^4$
1	$B_{1,0}^4$	$B_{1,1}^5$	$B_{1,2}^6$	$B_{1,3}^0$	$B_{1,4}^1$	$B_{1,5}^2$	$B_{1,6}^3$
2	$B_{2,0}^3$	$B_{2,1}^4$	$B_{2,2}^5$	$B_{2,3}^6$	$B_{2,4}^0$	$B_{2,5}^1$	$B_{2,6}^2$
3	$B_{3,0}^2$	$B_{3,1}^3$	$B_{3,2}^4$	$B_{3,3}^5$	$B_{3,4}^6$	$B_{3,5}^0$	$B_{3,6}^1$
4	$B_{4,0}^1$	$B_{4,1}^2$	$B_{4,2}^3$	$B_{4,3}^4$	$B_{4,4}^5$	$B_{4,5}^6$	$B_{4,6}^0$
5							
6	$B_{6,0}^0$	$B_{6,1}^1$	$B_{6,2}^2$	$B_{6,3}^3$	$B_{6,4}^4$	$B_{6,5}^5$	$B_{6,6}^6$

Figure 3: X-code array with $N = 7$ disks with parity group for $p(i) = B(5, i), 0 \leq i \leq 6$ with slope=+1 and parity group for $q(i) = B(6, j), 0 \leq i \leq 6$ at row 6 with slope=-1.

block. Hence RDP outperforms EVENODD in the number of XOR operations.

If the block size in RDP and EVENODD was a strip then a full stripe write would require updating the four diagonal parity strips. This inefficiency is alleviated by selecting the prime number $p = 2^n + 1$, which allows defining diagonal parities within a group of 2^n stripes. This allows the block size for RDP to be the usual system block size divided by 2^n . If the system's disk block size is 4 KB we can select $p = 17$, so that sixteen 256 B blocks per strip. This allows efficient processing of full stripe writes. EVENODD developed a similar scheme, but used $p = 2^{10} + 1 = 257$.

It is shown in Blaum and Roth 1999 [18] that the minimum update complexities of MDS codes for an $m \times n$ array with $k < n$ data and $r = n - k$ check columns are:

$$\text{MDS single bit update-cost} = \begin{cases} r = 2 & 2 + \frac{1}{m}(1 - \frac{1}{k}) \\ r = 3 & 3 + \frac{3}{m}(\frac{2}{3} - \frac{1}{k}). \end{cases}$$

In the generator matrix $G = [I|P]$, the update cost can be viewed as the number of 1's per row in P.

https://en.wikipedia.org/wiki/Generator_matrix

One is deducted because the number of 1's per row in P instead of in G are counted.

For $r = 2$ (resp $r = 3$) the equation is given as Proposition 5.2 (resp. 5.5) in the paper (Clarification by Prof. P. P. C. Lee at CUHK).

4.2 X-code 2DFT Array with Diagonal Parities

Given N disks, which is a prime number, we have segments consisting of $N \times N$ strips. Rows in a segment are indexed as $0 : N - 1$, rows $0 : N - 3$ hold data strips, row $N - 2$ holds P diagonal parities with positive slope, and row $N - 1$ Q parities with negative slope, thus the redundancy

Column 1	Column 2	Column 3	Column 4	Column 5	Column 6	Column 6
d_0	d_1	d_2	d_3	d_4	d_5	p_0
d_6	d_7	d_8	d_9	d_{10}	d_{11}	p_1
d_{12}	d_{13}	d_{14}	d_{15}	d_{16}	d_{17}	p_2
d_{18}	d_{19}	d_{20}	d_{21}	g_1	g_2^1	p_3

Figure 4: Layout of the local and global parities for Partial MDS with $r = 1$ and $s = 2$, The four local parities are $p_i, 0 \leq i \leq 3$ and g_1 and g_2 are the global parities.

level is $2/N$ and each data block is protected by two parity groups, which are diagonals with ± 1 slopes. hence we have an MDS array since it is shown in Xu and Bruck [243], where it is shown that recovery is possible for all two disk failures.

Figures 3 show the data layouts for $N = 7$ columns. $B_{i,j}$ denotes a data block (strip) at the i^{th} row (stripe) and the j^{th} column (disk). PG memberships are specified by the number for the corresponding P and Q parities. The two parities are independent and given that $\langle X \rangle_N \equiv X \pmod N$ then $p(i)$ and $q(i)$ for $0 \leq i \leq N - 1$ are computed as follows:

$$p(i) = B_{N-2,i} = \sum_{k=0}^{N-3} B_{k, \langle i-k-2 \rangle_N}, \quad q(i) = B_{N-1,i} = \sum_{k=0}^{N-3} B_{k, \langle i+k+2 \rangle_N}.$$

The parities to be updated are determined by the *Parity Group - PG* to which the block belongs. The PG size is $N - 1 = 6$ for both parities and either PG can be accessed to reconstruct a block, so that the load increase in degraded mode is the same as RAID6. Data recovery with two disk failures in X-code is investigated in Thomasian and Xu 2011 [216], where it is shown that the load increase is affected by the distance of two failed disks. A balanced load increase can be attained by rotating successive $N \times N$ segments.

4.3 Partial Maximum Distance Separable Code

Partial MDS - PMDS relies on local and global parities Blaum et al. 2013 [21]. Given an $m \times n$ array of sectors r erasures can be corrected in a horizontal row. The case of 1DFT $r = 1$ with $p_i, 0 \leq i \leq 3$ and $s = 2$ with two global parities g_1 and g_2 is shown in Figure 4, Given six check sectors as many failed sectors can be corrected.

Recoverable case I: One drive failure: $(d_3, d_9, d_{15}, d_{21})$ and two additional sector failures: d_2 and d_{12}

Recoverable case II: $r = 1$ failures per row $(d_2, d_11, d_{12}, d_{19})$ and two additional failures anywhere: d_4 and d_{19}

Recoverable case III: d_2 and d_4 in row zero and d_{12} and d_{14} in row 2. d_{11} and d_{19} in row 1 and three. d_1 and d_{12} can be recovered by g_1 and g_2^1 and then remaining blocks can be recovered using row parities.

RAID6 is an overkill to tolerate the failure of one disk and one sector according to Plank et al. 2023, Plank and Blaum 2014 [167, 168]. *Sector Disk - SD* is an erasure code based on the PMDS concept to cope with storage systems really fail. The decoding process in SD is based on straightforward linear algebra. A brief summary is as follows.

PMDS: Given a stripe defined by the parameters (n, m, s, r) a PMDS code tolerates the failure of any m blocks per row, and any additional blocks in the stripe. PMDS codes are maximally fault-tolerant codes that are defined with $m \times r$ local parity equations and s global parity equations [68]. However, PMDS codes make no distinction for blocks that fail together because they are on the same disk.

SD: Given a similarly defined stripe as PMDS SD code tolerates the failures of any m disks (columns of blocks) plus any additional s sectors in the stripe

For a given code construction, the brute force way to determine whether it is PMDS or SD is to enumerate all failure scenarios and test to make sure that decoding is possible. Given n disk and m as the number of coding disks s sectors per stripe are dedicated to coding, and there are r rows per stripe. A set of $m \times r + s$ equations are set up each of which sums to zero. For SD codes the number is: $\binom{n}{m} \binom{r(n-m)}{s}$

There are many constructions which are valid as SD codes, but not as PMDS codes. SD codes can recover the failure of a column 4 $(d_3, d_9, d_{15}, d_{21})$ and d_3 and d_{12} , but not not aforementioned case II.

“We provided a direct methodology and constructive algorithms to implement a universal and complete solution to the recoverability and non-recoverability of lost sectors. This method and algorithm meets the User Contract that says that what is theoretically recoverable shall be recovered. Our solution can be applied statically or incrementally. We demonstrated the power of the direct method by showing how it can recover data in lost sectors when these sectors touch more strips in the stripe than the fault tolerance of the erasure code. The direct method can be joined with any code-specific recursive algorithm to address the problem of efficient reconstruction of partial strip data. Alternatively, the incremental method can be reversed when some data is recovered to provide a completely generic method to address this same partial strip recovery problem. Finally, we provided numerical results that demonstrate significant performance gains for this hybrid of direct and recursive methods” Hafner et al. 2005 [76].

4.4 Tiger: Disk Adaptive Redundancy Scheme

Tiger Disk-Adaptive Redundancy - DAR scheme dynamically tailors itself to observed disk failure rates Kadekodi et al. 2022 [111]. Tiger results in significant space and cost savings with respect to existing DAR schemes, which are constrained in that they partition disks into subclusters with homogeneous failure rates.

The earlier Pacemaker DAR scheme is less desirable from the viewpoint of the fraction of viable disks for higher n-of-k’s as shown in Figure 2a for 7-of-9, 14-of-17, 22-of-25, and 30-of-33. Pacemaker also reduces intra-stripe diversity and is more susceptible to unanticipated changes in a make or model’s failure rate and only works for clusters committed to DAR.

Tiger avoids constraints by introducing eclectic stripes in which redundancy is tailored to diverse disk failure rates. Tiger ensures safe per-stripe settings given that device failure rates change over time. Evaluation of real-world clusters shows that Tiger provides better space-savings, less bursty IO to change redundancy schemes and better robustness than prior DAR schemes.

Appendix A in [112] derives MTTDL for eclectic stripes using the Poisson binomial distribution, whose disks have different failure rates.

https://en.wikipedia.org/wiki/Poisson_binomial_distribution

5 Multidimensional Coding for Higher Reliability

Several multidimensional coding methods are presented starting with Grid files in Subsection 5.1, a disk array referred to as RESAR in Subsection 5.2, and 2D and 3D arrays for archival storage in Subsection 5.3.

5.1 Grid Files

Grid files by Li et al. 2009 in [127] use coding in two dimensions to protect data strips. The Horizontal (H) and Vertical (V) *Parity Code - PC* or HVPC code is the simplest Grid code over k_1 rows and k_2 columns:

$$H_{i,k_2} = D_{i,1} \oplus D_{i,2} \oplus \dots \oplus D_{i,k_2}, \quad i = 1, \dots, k_1$$

$$V_{k_1,j} = D_{1,j} \oplus D_{2,j} \oplus \dots \oplus D_{k_1,j}, \quad j = 1, \dots, k_2$$

$$P_{k_1,k_2} = \bigoplus_{i=1}^{k_1} H_{i,k_2} = \bigoplus_{j=1}^{k_2} V_{k_1,j} = \bigoplus_{i=1}^{k_1} \bigoplus_{j=1}^{k_2} D_{i,j}$$

If the fault-tolerance of row and column codes are given as is t_r and t_c the total number of faults tolerated is:

$$t_{ft} = (t_r + 1)(t_c + 1) - 1. \quad (3)$$

Informally, the strips of a rectangle with $(t_r + 1)(t_c + 1)$ strips cannot be recovered, but just removing one failed strip allows recovery, hence the minus one in Eq. 3. An approximation (lower bound) to the reliability of grid files can be obtained by considering $k = t_{ft}$ in Eq. 39. In fact the summation can be carried up to the maximum number of failures tolerated for cases that do not lead to data loss with the reliabilities multiplied by the probability that so many failures can be tolerated. as given in Newberg and Wolf 1994 [150].

In addition to *Single Parity Code - SPC* or RAID5, EVENODD, STAR, and X-code codes are considered in this study. RDP which is computationally more efficient than EVENODD should be added to this list. SPC or RAID5 requires one row or column, EVENODD, RDP, X-code require two, and STAR code three. X-code requires a prime number of disks and unlike other codes is vertical, but can be placed horizontally and vice-versa.

In Figure 5 we consider a $p \times p$ X-code array, which is protected by a horizontal SPC code with P parities. There is data update, two parity updates for the X-code and three updates for the SPC code, total of five.

Data recovery in Grid files is carried alternating between row-wise and column-wise recovery and stops when there are no further fault strips (refer to Figure 6 in the paper).

5.2 Reliable Storage at Exabyte Scale - RESAR

RESAR has parity groups weaving through a 2-D disk array Schwarz et al. 2016 [191] As shown in Figure 6 has disklets numbered such that coordinates can be converted to a single number:

Column_1	Column_2	Column_3	Column_4	Column_5	Column_6
$D_{1,1}$	$D_{1,2}$...	$D_{1,p-2}$	$P_{1,p-1}$	$Q_{1,p}$
$D_{2,1}$	$D_{2,2}$...	$D_{2,p-2}$	$P_{2,p-1}$	$Q_{2,p}$
\vdots	\vdots	\ddots	\vdots	\vdots	\vdots
$D_{p,1}$	$D_{p,2}$...	$D_{p,p-2}$	$P_{p,p-1}$	$Q_{p,p}$
$P'_{p+1,1}$	$P'_{p+1,2}$...	$P'_{p+1,p-2}$	$P'_{p+1,p-1}$	$P'_{p+1,p}$

Figure 5: Data in the first p rows is protected by an X-code with P and Q parities in columns $p + 1$ and $p + 2$. (left upper corner) is inside a $((p + 2) \times (p + 2))$ X-code with P and Q parities. The $2 \times p$ space in upper right hand corner with D 's is only covered by the larger X-code. Data block updates affect P and Q parities and the P' parities.

$$(i, j) = i \times (k + 2) + j, \quad 0 \leq j \leq k + 1 \text{ with } k = 4, i = 2, \dots, k + 1$$

Disklet 39 = $6 \times 6 + 3$ is protected by P6 horizontally and D7 diagonally. If disklets 33, 35, 38, and 40 were placed on the same disk or disks on the same rack, then the failure of this disk or rack causes data loss, since the four disklets share two reliability stripes. Details on achieving appropriate placements are given in the paper.

	2	3	4	5	P_0
D_0	8	9	10	11	P_1
D_1	14	15	16	17	P_2
D_2	20	21	22	23	P_3
D_3	26	27	28	29	P_4
D_4	32	33	34	35	P_5
D_5	38	39	40	41	P_6
D_6	44	45	46	47	P_7
D_7	50	51	52	53	P_8
D_8	56	57			P_9
D_9					

Figure 6: A small bipartite RESAR layout connecting P_i and d_i parities for $0 \leq i \leq 9$ via intervening disklets. Each data disk is protected by a P parity in its row and a D parity at a lower row as member of diagonal parity group.

RESAR-based layout with 16 data disklets per stripe has about 50 times lower probability of suffering data loss in the presence of a fixed number of failures than a corresponding RAID6 organization. The simulation to estimate the probability of data loss for 100,000 disks required 10,000 hours.

5.3 2D- and 3-Dimensional Parity Coding

2D and 3D parity protection for disk arrays is discussed in Paris and Schwarz 2021 [157] A small example of 2D protection is given in Figure 7.

There are the following parity groups:

$$(P_1, D_1, D_3, D_8), (P_2, D_1, D_2, D_5, D_9), (P_3, D_3, D_4, D_7, D_{10}), (P_4, D_3, D_4, D_6, D_9), (P_5, D_5, D_6, D_7, D_8, D_9).$$

Three disk failures can result in data loss in this case. Two examples are (P_1, P_2, D_1) , and (D_1, D_5, D_8) . In the first case there is data loss since D_1 loses both of its parities. In the second case there are two failures in the three parity groups, which can support only one disk failure.

		P_1			
	P_2		P_3		
P_4				P_5	
		D_1			
	D_2		D_3		P_6
P_7				P_8	
		D_4			
	D_5		D_6		P_9
\vdots	\vdots	\vdots	\vdots	\vdots	\vdots

Figure 7: 3D parity where each data disk is protected by three parities one vertically and two diagonally.

A small example with 3-D parities with nine parity groups is given in Figure 7.

$$(P_1, D_1, D_4), (P_1, D_2, D_5), (P_3, D_3, D_6), (P_4, D_1, D_3), (P_5, D_1, D_2), (P_6, D_2, D_3), (P_7, D_4, D_6), (P_7, D_4, D_5),$$

As few as four disk failures can result in data loss with 3D coding, e.g., (P_2, P_5, D_2, P_6) , since D_2 has lost the three parities protecting it.

6 Local Redundancy Code

The *Local Redundancy Code - LRC* adds a few parity disks to provide speedier recovery by reducing the number of disks involved in recovery. There is also reduced data transmission cost in distributed storage systems with a large number of disks. LRC differs from CRAID in Section 9 which achieves faster rebuild by parallelizing disk accesses.

An early example of LRC is the (8,2,2) Pyramid code Huang et al. 2007 [90], which has two local parities, one over first four and the second over the next four disks; and the two global parities are over all eight disks. The recovery cost due to local parities is lower as shown in Table 1. also discussed in Section 7.1

Windows Azure Storage - WAS improves over Pyramid codes by reading less data from more fragments Huang et al. 2012 [91]. With the (12,2,2) code 100% of 3 and 86% of 4 disk failures are recoverable.

$$(X_0, X_1, X_2, X_3, X_4, X_5, X_6, p_X), (Y_0, U_1, Y_2, Y_3, Y_4, Y_5, Y_6, p_Y), P_0, P_1 [\forall X, \forall Y]$$

WAS design choices are justified in Table 2:

d_1	d_2	d_3	d_4	$c_{1,1}$
d_5	d_6	d_7	d_8	$c_{1,2}$
c_2	c_3			

Figure 8: An (8,2,2) pyramid code with 8 data and 4 check disks.

# of failed blocks		1	2	3	4
MDS code	recovery (%)	100	100	100	0
(11,8)	read overhead	1.64	2.27	2.91	-
Pyramid code	recovery (%)	100	100	100.0	68.89
(12,8)	read overhead	1.25	1.74	2.37	2.83

Table 1: Comparison between MDS code (11,8) and Pyramid code (12,8)

Scheme	Storage overhead	Reconstruction cost	Savings
RS(6+3)	1.5	6	
RS(12+4)	1.29	14	14%
LRC(12,2,2)	1.29	7	14%

Table 2: Choice of Windows Azure Storage

We continue the discussion with a smaller (6,2,2) example for which the MTDL is 2.6×10^{12} , versus 3.5×10^9 for replication and 6.1×10^{11} for (6,3) RS. i.e., a ten fold increase in MTDL at the cost of an extra disk.

$$(X_0, X_1, X_2, p_X), (Y_0, Y_1, Y_2, p_Y), p_0, p_1$$

This LRC can tolerate arbitrary 3 failures by using the following sets of coefficients:

$$q_{x,0} = \alpha_0 x_0 + \alpha_1 x_1 + \alpha_2 x_2, \quad q_{x,1} = \alpha_0^2 x_0 + \alpha_1^2 x_1 + \alpha_2^2 x_2 \quad q_{x,2} = x_0 + x_1 + x_2$$

$$q_{y,0} = \beta_0 y_0 + \beta_1 y_1 + \beta_2 y_2, \quad q_{y,1} = \beta_0^2 y_0 + \beta_1^2 y_1 + \beta_2^2 y_2 \quad q_{y,2} = y_0 + y_1 + y_2$$

$$p_0 = q_{x,0} + q_{y,0}, \quad p_1 = q_{x,1} + q_{y,1}, \quad p_x = q_{x,2}, \quad p_y = q_{y,2}$$

The values of α s and β s are chosen such that the LRC can decode all decodable four failures.

For disk failure rates: λ and repair rates ρ we have the following transitions among the states of a Markov reliability model, see e.g., Trivedi 2002 [228].

$$S_i \rightarrow S_{i-1} : i\lambda, \quad 10 \leq i \leq 8 \quad S_i \leftarrow S_{i-1} : \rho_i \quad 9 \leq i \leq 7$$

Let p_d be the fraction of decodable four disk failures

$$S_7 \rightarrow 7S_6 : \lambda p_d, \quad S_7 \rightarrow S_{Failed} : 7\lambda(1 - p_d)$$

With N storage nodes with capacity S and network bandwidth B the average repair rate of a single failure is $\rho_9 = \epsilon(N-1)B/SC$, where ϵ is the fraction of network bandwidth at each node. This is yet another option for rebuild processing. It takes 3 fragments to repair the 6 data fragments and 2 local parities. It takes 6 fragments to repair the 2 global parities. The *Average Repair Cost - ARC* is: $C = (3 \times 8 + 6 \times 2)/10 = 3.6$ Enumerating all failure patterns $p_d = 0.86$. The detection and triggering time $T = 30$ minutes dominates repair time for more than one fragment failure, so that $\rho_8 = \rho_7 = \rho_6 = 1/T$, $N = 300$, $S = 16$ TB, $B = 1$ GB per second, $\epsilon = 0.1$

6.1 A Systematic Comparison of Existing LRC Schemes

Xorbas, Azure’s LRCs, and Optimal-LRCs are compared using the *Average Degraded Read Cost - ADRC*, and the *Normalized Repair Cost - NRC* in Kolosov et al. 2018 [121]. The trade-off between these costs and the code’s fault tolerance offer different choices.

There are two types of (n, k, r) LRCs. With information-symbol locality, only the data blocks can be repaired in a local fashion by r blocks, while global parities require k blocks for recovery. Pyramid and Azure-LRC are examples of so-called data-LRCs.

In codes with all-symbol locality, all the blocks, including the global parities, can be repaired locally from r surviving blocks. Xorbas discussed in Subsection 7.2 is an example of a Full-LRC code.

The experimental evaluation on a Ceph cluster deployed on Amazon *Elastic Compute Cloud - EC2*

https://en.wikipedia.org/wiki/Amazon_Elastic_Compute_Cloud demonstrates the different effects of realistic network and storage bottlenecks on the benefit from various LRC approaches. Ceph is an open-source software-defined storage platform that implements object storage on a single distributed computer cluster and provides 3-in-1 interfaces for object-, block-, and file-level storage Maltzahn et al. 2010 [136]. The study shows the benefits of full-LRCs and data-LRCs depends on the underlying storage devices, network topology, and foreground application load.

The normalized repair cost metric can reliably identify the LRC approach that would achieve the lowest repair cost in each setup. The *Average Repair Cost - ARC* is based on the assumption that the probability of repair is the same for all blocks:

$$ARC = \sum_{i=1}^n \text{cost}(b_i)/n.$$

In the case of (10,6,3) Azure code is $ARC = (8 \times 3) + (2 \times 6)/10 = 3.6$.

The *Normalized Repair Cost - NRC* which amortizes the cost of repairing parity blocks over data blocks is given as:

$$NRC = ARC \times \frac{n}{k}, \quad NRC = [(8 \times 3) + (2 \times 6)]/6 = 6.$$

Degraded Read Cost - DRC is the full-node repair cost and which for (10,6,3) Azure LRC is $6 \times 3/6 = 3$.

Xorbas (16,10,5) has RS-based four global parities which can be recovered from local parities via an implied parity block as shown in Figure 2 in the paper.

$$(X_1, X_2, X_3, X_4, X_5, P_{1:5}, (X_6, X_7, X_8, X_9, X_{10}, P_{6:10}))$$

6.2 Combining Parity and Topology Locality in Wide Stripes

Wide stripes are used to minimize redundancy. There are n chunks, k data chunks, and $m = n - k$ which is 3 or 4 parity chunks [88]. For the ten examples given by Table 1: $1.18 \leq \text{redundancy} = n/k \leq 1.5$. The notation used in the paper is given in Table 3.

Challenges for wide stripes are: (i) Requiring k chunks to be retrieved is expensive, (ii) CPU cache may not be able to hold large number of chunks, (iii) updating $n - k$ check chunks is expensive.

Notation	Description
n	total # of chunks of a stripe
k	total # of data stripes of a chunk
r	# of retrieved chunks to repair a lost chunk
z	# of racks to store a stripe
c	# of chunks of a stripe in a rack
f	# of tolerable node failures of a stripe
γ	maximum allowed redundancy

Table 3: Notation for combined locality

D_1	D_3	D_5	D_7	D_9	D_{11}	D_{13}	D_{15}	D_{17}	D_{19}	Q_1
D_2	D_4	D_6	D_8	D_{10}	D_{12}	D_{14}	D_{16}	D_{18}	D_{20}	Q_2
P_1 [1,2]	P_2 [3,4]	P_3 [5,6]	P_4 [7,8]	P_5 [9,10]	P_6 [11,12]	P_7 [13, 14]	P_8 [15,16]	P_9 [17-18]	P_{10} [19-20]	

Figure 9: Azure parity locality LRC $(n,k,r)=(32, 20,2)$.

There is a trade-off between redundancy and repair penalty: (i) Parity locality incurs high redundancy. (ii) Topology locality incurs high cross-track repair bandwidth. The Azure LRC $(32,20,2)$ is given in Figure 9.

-	(n,k,r)	$(16,10,5)$
Azure-LRC	$f = n - k + \lceil k/r \rceil + 1$	$f = 5$
Xorbas	$f \leq n - k - \lceil k/r \rceil + 1$	$f = 4$
Optimal LRC	$f \leq n - k - \lceil k/r \rceil + 1$	$f = 4$
Azure LRC+1	$f \leq n - k - \lceil k/r \rceil$	$f = 4$

Table 4: Number of tolerable node failures f for different LRCs for $(n,k,r)=(16,10,5)$

$(n,k,r,z) = (26,20,5,9)$, where $z = 9$ is the number of elements in a column is given in Figure 10

6.3 Practical Design Considerations for Wide LRCs

The following discussion is based on Kadekodi et. al. 2023 [112]. With 4 data blocks (d_1, d_2, d_3, d_4) , 2 global parities c_1 and c_2 , and three local parities $\ell_1 = d_1 \oplus d_2$, $\ell_2 = d_3 \oplus d_4$, $\ell_g = c_1 \oplus c_2$. The generator matrix is:

$$G_C = \begin{pmatrix} 1 & 0 & 0 & 0 \\ 0 & 1 & 0 & 0 \\ 0 & 0 & 1 & 1 \\ 0 & 0 & 0 & 1 \\ c_{1,1} & c_{1,2} & c_{1,3} & c_{1,4} \\ c_{2,1} & c_{2,2} & c_{2,3} & c_{2,4} \\ 1 & 1 & 0 & 0 \\ 0 & 0 & 1 & 1 \\ c_{1,1} + c_{2,1} & c_{1,2} + c_{2,2} & c_{1,3} + c_{2,3} & c_{1,4} + c_{2,4} \end{pmatrix} \begin{pmatrix} d_1 \\ d_2 \\ d_3 \\ d_4 \\ \ell_1 \\ \ell_2 \\ \ell_g \end{pmatrix}$$

D_1	D_2	D_3
D_4	D_5	$P_1[1:5]$
D_6	D_7	D_8
D_9	D_{10}	$P_2[6:10]$
D_{11}	D_{12}	D_{13}
D_{14}	D_{15}	$P_3[11,15]$
D_{16}	D_{17}	D_{18}
D_{19}	D_{20}	$P_4[16:20]$
$Q_1[1:20]$	$Q_2[1:20]$	-

Figure 10: Combined locality (25,20,5,9).

Scheme	n	k	r	p	Rate
S1: 24-of-28	28	24	2	2	0.857
S2: 48-of-55	55	48	3	4	0.872
S3: 72-of-80	80	72	4	4	0.9
S4: 96-of-105	105	96	5	4	0.914

Table 5: Wide LRC schemes used to compare different LRC constructions with low level of redundancy $k/n > 0.85$. p is the # of parity groups and local parities and r the # of global parities.

Four different 48-of-55 Azure LRC constructions with four local parities and 3 global parities are specifiable as follows.

$$c_j = \bigoplus_{12 \times (j-1)+1}^{12 \times j} d_i, 1 \leq j \leq 4, \quad r_{s_1}, r_{s_2}, r_{s_3}$$

Azure-LRC+1 forms a local group of the global parities and protects them using a local parity.

$$c_j = \bigoplus_{16 \times (j-1)+1}^{12 \times j} d_i, 1 \leq j \leq 3, \quad c_{rs} = \bigoplus_{j=1}^3 r_{s_j}$$

In the case of 48-of-55 optimal Cauchy LRC the four local parities cover, similarly to Azure parities, but global parities cover parity blocks (as in Figure 4 (c)).

In the case of uniform Cauchy LRC the p local parities are uniformly distributed across the k data blocks and they are all XORed with the global parity checks.

$$c_1 = \bigoplus_{i=1}^{12} d_i \quad c_2 = \bigoplus_{i=13}^{25} d_i \quad c_3 = \bigoplus_{i=26}^{38} d_i \quad c_4 = \left[\bigoplus_{i=38}^{48} d_i \right] \oplus \left[\bigoplus_{j=1}^3 r_{s_j} \right].$$

The average cost of reconstructing any of the data blocks *Average Degraded Read Cost - ARC* and two other measures are defined as follows:

$$ADRC = \sum_{i=1}^k \text{cost}(b_i/k), \quad ARC_1 = \sum_{i=1}^n b_i/n \quad ARC_2 = \sum_{i=1, j \neq i}^n \text{cost}(b_{i,j} / \binom{n}{2}).$$

Locality (ℓ)	Uniform Cauchy LRC S1: 13, S2: 13, S3: 19, S4: 26
ADRC	Azure LRC - S1: 12, S2=12, S3=18, S4=24
ARC1	Azure LRC - S1: 12.85, S2: 12.76, S3:19, S4: 25.22
ARC2	Uniform Cauchy - LRC S1: 27.92; S2: 33.85, S3: 49.22, S4 67.69
Normalized MTTDL	S1, 1., S2, 1.01* S3, 1.0 S4: 1.0

Table 6: Best schemes based on analytic metrics used to compare different LRC constructions. Results are normalized with respect Uniform Cauchy. *Optimal Cauchy LRC.

Node ₁	Node ₂	Node ₃	Node ₄
A_1	B_1	$A_1 + B_1$	$A_2 + B_1$
A_2	B_2	$A_2 + B_2$	$A_1 + A_2 + B_2$

Figure 11: An MDS (4,2) code which can tolerate two disk failures.

Average repair or reconstruction cost takes into account local and global parity blocks in the computation as ARC₁ and ARC₂ is used as the cost of reconstructing 2 blocks. Best schemes for various metrics are given in Table 6.

The Markov chain to estimate the MTTDL for a 48-of-55 disk array can be specified as follows. Given that i denotes the number failed disks a failure at S_i leads to a transition to S_{i+1} for $i < 5$. Some of the transition for $5 \leq i \leq 7$ lead to failure. Transition probabilities are based on AFR. The MTTDL can be determined as the mean number of visits to each state and the holding time: $[(55 - i)\delta]^{-1}$ where δ is the failure rate.

7 Schemes to Reduce Rebuild Traffic in Distributed RAID

A survey of network codes for distributed storage is given in Dimakis et al. 2011 [47]. As an example consider a (4,2) MDS code is given in Figure 11, which can tolerate any two disk failures.

Assuming Node₁ fails then

$$B_2 \oplus (A_2 \oplus B_2) \rightarrow A_2 \quad (A_2 \oplus B_2) \oplus (A_1 \oplus A_2 \oplus B_2)$$

Assuming Node₄ fails then at Node₁ we compute $(A_2 \oplus B_2)$ at Node₂:

$$(A_2 \oplus B_2) \oplus (B_1 \oplus B_2) \rightarrow (A_2 \oplus B_1)$$

$$A_1 \oplus (A_2 \oplus B_2) \rightarrow (A_1 \oplus A_2 \oplus B_2)$$

To reproduce broken Node₁ and Node₂ we can proceed as follows:

$$\begin{aligned} (A_2 \oplus B_2) \oplus (A_1 \oplus A_2 \oplus B_2) &\rightarrow A_1 \rightarrow A_1, \\ A_1 \oplus (A_1 \oplus B_1) &\rightarrow B_1 \\ (A_1 \oplus B_1) \oplus (A_2 \oplus B_1) &\rightarrow (A_1 \oplus A_2) \\ (A_1 \oplus A_2) \oplus (A_1 \oplus A_2 \oplus B_2) &\rightarrow B_2 \\ B_2 \oplus (A_2 \oplus B_2) &\rightarrow A_2 \end{aligned}$$

node 1	a_1	b_1
node 2	a_2	b_2
node 3	$a_1 + a_2$	$b_1 + b_2$
node 4	$a_1 + 2a_2$	$b_1 + 2b_2 + a_1$

Figure 12: A toy example of piggybacking illustrated.

d_1	d_2	d_3	$d - 4$	d_5	d_6	$c_{1,1}$
d_7	d_8	d_9	d_{10}	d_{11}	d_{12}	$c_{1,2}$
c_2	c_3	c_4				

Figure 13: A pyramid code with 12 data and 5 check disks. $c_{1,1}$ and $c_{1,2}$ provide parity protection for the first six and second six disks, respectively.

Rashmi et al. 2013 [173] use Piggybacking to reduce the volume of transferred data. Consider four nodes with two bytes of data each as shown in Figure 12

If Node 1 fails its recovery would ordinarily require accessing two blocks from nodes 2 and 3 each, but with piggybacking we only need access the second byte from nodes Node 2, 3, and 4. Several methods to reduce rebuild traffic in a distributed environment are discussed in this section.

Piggybacking as defined by Muntz and Lui 1990 [147] writes blocks reconstructed on demand on the spare disk. Such small writes tend to be inefficient Holland et al. 1994 [84]. Piggybacking at the level of tracks on which data blocks resided is considered in Fu et al. [60]. There is a significant increase in disk utilization which affects response times since rebuild read times equalling disk rotation time are large, but rebuild time is reduced.

7.1 Pyramid Codes

Pyramid codes have a higher overhead than MDS erasures codes, but provide a much lower recovery cost Huang et al. 2007 [90]. Shown in Figure 13 are twelve data blocks subdivided into two groups of six blocks with local parities and three global parities. Microsoft's Azure is a *Local Reconstruction Code - LRC* which tolerates all three disk failures, but the repair of as many as four failed disks is possible Huang et al. 2012 [91].

A smaller example to shorten the discussion of data recovery is as follows:

$$(x_0, x_1, x_2), p_x, (y_0, y_1, y_2), p_y, c_0, c_1)$$

Consider the failure of x_0 , x_2 , and y_1 . Repair proceeds by repairing y_1 using p_y and x_0 and x_2 can then be repaired using c_0 and c_1 . Recovery with four disk failures is possible in 86% of cases, but is quite complex.

LRC can tolerate arbitrary 3 failures by choosing the following α 's and β 's.

$$q_{x,0} = \alpha_0 x_0 + \alpha_1 x_1 + \alpha_2 x_2, \quad q_{x,1} = \alpha_0^2 x_0 + \alpha_1^2 x_1 + \alpha_2^2 x_2, \quad q_{x,2} = x_0 + x_1 + x_2$$

$$q_{y,0} = \beta_0 y_0 + \beta_1 y_1 + \beta_2 y_2, \quad q_{y,1} = \beta^2 y_0 + \beta_1^2 y_1 = \beta^2 y^2 \quad q_{y,2} = y_0 + y_1 + y_2$$

The LRC equations are as follows:

$$p_0 = q_{x,0} + q_{y,0}, \quad p_1 = q_{x,1} + q_{y,1}, \quad p_x = q_{x,2} p_y = q_{y,2}$$

The values of α_s and β_s are selected, so that LRC can decide all information-theoretically decodable four failures.

1. None of four parities fails: The failures are equally divided between the two groups. We have the following matrix.

$$G = \begin{pmatrix} 1 & 1 & 0 & 0 \\ 0 & 0 & 1 & 1 \\ \alpha_i & \alpha_j & \beta_s & \beta_t \\ \alpha_i^2 & \alpha_j^2 & \beta_s^2 & \beta_t^2 \end{pmatrix}$$

$$\det(G) = (\alpha_j - \alpha_i)(\beta_t - \beta_s)(\alpha_i + \alpha_j - \beta_s - \beta_t).$$

2. Only one of p_x and p_y fails: Assume p_y fails. The remaining three failures are two in group x and one in group y . We have three equations with coefficients given by:

$$G' = \begin{pmatrix} 1 & 1 & 0 \\ \alpha_i & \alpha_j & \beta_s \\ \alpha_i^2 & \alpha_j^2 & \beta_s^2 \end{pmatrix} \det(G') = \beta_s(\alpha_j - \alpha_i)(\beta_s - \alpha_j - \alpha_i)$$

3. Both p_x and p_y fail The remaining two failures are divided between the two groups.

$$G'' = \begin{pmatrix} \alpha_i & \beta_s \\ \alpha_i^2 & \beta_s^2 \end{pmatrix} \det(G') = \alpha_i \beta_s (\beta_s - \alpha_i)$$

To ensure all cases are decodable all three matrices should be non-singular.

The repair savings of an ($n = 16, k = 12, r = 6$) LRC compared to that of an ($n = 16, k = 12$) RS code in the Azure production cluster are demonstrated in Huang et al. [91]. The ($n = 18, k = 14, r = 7$) LR code in WAS - Windows Azure Storage has repair degree comparable to that of an ($9, 6$) RS code, in the Azure production cluster are demonstrated in this work. This code has reportedly resulted in major savings for Microsoft.

<https://www.microsoft.com/en-us/research/blog/better-way-store-data/>

7.2 Hadoop Distributed File System - HDFS-Xorbas

Hadoop Distributed File System - HDFS Borthakur 2007 [24], which employs $n \geq 3$ replications for high data reliability is based on the following assumptions: 1. Hardware failures the norm rather than the exception. 2. Batch processing. 3. Large datasets. 4. Files once created are not changed, i.e., *Write-Once, Read-Many - WORM*. 5. Moving computation cheaper than moving data. 6. Portability across heterogeneous platforms required.

HDFS Xorbas was implemented at U. Texas at Austin for Facebook. This is an LRC build on top of an RS code by adding extra local parities Sathiamoorthy et al. 2013 [182]. The experimental evaluation of Xorbas was carried out in Amazon EC2 and a Facebook cluster, in which the repair performance of ($n = 16, k = 10, r = 5$) LR code was compared against a [$14, 10$] RS code. Xorbas reduced disk I/O and repair network traffic compared to RS codes. In addition

Scheme	Storage overhead	Repair traffic	MTTDL (days)
3-replication	2x	1x	2.31E+10
RS(10,4)	0.4x	10x	3.31E+13
LRC(10,6,5)	0.6x	5x	1.21E+15

Table 7: Comparison of three redundancy schemes.

to the four RS parity blocks associated with ten file blocks, LRC associates local parities as shown below:

$$\begin{aligned}
S_1 &= c_1X_1 + c_2X_2 + c_3X_3 + c_4X_4 + c_5X_5 \\
S_2 &= c_6X_6 + c_7X_7 + c_8X_8 + c_9X_9 + c_{10}X_{10} \\
S_3 &= c'_5S_1 + c'_6S_2 \text{ with } c'_5 = c'_6 = 1
\end{aligned}$$

With three local parities the storage overhead is 17/10, but S_3 need not be stored by choosing $c_i, 1 \leq i \leq 10$ satisfy the additional alignment equation $S_1 + S_2 + S_3 = 0$. It is shown that this code has the largest possible distance ($d = 5$) for this given locality ($r = 5$) and blocklength ($n = 16$). This is an LRC (10,6,5) code.

The reliability analysis of the system with the birth-death model (Kleinrock 1975 [118]) is given in Ford et al. [59]. Chunks fail independently with rate λ_i and recover with rate ρ_i . The failure transition rates are $S_i \rightarrow S_{i+1}: \lambda_i, 0 \leq i \leq 4$ and repair transition rates $S_i \leftarrow S_{i+1} \rho_i, 0 \leq i \leq 3$. Starting with state s and given that the system can tolerate r failures we are interested in the time to failure (the time to reach \mathcal{D}_{r-1}).

$$\text{MTTDL} = \frac{1}{\lambda} \left(\sum_{k=0}^{s-r} \sum_{i=0}^k \left(\frac{\rho^i}{\lambda^i} \right) \frac{1}{(s-k+i)_{i=1}} \right) \quad (4)$$

where $(a)_{(b)} \stackrel{\text{def}}{=} a(a-1)(a-2)\dots(a-b+1)$. Since recovery takes much less time than time to failure ($\rho \gg \lambda$) the MTTF can be approximated as:

$$\text{MTTDL} \approx \frac{\rho^{s-r}}{\lambda^{s-r+1}} \frac{1}{(s)_{(s-r+1)}} + \mathcal{O} \left(\frac{\rho^{s-r-1}}{\lambda^{s-r}} \right)$$

A comparison of three redundancy methods is given in Table 7

7.3 Hadoop Adaptively-Coded Distributed File System - HACDFS

HACDFS uses two codes: a fast code with low recovery cost and a compact code with low storage overhead Xia et al. [239]. It exploits the data access skew observed in Hadoop workloads to decide on the initial encoding of data blocks. HACDFS uses the fast code to encode a small fraction of the frequently accessed data and provides overall low recovery cost for the system. The compact code encodes the majority of less frequently accessed data blocks with a low storage overhead.

After an initial encoding, e.g., with the compact code, HACDFS dynamically adapts to workload changes by using upcoding and downcoding to convert data blocks between the fast and

compact codes. Blocks initially encoded with fast code are upcoded into compact code enabling HACDFS system to reduce the storage overhead. Downcoding data blocks from compact code to fast code representation lowers the overall recovery cost of the HACDFS system. The upcode and downcode operations are efficient and only update the associated parity blocks. HACDFS exploits the data access skew observed in Hadoop workloads.

<http://blog.cloudera.com/blog/2012/09/what-do-real-life-hadoop-workloads-look-like/>

D	D	D	D	D	P
D	D	D	D	D	P
P	P	P	P	P	P

D	D	D	D	D	P
D	D	D	D	D	P
P	P	P	P	P	P

D	D	D	D	D	P
D	D	D	D	D	P
P	P	P	P	P	P

D	D	D	D	D	P
D	D	D	D	D	P
D	D	D	D	D	P
D	D	D	D	D	P
D	D	D	D	D	P
D	D	D	D	D	P
P	P	P	P	P	P

Figure 14: Parity encodings to attain reliability in Hadoop. Upcoding (2x5) arrays to 6x5 results in a reduced redundancy from 18/10=1.8 to 42/30=1.4. Horizontal parity codes are simply copied, while the vertical parity bits are the XOR of the parities in the high density code.

Fewer data accesses are required for rebuild strips with 2×5 encoding, i.e., two strips accesses to rebuild a strip.

8 Copyset Replication for Reduced Data Loss Frequency

Copyset Replication - CR is a technique to significantly reduce the frequency of data loss events with triplicated data. It was implemented and evaluated on two open source data center storage systems by Cidon et al. in [36]. HDFS in Subsection 7.2 and RAMCloud in Subsection 29.5).

Data replicas are ordinarily randomly scattered across several nodes for parallel data access and recovery. CR presents a near optimal trade-off between the number of nodes on which the data is scattered and the probability of data loss. It is better to lose more data less frequently than vice-versa as stated by a Facebook engineer in the paper.

“Even losing a single block of data incurs a high fixed cost, due to the overhead of locating and recovering the unavailable data. Therefore, given a fixed amount of unavailable data each year, it is much better to have fewer incidents of data loss with more data each than more incidents with less data. We would like to optimize for minimizing the probability of incurring any data loss. in other words fewer events are at a greater loss of data are preferred.”

Replication characteristics of three data centers are given in Table 8.

In *Random Replication - RR* assuming that the primary replica is placed at node i the secondary replica is placed at node $i + 1 \leq j \leq i + S$ and if $S = N - 1$ the secondary replicas are

System	Chunks per node	Cluster size	Scatter width	Replication scheme
Facebook	10,000	1000-5000	10	Small group
RAMCloud	8000	100-10,000	N-1	Across all nodes
HDFS	10,000	100-10,000	200	Large group

Table 8: Three replication schemes. In the case of Facebook and HDFS 2nd and 3rd replica is on same rack.

drawn uniformly from all the nodes in the cluster. The scatter width (S) is the number of nodes that may store copies of a node’s data.

For example, for $N = 9$ nodes, degree of replication $R = 3$, $S = 4$ if the primary replica is on Node 1 then the secondary replica is on Nodes (2,3,4,5). P_{DL} is the ratio $\#copysets = 54$ and the maximum number of sets $\binom{9}{3}$ or 0.64. A lower scatter width decreases recovery time, while a high scatter width increases the frequency of data loss.

Correlated failures such as cluster power outages are poorly handled by RR and (0.5%-1%) of nodes do not power up. There is a high probability that all replicas of at least one chunk in the system will not be available. According to Figure 1 in the paper as the number nodes exceeds 300 nodes with degree of replication ($R = 3$) the probability of data loss $P_{DL} \approx 1$.

CR - Copyset Replication splits the nodes into groups of R chunks, so that the replicas of a single chunk can only be stored in a copyset. Data loss occurs when all the nodes of a copyset fail together, e.g., with $N = 9$ nodes and $R = 3$ nodes per copyset: (1, 2, 3), (4, 5, 6), (7, 8, 9), so that data loss occurs if (1, 2, 3), (4, 5, 6), or (7, 8, 9) are lost. When a CR node fails there are $R - 1$ other nodes that hold its data.

The goal of CR is to minimize the probability of data loss, given any S by using the smallest number of copysets. When the primary replica is on node i the remaining $R - 1$ replicas are chosen from $(i + j)$, $j = 1, \dots, S$. With $S = 4$ (1, 2, 3), (4, 5, 6), (7, 8, 9), (1, 4, 7), (2, 5, 8), (3, 6, 9). Node 5’s chunks can be replicated as nodes (4,6) and nodes (2,8). There are $\#copysets=6$ and if three nodes fail $P_{DL} = 0.07$. Note that the copysets overlap each other in one node and that copysets cover all nodes equally,

Two permutations of node numbers can be used to define copysets. The overall scatter width is $S = P(R - 1)$. The scheme creates PN/R or $SN/(R(R - 1))$ copysets.

Simulation results are used to estimate P_{DL} versus the number of RAMCloud nodes for $3 \leq R \leq 6$. As shown in Figure 2 $P_{DL} \approx 0$ for $R = 6$ beyond a 1000 nodes, and increases linearly from 0 to 50% for 10,000 nodes.

Figure 3 in the paper plots P_{DL} with $N = 5000$, $R = 3$, with RR and CR versus $1 \leq S \leq 500$ when 1For RR $P_{DL} \approx 1$ for $S \geq 50$, which is the case for Facebook HDFS and $P_{DL} > 0.0$ for $S = 500$.

Consider the case when the system replicates data on the following copysets:

$$(1, 2, 3), (4, 5, 6), (7, 8, 9), (1, 4, 7), (2, 5, 8), (3, 6, 9).$$

That is, if the primary replica is placed on node 3, the two secondary replicas can only be randomly on nodes 1 and 2 or 6 and 9. Note that with this scheme, each node’s data will be split uniformly on four other nodes. With this scheme there are six copysets and $P_{DL} = \#copysets/84 = 0.07$.

Power outage in the case of a 5000-node RAMCloud cluster with CR reduces the probability of data loss from 99.99% to 0.15%. For Facebook’s HDFS cluster it reduces the probability from 22.8% to 0.78%.

8.1 More Efficient Data Storage: Replication to Erasure Coding

DiskReduce is a modification of HDFS enabling asynchronous compression of initially triplicated data down to RAID6. This increases cluster’s storage capacity by a factor of three and this is delayed long enough to deliver the performance benefits of multiple data copies

Also considered in this study was mirrored RAID - RAID1/5 which was mirrored RAID5 within and across files. A plot of space overhead versus RAID group size $2^i, 1 \leq i \leq 5$ shows a less than 5% overhead for $i = 5$ for RAID6 and across files.

If the encoding is delayed for t seconds, we can obtain the full performance of having three copies from a block’s creation until it is t seconds old. The penalty is modeled by r , which stands for $100(1 - r)\%$ degradation. Different r gives different expected performance bounds, a The expected performance achieved by delaying encoding can be bounded as:

$$\text{Penalty}(t) = 1 \times \Phi(t) + r \times (1 - \Phi(t)),$$

where $\Phi(t)$ is CDF of block access with regard to blockage, which is derived from the trace (Figure 4 in paper), Plotting $\text{Penalty}(t)$ versus t it can be seen in Figure 5 in the paper, that for $r = 0.8, 0.5, 0.333$ there is very little system performance penalty after an hour.

Based on traces collected from Yahoo!, Facebook, and Opencloud cluster the following issues are explored,

1. The capacity effectiveness of simple and not so simple strategies for grouping data blocks into RAID sets;
2. Implications of reducing the number of data copies on read performance and how to overcome the degradation;
3. Different heuristics to mitigate SWP.

The framework has been built and submitted into the Apache Hadoop project.

The *Quantcast File System - QFS* [156] is a plugin compatible alternative to HDFS/MapReduce offering efficiency improvements:

- (1) 50% disk space savings through erasure coding instead of replication,
- (2) doubling of write throughput,
- (3) a faster name node,
- (4) support for faster sorting and logging through a concurrent append feature,
- (5) a native command line client much faster than Hadoop file system,
- (6) global feedback-directed I/O device management.

9 Clustered RAID5

Clustered RAID - CRAID proposal Muntz and Lui 1990 [147] was focused on the reduction of load increase in degraded mode. The *Parity Group - PG* size: G is set to be smaller than the stripe

width set equal to the number of disks (N). The read load increase is given by the declustering ratio $\alpha = (G - 1)/(N - 1) < 1$, since each access to the failed disk results in accesses to surviving disks in the PG. CRAID will result in a reduction of $R_n^{F/J}(\rho)$ due to a reduced ρ in degraded mode and that that a $n = G < N$ -way F/J requests are required.

The load decrease in RAID5 is tantamount to reduced rebuild time according to Eq. (36), which is due to reduced load and the fact that rebuild reading is parallelized. With dedicated sparing that disk may become a bottleneck even if there is no read redirection, but curtailing redirection by monitoring the load of the spare disk can be used to reduce rebuild time. Distributed sparing is a possible solution.

The load in clustered RAID5 and RAID6 is obtained using decision trees in Thomasian 2005b [207]. Let \bar{T} denotes read, write, and *Read-Modify-Write* - *RMW* mean disk service times. RMW is a read followed by a write after a disk rotation and can be substituted by independent single reads and writes. With arrival rate Λ to a RAID5 with N disks disk utilizations factors due to read and write requests with one failed disk are:

$$\begin{aligned} \rho_{read}^{RAID5/F1} &= \frac{\Lambda f_{read}}{N-1} \left[\frac{N+G-2}{N} \bar{T}_{read} \right] \\ \rho_{write}^{RAID5/F1} &= \frac{\Lambda f_{write}}{N-1} \left[\frac{G-2}{N} \bar{T}_{read} + \frac{2}{N} \bar{T}_{write} + \frac{2(N-2)}{N} \bar{T}_{RMW} \right] \end{aligned} \quad (5)$$

Six properties for ideal layouts for CRAID are presented in Holland et al. 1994 [84], but not all six properties are attainable as shown in the study:

- (i) Single failure correcting, the strips in the same stripe are mapped to different disks.
- (ii) Balanced load due to parity, all disks have the same number of parity strips.
- (iii) Balanced load in failed mode, the reconstruction workload should be balanced across all disks.
- (iv) Large write optimization, each stripe should contain $N - 1$ contiguous strips, where N is the parity group size.
- (v) Maximal read parallelism is attained, i.e., the reading of $n \leq N$ disk blocks entails in accessing n disks.
- (vi) Efficient mapping, the function that maps physical to logical addresses is easily computable.

According to Alvarez et al. 1998 [5] for declustering with $n \geq 2$ disk drives, b parity groups, $k \leq n$ strips per group, and r strips per disk the equality $bk = nr$ holds. According to Theorem 5 in the paper there is a placement-ideal layout with parameters n, k, r , *if and only if* - *iff* $k|r$ and $(n-1)|k(r-1)$ and one of the following holds: (1) $k = n$, (2) $k = n - 1$, (3) $k = 2$, (4) $k = 3$ and $n = 5$ (5) $k = 4$ and $n = 7$.

The *Permutation Development Data Layout* - *PDDL* is a mapping function described in Schwarz et al. 1999 [190]. It has excellent properties and good performance both in light and heavy loads like the PRIME Alvarez et al. 1998 [5] and the DATUM data layout Alvarez et al. 1997 [4], respectively.

In what follow we discuss four other CRAID organizations.

9.1 Balanced Incomplete Block Design - BIBD

The *Balanced Incomplete Block Design* - *BIBD* incurs a small cost for mapping PGs with balanced parities Holland et al. 1994 [84]. Four parameters for a declustering layout are given as

follows: $n \geq 2$ is the number of disks, $k \leq n$ is the PG size G , b is the number of PGs, the number of stripes (rows) per disk is r . An additional parameter L which is the number of PGs common to any pair of disks is specified in Ng and Mattson 1994 [151], Because of the following two equalities, only three out of five variables are free,

$$bk = nr \text{ and } r(k - 1) = L(n - 1).$$

For $N = 10$, $k = G = 4$, and $L = 2$, $r = 2 \times 9/3 = 6$, and $b = N \times r/G = 10 \times 6/4 = 15$. Figure 15 is a BIBD layout given in Ng and Mattson [151] extracted from Hall 1986 [78].

Each set of six consecutive stripes constitute a segment. The $r = 6$ strips in each column of the segment can be rebuilt by accessing three strips per PG for $G = k = 4$ or $r(k - 1) = 18$ strips.

The following disk accesses are required to reconstruct the six strips on failed Disk#3 specified as strip#(disk#1,disk#2,disk#3): 2(1,6,9), 4(1,2,4), 5(4,5,8), 7(2,7,10), 10(5,7,9), 14(6,8,10), Two strips are read from each one of surviving disks denoted by D#i.

D#1(2,4), D#4(7), D#4(4,5), D#5(5,10), D#6(2,14), D#7(7,10), D#8(5,14), D#9(2,10), D#10(7,14). The on-demand reconstruction load is balanced and there is a 3-fold increase in rebuild bandwidth.

One of the strips, say the first (or the last), in all PGs, may be set consistently to be the parity. Given $b = 15$ PGs and $N = 10$ disks there should be 1.5 parities per disk on the average. Inspection shows that five disks have one parity and another five two parities per segment. Ten rotations of segments balance parity loads with 15 parities in each column or an average of 1.5 parities per segment.

An example for BIBD parity placement for $N = 5$ and $G = 4$ is given in Holland et al. 1994 [84]. BIBD designs are not available for all N and G values, e.g., layouts for $N = 33$ with $G = 12$ do not exist, but designs with $G = 11$ and $G = 13$ can be used instead.

9.2 CRAID Implementation Based on Thorp Shuffle

The Thorp shuffle to implement CRAID is proposed in Merchant and Yu [145]. It is stated that unlike BIBD it can generate layouts for arbitrary N and G , but provided examples are restricted to $N/G = 2^i, 0 \leq i \leq 3$ with $G = 8$.

The Thorp shuffle cuts a deck of cards into two equal half decks A and B and then the following is repeated until no cards are left: “Pick deck A or B randomly and drop its bottom card and then drop the bottom card from the other half deck atop it” Thorp 1973 [226].

A shuffle-exchange network where the propagation through the network is determined by random variables was used for this purpose. With N disks and B strips per disk the overall time complexity of computing block addresses is $O(\log(B) + \log(N))$.

Disk #	1	2	3	4	5	6	7	8	9	10
Parity Groups	1	1	2	3	1	2	3	1	2	3
	2	4	4	4	5	6	7	5	6	7
	3	6	5	5	8	8	8	9	10	11
	4	7	7	6	10	9	9	12	12	12
	8	9	10	11	11	11	10	14	13	13
	12	13	14	15	13	14	15	15	15	14

Figure 15: BIBD data layout of a segment with $N = 10$ disks and PG size $G = k = 4$.

The Thorp shuffle method has the disadvantage of incurring high computational cost per block access Holland et al. 1994 [84], 14 μ s (microseconds) on an SGI computer,

https://en.wikipedia.org/wiki/Silicon_Graphics

but disk capacities which affect B have increased by orders of magnitude in the last quarter century, making the Thorp shuffle more costly to implement, In addition it seems sufficient load balancing can be attained by the following simpler methods.

9.3 Nearly Random Permutation - NRP

The *Nearly Random Permutation - NRP* in Fu et al. 2004 [61] incurs less mapping cost by permuting individual stripes (rows). This is different from the scheme in Section 9.2 given this name. To build the mapping consecutive PGs of size $G < N$ are placed consecutively in the matrix with N columns in as many rows as disk capacity allows, so that PG_i occupies strips $iG : iG + (G - 1)$. In the case of RAID5 (resp. RAID6) the P (resp. P and Q) parities are consistently placed as the first or last two strips in each PG.

According to this placement P parities appear on half of the disks as shown by “Initial allocation” in Figure 16. This imbalance is alleviated by randomizing strip placement, so that approximately the same number of parity blocks are allocated per disk. Load balance can be attained by rotating columns in segments of K rows defined below and placing parity blocks on odd numbered disks and use this layouts alternatively.

Algorithm 235 in Durstenfeld 1964 [49] for randomly permuting:

```

Consider an array  $A$  with  $N$  elements. Set  $n = N$ .
L: Pick a random number  $k$  between 1 and  $n$ .
If  $k \neq n$  then  $A_n \leftrightarrow A_k$ .
Set  $n = n - 1$  and go back to L if  $n < 2$ .

```

If $N \bmod(G) = 0$ then the random permutation is applied once and otherwise it is repeated at $K = \text{GCD}(N, G)$ rows. A permutation obtained using an easy to compute polynomial function $f(I)$ with $I = jK, j \geq 0$ is used as a seed. The same permutation is applied to stripes $jK, jK + 1, \dots, jK + (K - 1)$.

A pseudo-*Random Number Generator - RNG* yields a random permutation of $\{0, 1, \dots, N - 1\}$ as: $P_I = \{P_0, P_1, \dots, P_{N-1}\}$.

For example, consider an example $N = 10$ and $G = 4$ so that $K = \text{GCD}(10, 4) = 2$. The permutation

$$\mathbf{P} = \{0, 9, 7, 6, 2, 1, 5, 3, 4, 8\}$$

should be applied to two rows at a time in Figure 16 as show in Figure 17. This assures that a PG straddling two rows is mapped onto different disks, since initially all strips were on different disks (this is the case for $D_6, D_7, D_8, P_{6:8}$). Since data strips in a PG are assigned to different disks they can be accessed in parallel.

9.4 Shifted Parity Group Placement

When N is divisible by G or $N \bmod G = 0$ the following approach can be used to balance parity loads. For $N = 12, G = 4, L = \text{LCM}(N, G) = 12, p = L/G = 3$ PGS in each row. PGs in one row need be shifted $G - 1 = 3$ times in following rows.

Disk #	1	2	3	4	5	6	7	8	9	10
Initial allocation	D_1	D_2	D_3	$P_{1:3}$	D_4	D_5	D_6	$P_{4:6}$	D_7	D_8
allocation	D_9	$P_{7:9}$	D_{10}	D_{11}	D_{12}	$P_{10:12}$	D_{13}	D_{14}	D_{15}	$P_{13:15}$

Figure 16: The two rows show the preliminary allocation of strips before they are permuted using nearly random permutation method ($N = 10, G = 4, K = 2$).

Disk#	1	2	3	4	5	6	7	8	9	10
Final allocation	D_1	D_5	D_4	$P_{4:6}$	D_7	D_6	$P_{1:3}$	D_3	D_8	D_2
allocation	D_9	$P_{10:12}$	D_{12}	D_{14}	D_{15}	D_{13}	D_{11}	D_{10}	$P_{13:15}$	$P_{7:9}$

Figure 17: Permuted data blocks with nearly random permutation method ($N=10, G=4$). Only first two rows are shown.

If G is coprime with N , i.e., if $m = \text{GCD}(N, G) = 1$ then $iG \bmod N, i \geq 1$ generates all values $0 : N - 1$ in a periodic manner. For $N = 10, G = 3, L = 30, K = 3, p = 10, m = \text{GCD}(10, 3) = 1$, with 10 PGs in $K = 3$ rows. When parities are the first element of a PG they will appear in columns:

$$(1, 4, 7, 10, 3, 6, 9, 2, 5, 8).$$

For $N = 11, G = 4, L = 44, K = 4, m = 1, p = L/G = 11$ PGs in four rows. Shifting not required.

For $N = 15, G = 6, L = 30, K = 2, r = N \bmod G = 3, r - 1 = 2$ shifts to two rows. Figure 18 $N = 10, G = 4, L = 20, K = 2, r = N \bmod G = 2$, hence $r - 1 = 1$ shift applied to the second set of two rows.

10 Miscellaneous Topics Related to RAID5

The following topics are covered in this section. Distributed sparing in RAID5 in Subsection 10.1. Permanent Customer Model - PCM versus VSM in Subsection 10.2. Rebuild processing in Heterogeneous Disk Arrays - HDAs in Subsection 10.3. Optimal single disk rebuild in EVENODD, RDP, X-code in Subsection 10.4.

10.1 Distributed Sparing

Distributed sparing in RAID5 allocates sufficient spare areas on surviving disks to accommodate a single disk failure, i.e., to hold the data blocks of a failed disk as shown in Figure 1 in [203]. Empty strips are placed diagonally in parallel with parity strips at each disk. The advantage of

Disk #	1	2	3	4	5	6	7	8	9	10
Initial allocation	D_1	D_2	D_3	$P_{1:3}$	D_4	D_5	D_6	$P_{4:6}$	D_7	D_8
allocation	D_9	$P_{7:9}$	D_{10}	D_{11}	D_{12}	$P_{10:12}$	D_{13}	D_{14}	D_{15}	$P_{13:15}$
Shifted allocation)	D_{17}	D_{18}	$P_{17:18}$	D_{19}	D_{20}	D_{21}	$P_{19:21}$	D_{22}	D_{23}	D_{24}
allocation)	$P_{22:24}$	D_{25}	D_{26}	D_{27}	$P_{25:27}$	D_{28}	D_{29}	D_{30}	$P_{28:30}$	D_{16}

Figure 18: Shifted allocation of PGs with $N = 10, G = 4$.

distributed sparing with respect to dedicated sparing is all disks contribute to the processing of the workload in normal mode.

Rebuild reading time is slowed down because surviving disks in addition to being read are written reconstructed RUs. An iterative solution is used in [203] to equalize the rate at which RUs are being read and written to prevent the overflow of DAC' buffer capacity. Once a spare disk becomes available the contents of spare areas are copied onto it in copyback mode This mode is also required with restriping discussed in Section 26.2 to return the system to its original state.

10.2 Rebuild Processing Using the Permanent Customer Model

The *Permanent Customer Model - PCM* is proposed and analyzed in Boxma and Cohen 1991 [26] postulates a circulating permanent customer in an M/G/1 queue, which also serves external customers arriving according to a Poisson process. The permanent customer once completed rejoins a FCFS queue from which all customers are served. PCM is adopted in Merchant and Yu 1996 [145] to model rebuild processing. FCFS scheduling is not compatible with modern disk scheduling policies such as SATF.

VSM for rebuild processing outperforms PCM by attaining a lower response times for external disk requests, since it processes rebuild read requests at a lower priority than external requests.

In PCM rebuild reads spend more time in the FCFS queue and this reduces the probability of consecutive rebuild reads with respect to VSM. The probability that rebuild requests are intercepted by user requests arriving with rate λ with VSM and PCM rebuild are given in [60]:

$$P_{VSM} = 1 - \exp(-\lambda \bar{x}_{RU}), \quad P_{PCM} = 1 - \exp(-\lambda(\bar{x}_{RU} + W_{RU})),$$

x_{RU} is the time to read an RU and W_{RU} is the mean waiting time in the queue for rebuild reads in PCM. Since $\bar{x}_{RU} + W_{RU} > \bar{x}_{RU}$ implies $P_{VSM} < P_{PCM}$.

Both effects are verified via simulation in Fu et al. 2004a [60], where it is shown that VSM outperforms PCM on both measures.

Given that rebuild time with VSM takes less time than rebuild time with PCM fewer external requests are processed while rebuild processing is in progress.

10.3 Rebuild in Heterogeneous Disk Arrays

Heterogeneous Disk Array - HDA postulates a DAC, which can control multiple RAID levels, e.g., RAID1 and RAID5 sharing space in a disk array Thomasian and Xu 2011 [217]. The choice of RAID1 and RAID5 is based on their suitability, e.g., RAID1 for OLTP workloads and RAID5 for parallel access. Data allocation in early version of HDA used a two level allocation into areas dedicated to RAID1 and RAID5 which were also allocated dynamically as such storage was exhausted Thomasian et al. [205]. Another aspect of HDA is that VAs with higher dependability levels are allocated as RAID(4+k), $k > 1$ or with 3-way replication.

The study is concerned with alternative data allocation method of *Virtual Disks - VDs* constituting *Virtual Arrays - Array - VAs*. Two dimensional disk bandwidth and capacity per VD are considered in this study, but the latter is of less relevance for terabyte disks.

The VA width W is selected to limit the physical disk load per VD below a certain percentage of its bandwidth expressed in IOPS. Allocations are carried out in degraded mode, as if one of VDs of a VA has failed to avoid overload if a disk fails.

Given that disk layout is known there is no need to read unallocated disk areas. It is also possible to prioritize the rebuild processing of VAs used by more critical applications, e.g., OLTP for e-commerce generates more revenue than data mining.

URSA minor cluster based storage in Abd-el-Malek et al. 2005 [2] is described as follows: “No single encoding scheme or fault model is optimal for all data. A versatile storage system allows them to be matched to access patterns, reliability requirements, and cost goals on a per-data item basis. Ursa Minor is a cluster-based storage system that allows data-specific selection of, and on-line changes to, encoding schemes and fault models. Thus, different data types can share a scalable storage infrastructure and still enjoy specialized choices, rather than suffering from “one size fits all.” Experiments with Ursa Minor show performance benefits of 2–3x when using specialized choices as opposed to a single, more general, configuration. Experiments also show that a single cluster supporting multiple workloads simultaneously is much more efficient when the choices are specialized for each distribution rather than forced to use a “one size fits all” configuration. When using the specialized distributions, aggregate cluster throughput nearly doubled.”

The IBM *RAID Engine and Optimizer - REO* project described in Kenchamana-Hosekote et al. 2007 [115] has similarities to HDA in that it can accommodate different RAID levels on shared disks. REO works for any XOR-based erasure code and can systematically deduce a least cost reconstruction strategy for a read to lost pages Two plausible measures for an I/O plan are: (1) The number of distinct disk read and write commands needed to execute an I/O plan. (2) The number of cache pages input to and output from XOR operations in executing an I/O plan. Minimizing XOR leads to lower memory bandwidth usage.

10.4 Optimal Single Disk Rebuild in RAID6 Arrays

An optimal data recovery method was proposed in the context of RDP in Xiang et al. 2010 [241]. The method is optimal in the number of accessed pages and balancing disk loads, but erroneously assumes that that symbols are as large as strips. The method was extended to the EVENODD layout in Xiang et al. 2011 [242], whose implementations uses small symbol sizes like RDP as discussed in Section 4.1.

The method is applicable to X-code described in Subsection 4.2 since it applies coding at strip level size Xiang et al. 2014 [244]. A similar method to minimize page accesses was informally proposed in Thomasian and Xu 2011 [216].

The method should be evaluated in reducing computational cost for reconstruction because blocks would be reused in caches. More efficient recovery methods should be similarly applicable to Grid files in Section 5.1.

11 Evaluation of RAID5 Performance

With the advent of faster CPUs, the performance of applications with stringent response time requirements, such as OLTP, rely heavily on storage performance, which is especially a problem for disks. Potential storage accesses are obviated by caching, e.g., higher levels of B+ tree indices are held in main memory. Storage performance can be improved by utilizing larger caches and improved cache management policies. Further improvement is possible adopting improved data

organizations on disk and disk scheduling as discussed in Subsection 2.1 and more detail in Chapter 9 in Thomasian 2021 [224].

OLTP workloads generate accesses to small randomly placed blocks, which are costly since they incur high positioning time, as in the case of the TPC-C order-entry benchmark.

<https://www.tpc.org/tpcc/>

Disks have an onboard cache for fetching sectors preceding/following requested sectors on a track Jacob et al. 2008 [104]. The DAC provides a much larger cache for data from the RAID disks. Part of the DAC cache is NVRAM and duplexed NVRAM is as reliable as disk storage for logging according to Menon and Cortney 1993 [141], Logging for database recovery is discussed in Chapter 18 on Crash Recovery in Ramakrishnan and Gehrke [171]. This allows a fast-write capability and deferred destaging of dirty blocks. Dirty blocks can be overwritten several times before they are destaged to disk, thus reducing the disk load. Batch destaging allows disk scheduling to minimize disk utilization.

Results obtained by investigating I/O traces by Treiber and Menon 1995 [227] were incorporated into the analysis in Thomasian and Menon 1997 [203], e.g., occurrences of two blocks a short distance apart on a track, treated as one disk access. Note similarity to proximal I/O to increase disk bandwidth in Schindler et al. 2011 [185]. Large database or filesystem buffers are provided in the main memory of computers running such applications. Disk cache miss ratio analysis and design considerations are discussed in Smith 1985 [193].

Self-similarity was first observed in nature by B. Mandelbrot.

<https://en.wikipedia.org/wiki/Self-similarity>

It is discussed in detail by Peitgen et al. 2004 [161]. The fractal structure of cache references model by a statistically self-similar underlying process, which is transient in nature is discussed in McNutt 2002 [140].

IBM z16 mainframe supports up to 40 terabytes (TB=10¹² bytes) main memory.

https://www.ibm.com/common/ssi/ShowDoc.wss?docURL=/common/ssi/rep_sm/1/897/ENUS3931-_h01/index.html

The very large capacity of caches requires very long traces making trace-driven simulation difficult if not impossible. Online measurement of page miss ratios versus memory size using hardware and a software is explored in Zhou et al. 2004 [250].

Two examples of main memory databases are IMS FastPath and Oracle's TimesTen Lahiri et al. 2013 [123]. The sizes of largest databases at this time are as follows.

<https://www.comparebusinessproducts.com/fyi/10-largest-databases-in-the-world>

12 Analysis of RAID5 Performance*

An M/G/1 queueing model is adopted in this section with Poisson arrivals with exponential interarrival times with mean $\bar{t} = 1/\lambda$ (**M**) standing for Markovian) and generally distributed disk service times (**G**) with their i^{th} moment denoted by \bar{x}^i .

12.1 Components of Disk Service Time w/o and with ZBR*

The CPU checks if a referenced block by a program is cached in the database or file buffer in main memory. If not it issues an I/O request and the DAC checks if it caches the block. If not the requests is past on to the disk where it is sought on the onboard disk cache before accessing

the disk taking into account faulty reallocated sectors Ma et al. 2015 [133]. Disk are discussed in Part III of Jacob et al. 2008 [104].

Disk service time is the sum of seek (s), latency (ℓ), and transfer time (t), Given the mean and variance of service time components we have the following mean and variance for disk service time:

$$\bar{x}_{disk} = \bar{x}_s + \bar{x}_\ell + \bar{x}_t, \quad \sigma_{disk}^2 = \sigma_s^2 + \sigma_\ell^2 + \sigma_t^2. \quad (6)$$

The latter equality requires the independence of random variables, especially latency and transfer time which is true for accesses to small blocks. The second moment of disk service time required in the analysis is given as follows:

$$\overline{x^2}_{disk} = \sigma_{disk}^2 + (\bar{x}_{disk})^2.$$

Seagate Cheetah 15k.5 model ST3146855FC parameters extracted in 2007 at CMU's *Parallel Data Laboratory - PDL* are given as follows:

<https://www.pdl.cmu.edu/DiskSim/diskspecs.shtml>

146 GB, maximum logical block number $b=286749487$ (number of 512 B sectors), $c=72,170$ cylinders, number of surfaces 4, 15015 RPM, $h = 4$ heads, The disk rotation time for 7200 RPM disks is $T_{rot} \approx 60,000/RPM = 8.33$ ms. The mean number of sectors per track is: $b/(c \times h) \approx 993$, so that the transfer time for 4 KB blocks with 8 sectors is negligible.

12.2 Seek Distance Distribution without and with ZBR*

Most analytic studies make the false assumption that disk are fully loaded, which is not true in practice. Before striping in RAID was introduced it was observed in a 1970s study that disk arms rarely move, which might have been the case for reading successive blocks of a file in batch processing. The probability of not moving the disk arm is to set $0 \leq p \leq 1$ and with probability $1 - p$ the remaining disk cylinders are accessed uniformly. With these two assumptions the seek distance is given in Lavenberg 1983 [124] by Eq. 7

$$P_D[d] = \begin{cases} p, & \text{for } d = 0, \\ (1 - p) \frac{2(C-d)}{C(C-1)}, & \text{for } 1 \leq d \leq C - 1 \end{cases} \quad (7)$$

There are $2(C - d)$ ways to move $1 \leq d \leq C - 1$ cylinders, which are normalized by $\sum_{d=1}^{C-1} 2(C - d) = C(C - 1)$. For uniform distribution across all cylinders:

$$p = P_D[0] = \frac{1}{C} \text{ and } P_D[d] = \frac{2(C-d)}{C^2}, 1 \leq d \leq C - 1. \quad (8)$$

The seek time characteristic $t_{seek}(d)$ is the seek time versus seek distance in cylinders or tracks (d). Curve-fitting to experimental results yields equations of the following forms Hennessey and Patterson 2019 [83]:

$$t_{seek}(d) = a + b\sqrt{d-1}, \quad 1 \leq d \leq C - 1$$

$$t_{seek}(d) = a + b\sqrt{d-1} + c(d-1) \quad 1 \leq d \leq C-1$$

The average seek time can be obtained by plugging in the average seek distance $C/3$ for uniform accesses, but it is argued in Thomasian and Liu 2005 [206]) that a more accurate method to obtain seek time:

$$\bar{x}_s^i = \sum_{d=1}^{C-1} P_D(d) t_{seek}^i(d), \quad \sigma_s^2 = \bar{x}_s^2 - (\bar{x}_s)^2$$

The analysis in Merchant and Yu 1996 [145] postulates a seek-time formula of the form: $t_{seek}(f) = a + b\sqrt{f}$, where f is the fraction of traversed cylinders. It is implicitly assumed that the seek distance is uniform $0 \leq f \leq 1$, hence $\bar{f} = 1/2$. This is not true according to Eq. (8) when disk accesses are uniform over all disk cylinders, since $P_D[0] = 1/C$ and drops from $P_D[1] \approx 2/C$ to $P_D[d = C-1] = 2/C^2$ and the mean seek distance is then $\bar{d} \approx C/3$. This issue is discussed in Thomasian and Li 2005 [206], in pointing out the same error in Varki et al. 2004 [230].

The analysis of disk seek times for disks with ZBR should take into account the variability of track capacities as in Thomasian et al. 2007 [212]. The number of sectors on cylinder c is $s_c, 1 \leq c \leq C$. With the assumption that disk is fully loaded and its sectors are uniformly accessed the probability of accessing cylinder c is proportional to the number of sectors it holds:

$$P_c = s_c/C_d \text{ where the disk capacity is } C_d = \sum_{c=1}^C s_c.$$

Starting with the probability of seek distance d starting at cylinder c , requires $C > d$ and $c + d < C$. This requires unconditioning on c :

$$P_D(d|c) = P_c(c+d) + P_c(c-d), \quad P_D(d) = \sum_{c=1}^C P_D(d|c)P_c$$

Rebuild analysis requires the *Laplace-Stieltjes Transform - LST* of seek time and transfer time. Provided that the *Rebuild Unit - RU* is a track after a seek is completed there is no latency due to *Zero Latency Access - ZLA*, which allows track reading to start at the first encountered sector. Given that transfer time equals disk rotation time, the LST is: $\mathcal{L}_t^*(s) = T_R/s$.

Latencies to access small blocks are uniformly distributed over tracks. The LST and i^{th} moment of latency which is uniformly distributed over $(0, T_R)$ are given as:

$$\mathcal{L}_\ell^*(s) = (1 - e^{-sT_R})/(sT_R), \quad \bar{x}_\ell^i \approx T_R^i/(i+1).$$

Given that the transfer time of j sectors from cylinder c is $x_t(j) = jT_{rot}/s_c$, it follows that the mean over all cylinders is:

$$\bar{x}_t^i(j) = \sum_{c=1}^C x_t^i(j)P_c, \quad \sigma_t^2 = \bar{x}_t^2 - (\bar{x}_t)^2.$$

$j = 8$ sectors is assumed in the discussion.

Shingled Magnetic Recording - SMR

SMR is a technique for writing data to HDDs whereby the data tracks partially overlap to increase the areal density radially and hence increase disk capacity. While ZBR increases recording capacity linearly, while SMR increases this density radially.

https://en.wikipedia.org/wiki/Shingled_magnetic_recording

The emergence of SMR has been attributed to slowdown in disk capacity after 2010 after fast growth in the period 2000-2010. An influential paper on disk developments in earlier disk storage technology is Gray and Shenoy 2000 [74].

Design issues in SMR are presented in Amer et al. 2010 [6]. Theoretical justifications for SMR are given in Sanchez 2007 [181], which in Section 1.2 introduces the trilemma: Thermal stability, Writeability, and Media *Signal to Noise Ratio* - *SNR*. A technical description of SMR drives is given in Feldman and Gibson 2013 [53].

The performance of SMR drive is less predictable in that clean drives can be written quickly, but if the drive has too many writes queued, or has insufficient idle time to reorganize or discard overwritten data, then write speeds can be significantly lower than the usual disk bandwidth, e.g., 50-150 MB/s. Because of their access time variability SMR disks should be excluded from RAID5 disk arrays.

https://en.wikipedia.org/wiki/Hard_disk_drive_performance_characteristics

13 RAID5 Performance in Normal Mode*

Let f_r and $f_w = 1 - f_r$ denote the fraction of logical read and write requests, respectively. Each read request results in a *Single Read* - *SR* access if the data is not cached and each logical write may require two SR and two *Single Write* - *SW* accesses:

$$f_{SR} = (f_r + 2f_w)/(3f_r + 2f_w), \quad f_{SW} = 1 - f_{SR}.$$

The moments of disk service time are given as follow:

$$\bar{x}_{disk}^i = f_{SR}\bar{x}_{SR}^i + f_{SW}\bar{x}_{SW}^i. \quad (9)$$

Given that the arrival rate to the RAID5 disk array is Λ . then RAID striping results in uniform accesses to $N + 1$ disks. Due to striping the arrival rate to the $N + 1$ disks are balanced: $\lambda = \Lambda/(N + 1)$, so that the disk utilization factor is:

$$\rho = \lambda\bar{x}_{SR} + 2f_w(\bar{x}_{SR} + \bar{x}_{SW}).$$

Given the mean and variance of disk service time with FCFS scheduling the coefficient of variation of disk service time is: $c_X^2 = \sigma_{disk}^2/(\bar{x}_{disk})^2$. The mean and variance of waiting time in M/G/1 queues is given by the Pollaczek-Khinchine formula in Kleinrock 1975 [118]:

$$W = \frac{\lambda\bar{x}_{disk}^2}{2(1 - \rho)} = \frac{\rho\bar{x}(1 + c_X^2)}{2(1 - \rho)}, \quad \bar{W}^2 = 2W^2 + \frac{\lambda\bar{x}_{disk}^3}{3(1 - \rho)}. \quad (10)$$

The prioritized processing of SR requests on behalf of logical reads is only affected by disk utilization due to other logical read requests. The fraction of such requests is $f'_{SR} = f_r / (f_r + 4f_w)$ and moments of x_{disk} should be recomputed with f'_{DR} . The waiting of SR requests with nonpreemptive priorities is given in Kleinrock 1976 [119].

$$W_{pr} = \frac{\lambda \bar{x}_{disk}^2}{2(1 - \rho_{SR})} \text{ with } \rho_{SR} = f'_r \lambda \bar{x}_{SR}. \quad (11)$$

The read response without and with priorities is $R_{SR} = \bar{x}_{SR} + W$ and $R_{SR} = \bar{x}_{SR} + W_{pr}$.

A write is considered completed when both the data and parity blocks are written to disk, which is an instance of F/J processing discussed in Section 14 given by Eq. (21) in Section 14. Due to the fast write capability write response times are of little interest.

Since for the FCFS policy the waiting time is independent from service time then: $E[\tilde{W}_{SR} \tilde{x}_{SR}] = \bar{W}_{SR} \times \bar{x}_{SR}$ and the second moment of SR requests is:

$$\overline{R^2}_{SR} = \overline{W^2}_{SR} + \overline{x^2}_{SR} + 2W\bar{x}_{SR}. \quad (12)$$

$\sigma^2_{SR} = \overline{R^2}_{SR} - (R_{SR})^2$ is used in the Fork/Join analysis in Section 14.

14 Methods to Obtain Response Times for Fork/Join Requests*

In the case of a RAID5 with $N + 1$ disks an N -way (resp. $N - 1$ -way) F/J request is required to process read (resp. write) requests involving failed disks in degraded mode of operation. The expected mean of n -way F/J requests with Poisson arrivals and general service times is not known, but can be approximated with the maximum of n -way requests as follows: $R_n^{F/J}(\rho) \approx R_n^{max}(\rho)$ as discussed below.

Before rebuild processing starts F/J requests on behalf of read requests constitute one-half of read requests processed by surviving disks, but this fraction gets smaller as rebuild progresses due to “read redirection” Muntz and Lui 1990 [147]. Read redirection simply reads reconstructed data from the spare disk, but the term is a misnomer since redirection is also used for write requests to a failed disk when d_{old} is already reconstructed on a spare to compute the parity block. Otherwise an F/J request to surviving disks in the parity group. When p_{old} is not reconstructed yet there is no need update it by computing and writing p_{new} , since this is done more efficiently later as part of rebuild.

Given the response time distribution in M/M/1 queues $R(\rho)$, which was given by Eq. (1) the only exact mean response time known is for 2-way F/J requests is given by Flatto and Hahn 1984 [55].

$$R_2^{F/J}(\rho) = \left[H_2 - \frac{\rho}{8} \right] R(\rho) = \frac{12 - \rho}{8} R(\rho), \text{ where the Harmonic sum is: } H_K \stackrel{\text{def}}{=} \sum_{k=1}^K \frac{1}{k}. \quad (13)$$

Note that $R_2^{F/J}(0) = R_2^{max}(0) = \frac{H_2}{\mu}$. The following approximate equation for $2 \leq n \leq 32$ -way M/M/1 F/J queueing systems is derived in Nelson and Tantawi 1988 [149].

$$R_n^{F/J}(\rho) = \left[\frac{H_n}{H_2} + \left(1 - \frac{H_n}{H_2}\right) \alpha(\rho) \right] R_2^{F/J}(\rho), \quad (14)$$

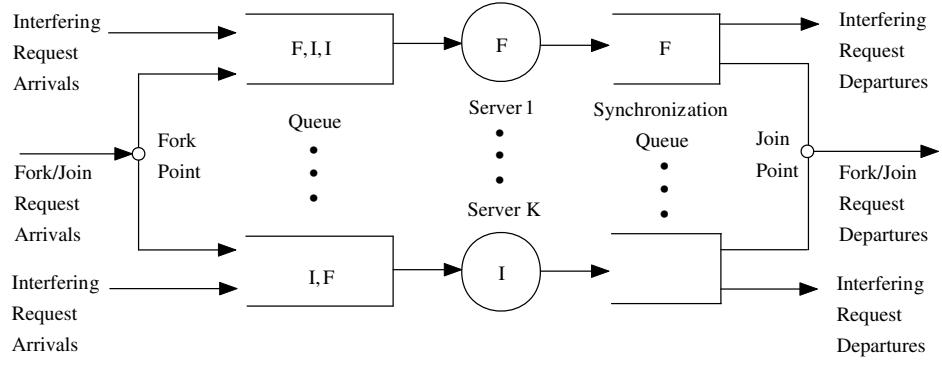


Figure 19: Fork/join processing with interfering requests processing

Curve-fitting to simulation results yielded $\alpha(\rho) \approx (4/11)\rho$.

This equation was used in Menon 1994 [142] for estimating F/J response times in degraded mode, which is not the case in this study because of interfering requests.

The processing of F/J requests with interfering requests is shown in Figure 19. Simulation results for the mean F/J response time versus server utilization by varying the fraction of F/J requests, while the total is kept fixed for different service time distributions is given in Thomasian and Tantawi 1994 [201]. The graphs show that as the fraction of F/J requests decreases with respect to interfering requests, their mean response times increases and tends to the expected value of the maximum.

$$R_n^{F/J} \approx R_n^{max}.$$

An approximation for the expected value of the maximum of n i.i.d. random variables is given as a function of the mean μ_X and standard deviation σ_X in order statistics, see e.g., David and Nagaraja 2003 [40]:

$$\bar{X}_n^{max} \approx \mu_X + \sigma_X G(n). \quad (15)$$

$G(n) = H_n - 1$ and $\sigma_X = \mu_X$ for the exponential distribution: $\bar{X}_n^{max} = \mu_X H_n$, which is also given by Eq. (17).

Eq. (16) in Thomasian and Tantawi 1994 [201] was motivated by Eq. (15):

$$R_n^{F/J}(\rho) = R(\rho) + F_n \sigma_R(\rho) \alpha_n(\rho), \quad (16)$$

where $R(\rho)$ and $\sigma_R(\rho)$ are the mean and standard deviation of response time at utilization factor ρ . In a limited study surface-fitting to simulation results was used to obtain $\alpha_n(\rho)$ for a few distributions.

The *Probability Distribution Function - PDF* of the maximum of n random variables with PDF $F_Y(y)$ is also the n^{th} order statistic Trivedi 2002 [228]:

$$F_{Y_n^{max}}(y) = [F_Y(y)]^n.$$

Given that response times in an M/M/1 queueing system are exponentially distributed applying the formula for the maximum of n exponentials in Trivedi [228]:

$$R_n^{max}(\rho) = H_n R(\rho). \quad (17)$$

It is shown in Nelson and Tantawi 1988 [149] that $R_n^{max}(\rho)$ is an upper bound to $R_n^{F/J}(\rho)$ for the exponential distribution. This effect is observed via simulation in Thomasian and Tantawi 1994 [201] for other distributions and that $R_n^{max}(\rho)$ is a good approximation to $R_n^{F/J}(\rho)$ when F/J requests constitute a small fraction of processed requests. This is the case for RAID5 in degraded mode as rebuild progresses and most requests to the failed disk are satisfied by redirection.

A simple method to obtain the maximum of n i.i.d. random variables is to approximate it with the two-parameter *Extreme Value Distribution - EVD* Johnson et al. 1995 [110], Kotz and Nadarajah 2000 [122].

$$F_Y(y) = P(Y < y) = \exp(-e^{-\frac{y-a}{b}}), \quad \bar{Y} = a + \gamma b, \quad \sigma_Y^2 = \frac{\pi^2 b^2}{6},$$

where $\gamma = 0.577721$ is the Euler constant. Matching the first two moments: $\bar{Y} = R(\rho)$ and $\sigma_Y = \sigma_R$: we obtain a and b given the first two moments of Y :

$$b = \sqrt{\frac{6}{\pi}} \sigma_Y \text{ and } a = \bar{Y} - \gamma b.$$

The maximum of n random variables with EVD has a simple form:

$$\bar{Y}_n^{max} = (a + \gamma b) + b \ln(n) = \bar{Y} + \frac{\sqrt{6}}{\pi} \sigma_Y. \quad (18)$$

It follows from simulation results in Thomasian et al. 2007 [212] that a better approximation to Y_n^{max} is obtained if the second summation term is divided by 1.27.

The coefficient of variation of response times of M/G/1 queues for accesses to small randomly placed disk blocks for given disk characteristics with $c_R^2 < 1$ observed in Thomasian and Menon 1997 [203].

$$c_R^2(\rho) = \frac{\sigma_R^2(\rho)}{R^2(\rho)} = \frac{c_X^2 + \frac{\rho s_X}{3(1-\rho)} + \frac{\rho(1+c_X^2)}{4(1-\rho)^2}}{1 + \frac{\rho(1+c_X^2)}{1-\rho} + \frac{\rho(1+c_X^2)}{4(1-\rho)^2}}, \quad (19)$$

where $s_X = \bar{x}_{SR}^3 / (\bar{X}_{SR})^3$. Where $c_R = c_X$ for $\rho = 0$ and that as $\rho \rightarrow 1$ $c_R \rightarrow 1$, i.e., an exponential distribution, hence $c_R < 1$ for $C_X < 1$.

Approximating the response time distribution with with a distribution, which is an exponential in form has the advantage that its maximum can be computed easily by integration. The number of stages in the Erlang distribution is: $k = \lceil 1/c^2 \rceil$ and the mean delay per stage is $1/\mu = R(\rho)/k$ $R_n^{max}(\rho)$ for an n -way k -stage Erlang distribution is then:

$$R_n^{max}(\rho) = \int_0^\infty \left[1 - \prod_{i=1}^n \left(1 - e^{-\mu_i t} \sum_{j=0}^{k_i-1} \frac{(\mu_i t)^j}{j!} \right) \right] dt. \quad (20)$$

Provided disks have an XOR capability updating parities results in a 2-way F/J request with unequal service times: d_{new} and the block address is sent to the disk and after d_{old} is read d_{diff} is computed and d_{new} overwrites d_{old} after a disk rotation. d_{diff} and the address of P_{old} are then sent via the DAC to the parity disk where it is XORed with p_{old} to compute P_{new} , which overwrites p_{old} after one disk rotation. The mean write response time is the maximum of data and parity writes.

$$R_2^{max}(\rho) = \sum_{i=1}^2 R_i(\rho) - \sum_{m=0}^{k_1-1} \sum_{n=0}^{k_2-1} \binom{m+n}{m} \frac{\mu_1^m \mu_2^n}{(\mu_1 + \mu_2)^{m+n+1}}, \quad (21)$$

where $\mu_1 = k_1/R_1(\rho)$ and $\mu_2 = k_2/R_2(\rho)$.

The more flexible Coxian distribution used by Chen and Towsley 1993 [34]. can be applied to any response time distribution regardless of the value of c_R .

15 Rebuild Processing in RAID5

The discussion in this section is based on HDDs where rebuild time is a problem, but while it is less of a problem in Flash SSDs as discussed in Section 29 RAID availability is critical for some applications such as OLTP and e-commerce. RAID with one disk failure is vulnerable to data loss if a second disk fails or an unreadable disk sector is encountered. The possibility of a second disk failure is high because of high rebuild time. RAID repair requires rebuilding the contents of a failed disk and this should be carried out concurrently with the processing of external requests due to the high cost of downtime.

<https://queue-it.com/blog/cost-of-downtime/>

Rebuild time is lengthened due to the interference of external disk requests and conversely response times are increased by rebuild reads.

Reconstructed data is written onto a spare disk in dedicated sparing or spare areas on N surviving disks in distributed sparing Thomasian and Menon 1994/1997 [200, 203]. Restriping which is overwriting check strips was proposed in Rao et al. 2011 [172]. In parity sparing two RAID5 arrays are merged and parity blocks on one RAID5 are used as spare areas Reddy et al. [175].

RAID5 rebuild time is investigated via simulation in Holland et al. 1994 [84], where it is concluded that *Disk-Oriented Rebuild - DOR* is superior to *Stripe-Oriented Rebuild - SOR*, which proceeds by reading disk strips one stripe at a time. SOR introduces unnecessary synchronization delays at the cost of reducing buffer requirements with respect to DOR, where *Rebuild Units - RUs* are read from disks independently when the disk is idle.

Before the introduction of ZBR the RU size was set to be fixed size tracks. Fixed RU sizes can also be adopted with ZBRs. RUs are read into the DAC cache where corresponding RUs are XORed to produce successive RUs on the failed disk. The analysis is complicated by the fact disks continue processing external disk requests, which interfere with rebuild reads. Reading of successive RUs on surviving disks starts when the disk is idle.

With ZBR rather than *Constant Angular Velocity - CAV* disks a higher data transfer rate is achieved at outer disk tracks. With ZBR the RAID stripe unit (strip) size can be varied across tracks and then RU sizes could be set to be a fraction or multiple of strip sizes.

Rebuild time decreases with increased RU size due to the fact that fewer seeks are incurred in rebuild processing, but large RU sizes will result in an unacceptable increase in disk response

times. Seek times can be reduced by utilizing several anchor points to reduce seek distances from the point where the last external requests was served Holland et al. 1994 [84]. Seek affinity can be exploited in copying the contents of a failing disk or the surviving mirrored disk where the other disk has failed.

While RAID5 during rebuild is vulnerable to data loss due to additional disk failures, most rebuild failures are due to *Latent Sector Errors - LSEs* Dholakia et al. 2008 [46]. A queuing model to estimate rebuild time in RAID5 with HDDs is discussed in the next section.

16 Vacationing Server Model for Analyzing Rebuild Processing*

The *Vacationing Server Model - VSM* with multiple vacations with two types based on the analysis in Doshi 1985 [48], Takagi 1991 [196] was adopted in Thomasian and Menon 1994, 1997 [200, 203] to analyze rebuild processing. The analysis yields the increased response time of external disk requests due to rebuild processing and the effect of external disk requests on expanding rebuild processing time. The accuracy of the analyses was verified using a random-number driven simulations in aforementioned studies.

VSM starts reading successive *Rebuild Units - RUs* after the processing of external disk requests is completed, or a busy period ends using queuing theory terminology. Rebuild reads are resumed at the point where the last read was halted as there was an external disk requests.

The initial RU read request takes longer, since it involves a seek and latency (estimated in Section 18) as shown in Figure 20). The reading of succeeding RUs takes less time, since a seek is not required, e.g., a disk rotation if the RU size is a track.

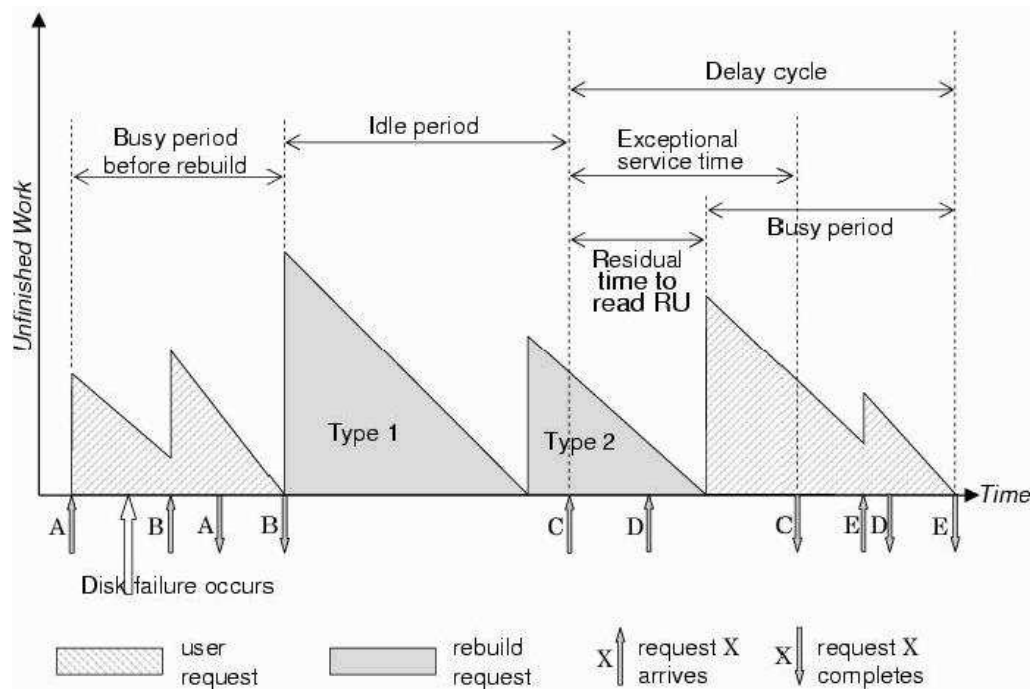


Figure 20: Key VSM parameters associated with rebuild processing.

The delay encountered by an external request requests with VSM follows from the fact that

Poisson Arrivals See Time Averages - PASTA Wolff 1982 [237]: The mean waiting time for external disk requests is the sum of three delays:

- (1) the mean waiting time in the queue, which is a product of mean queue size (\bar{N}_q) and mean service time (\bar{x}).
- (2) if the server is busy with probability ρ in which case there is an additional delay given by the mean residual service time ($\bar{x}_r = \bar{x}^2 / (2\bar{x})$ Kleinrock 1975 [118]).
- (3) the system is idle with probability $1 - \rho$, in which case the delay is the mean residual vacation (RU reading) time ($\bar{v}_r = \bar{v}^2 / (2\bar{v})$, where the \bar{v}^i is the i^{th} moment of vacation time).

$$W = \bar{N}_q \bar{x} + \rho \bar{x}_r + (1 - \rho) \bar{v}_r \text{ due to Little's result: } \bar{N}_q = \lambda W, \quad \rho = \lambda \bar{x}$$

Simplifying the above equation using the two substitutions yields:

$$W_{VSM} = W_{M/G/1} + \bar{v}_r = \frac{\lambda \bar{x}^2}{2(1 - \rho)} + \bar{v}_r. \quad (22)$$

An analysis of VSM with multiple vacations of two types is repeated in Section 17.

There is little variation in the completion time of disk rebuild reading times (see e.g., Figure 4 in Thomasian and Menon 1997 [203]). The spare disk is not a bottleneck unless the system is clustered RAID, which is discussed in Section 9, so that rebuild time can be approximated with rebuild read time.

Assuming that the RU is a track, the number of disk tracks: N_{track} and the mean number of tracks read per cycle: \bar{n}_{track} , where the cycle time (T_{cycle}) is defined and below by Eq. (26).

$$T_{rebuild}(\rho) = \frac{N_{track}}{\bar{n}_{track}} \times T_{cycle}. \quad (23)$$

The M/G/1 queue alternates between busy periods with mean \bar{g} during which external disk requests are served and idle periods given by mean interarrival time ($1/\lambda$) during which rebuild reads are processed, although the the processing of the first external request is delayed until a rebuild request is completed, unless preemption is allowed as discussed in Thomasian 2005b [207]. The utilization factor ρ is the fraction of time the server is busy, which can be expressed as follows:

$$\rho = \frac{\bar{g}}{\bar{g} + 1/\lambda} \implies \bar{g} = \frac{\bar{x}_{disk}}{1 - \rho}. \quad (24)$$

The delay cycle is different from a busy period in that it starts with a special request whose mean is the sum of mean residual rebuild time (\bar{v}_r) and \bar{x}_{disk} as shown in Fig. 20. The mean duration of the delay cycle using the intuitive argument expressed by Eq. (24) is then Thomasian 2018 [223]:

$$\rho = \frac{\bar{T}_{dc}(\rho) - \bar{v}_r}{\bar{T}_{dc}(\rho) + 1/\lambda} \implies \bar{T}_{dc}(\rho) = \frac{\bar{x}_{disk} + \bar{v}_r}{1 - \rho}. \quad (25)$$

The cycle time is defined as the time between the start of successive busy periods and is given by Eq. (26):

$$\bar{T}_{ct}(\rho) = \bar{T}_{dc}(\rho) + \frac{1}{\lambda}. \quad (26)$$

Given their LSTs of busy period and delay cycle Kleinrock 1975 and 1976 [118, 119] leads to their moments. The variances obtained in this manner can be used to obtain a better estimate of rebuild time as given by Eq. (15)

17 M/G/1 VSM Analysis of Multiple Vacations with Two Types*

The analysis in this section is based on Doshi 1985 [48], which is summarized in Takagi 1991 [196] and was adopted in Thomasian 1994/1997 [200, 203]. The analysis assumes that the RU size is a track.

The first RU/track read at the start of an idle period requires a seek followed by the reading of a track, while successive rebuild reads just take a disk rotation, as shown in Figure 20. Due to ZLA reading of a track starts with the first encountered sector, i.e., the rotational latency is negligible. Track and cylinders skew in reading successive tracks is negligible Jacob et al. [104].

17.1 The Laplace Stieltjes Transform for Seek Time*

LSTs are discussed in Appendix I in Kleinrock 1975 [118] and Appendix D in Trivedi 2002 [228]. To obtain the LST of seek time required for type 1 vacations we approximate the distribution in Eq. (7) by a continuous function, whose *probability density function - pdf* is:

$$f_X(x) = p\delta(x) + (1-p)\frac{2(C-x)}{C(C-2)}, \quad (27)$$

where $\delta(x)$ is the unit impulse at $x = 0$. $(C-2)$ is used instead of $(C-1)$ in the denominator, so that $\int_{x=1}^{C-1} \frac{2(C-x)}{C(C-2)} dx = 1$.

Motivated by Abate et al. 1968 [1] to derive the LST of seek time by first using a piecewise linear approximation to the seek time characteristic: seek time T_k versus seek distance C_k , where $C_1 = 1$ and $C_{K+1} = C - 1$.

$$t(x) = \alpha_k x - \beta_k \quad C_k \leq x \leq C_{k+1}.$$

$$\alpha_k = \frac{C_{k+1} - C_k}{T_{k+1} - T_k} \text{ and } \beta_k = \alpha_k T_k - C_k.$$

Given that x denotes the number of moved tracks:

$$x = \sum_{k=1}^K (\alpha_k t - \beta_k) [u(t - C_k) - u(t - C_{k+1})], \quad (28)$$

where $u(x)$ is the unit step function Kleinrock 1975 [118].

$$u(x) = \begin{cases} 1 & \text{for } x \geq 0 \\ 0 & \text{for } x < 0. \end{cases}$$

The LST of seek time using Eq. (27) and Eq. (28) is, but $p = 1/C$ was used in the study:

$$\mathcal{L}_s^*(s) = \frac{p}{s} + \frac{2(1-p)}{C(C-2)} \sum_{k=1}^K \alpha_k (C + \beta_k) \frac{e^{-sT_k} - e^{-sT_{k+1}}}{s} \quad (29)$$

$$- \alpha_k^2 \left(\frac{T_k e^{-sT_k} - T_{k+1} e^{-sT_{k+1}}}{s} - \frac{e^{-sT_k} - e^{-sT_{k+1}}}{s^2} \right)$$

The LST of disk service time according to Eq. (refeq:diskservice) is the product of the LSTs of its components:

$$\mathcal{L}_{disk}^*(s) = \mathcal{L}_s^*(s) \times \mathcal{L}_\ell^*(s) \times \mathcal{L}_t(s).$$

The moments of disk service time can be obtained by taking the derivatives of \mathcal{L}_{disk}^* , such as Eq. (34).

Reading of RUs is modeled as two vacation types: Type 1 vacations start once the disk is idle and require a seek to access the next RU to be read. Type 2 vacations are reads of consecutive RUs until an external request arrives.

The PDFs of two vacation types are denoted by $V_i(t)$, $i = 1, 2$. In the case of Poisson arrivals the probability of no arrival (resp. an arrival) is $e^{-\lambda t}$ (resp. $1 - e^{-\lambda t}$) in time interval $(0, t)$. Let p_i denote the probability that a request arrives during the i^{th} vacation. Unconditioning on $V_i(t)$

$$p_i = \left[1 - \int_0^\infty e^{-\lambda t} dV_i(t) \right] \prod_{j=1}^{i-1} \int_0^\infty e^{-\lambda t} dV_j(t) = [1 - V_i^*(\lambda)] \prod_{j=1}^{i-1} V_j^*(\lambda). \quad (30)$$

where $V_j^*(\cdot)$ is the LST of the j^{th} vacation time. The mean number of tracks read per idle period is:

$$\bar{n}_{track} = \bar{J} = \sum_{j=1}^{\infty} j p_j = 1 + \frac{V_1^*(\lambda)}{1 - V_2^*(\lambda)} \quad (31)$$

The split seek-option skips track reading following a seek if there is an arrival during the rebuild seek Thomasian and Menon 1994 [200]. Preemption during the latency and even track transfer phases are studied via simulation in Thomasian 1995 [202]. While preemption results in an improvement in disk response times, rebuild time is elongated since more requests are processed and this results in an increased number of requests during rebuild processing (with increased response times). The cumulative sum of response times is an appropriate metric in comparing rebuild options.

The probability of an arrival during the first and i^{th} vacation is:

$$p_1 = 1 - V_1^*(\lambda) \quad p_i = [1 - V_2^*(\lambda)] V_1^*(\lambda) [V_2^*(\lambda)]^{i-2} \quad (32)$$

The probability that the i^{th} vacation occurs is $q_i = p_i / \bar{J}$, where \bar{J} was given by Eq. (31). The probability q_i , $i = 1, 2$ that an external arrival occurs during a type one or two vacation is:

$$q_1 = \frac{1}{1 + V_1^*(\lambda)/(1 - V_2^*(\lambda))}, \quad q_2 = 1 - q_1.$$

It follows that overall LST for vacations is:

$$V^*(\lambda) = \frac{(1 - V_2^*(\lambda))V_1^*(s) + V_1^*(\lambda)V_2^*(s)}{1 - V_2^*(\lambda) + V_1^*(\lambda)}. \quad (33)$$

Derivatives of the LST Eq. (33 set to zero yield the j^{th} moment of vacation/rebuild time:

$$\bar{v}^j = (-1)^j \frac{dV^j(\lambda)}{d\lambda} \Big|_{\lambda=0} = \sum_{i=1}^{\infty} q_j v_i^j = \frac{(1 - V_2^*(\lambda))\bar{v}_{1j} + V_1^*(\lambda)\bar{v}_{2j}}{1 - V_2^*(\lambda) + V_1^*(\lambda)}. \quad (34)$$

The mean residual vacation/rebuild time is the second moment divided by twice the mean, as noted earlier: $\bar{v}_r = \bar{v}^2 / (2\bar{v})$.

The variation in disk utilization due to redirection in computing $T_{rebuild}(\rho_i)$ is taken into account by computing rebuild processing time over k intervals. A read only workload to simplify the discussion results in the doubling of disk loads, but otherwise the load decrease as rebuild progresses are given by Eq. (2). The rate of rebuild processing accelerates as disk utilizations drop due to redirection.

$$T_{rebuild}(\rho) = \sum_{i=1}^k T_{rebuild}(\rho_i), \quad \rho_i = [2 - \frac{i}{k}] \rho. \quad (35)$$

RAID5 rebuild time at an initial disk utilization ρ can be approximated by Eq. (refeq:beta), where ρ is the disk utilization when rebuild starts with all read requests, which results in highest increased load in degraded mode.

$$T_{rebuild}(\rho) = \frac{T_{rebuild}(0)}{1 - \beta\rho}, \quad \text{where } \beta \approx 1.75. \quad (36)$$

18 An Alternate Method to Estimate Rebuild Time*

Memory bandwidth does not constitute a bottleneck in determining disk rebuild time, as shown in Section 5.2 of Dholakia et al. 2008 [46], so we only consider disk bandwidth. Rebuild time is estimates as the ratio of utilized disk capacity (U) and mean rebuild bandwidth: b_d is presented in this section.

With varying track circumference the number of sectors do not vary track to track. Zoning subdivides disk tracks into I bands with the same number of sectors, There are n_i tracks with c_i sectors per track in the i^{th} band.

The sector size in FBA disks used to be 512 bytes, but there was a transition to 4096 byte sectors circa 2010. It follows that the mean disk transfer rate is:

$$t_d = \sum_{i=1}^I n_i \times c_i \times s / T_{rot}.$$

Given that the RU size is s_{RU} the transfer time per RU is s_{RU}/t_d , but the first RU according to VSM requires a seek (\bar{x}_s) plus rotational latency estimated as follows. Let f denote the size

of RU as a fraction of the tracks size, then if the R/W head lands inside the RU then we need a full disk rotation to transfer an RU ($f \times T_{rot}$) and otherwise the cost is $(1 - f)^2 T_{rot}/2$, hence:

$$\bar{x}_\ell = (1 + f^2)T_{rot}/2$$

The following RU accesses incur a track or cylinder skew Jacob et al. 2008 [104].

The number of bytes transferred per cycle is the product of the number of RUs transferred (\bar{n}_{RU}) and RU size (s_{RU}). The cycle time is the sum of interarrival time ($1/\lambda$), the delay cycle for processing external disk requests given by Eq. (25),

$$\bar{T}_{dc} = \frac{\bar{x}_{disk} + \bar{v}_r}{1 - \rho}$$

Given $\bar{x}_{RU} = s_{RU}/t_d$ the mean transfer rate for RUs is:

$$b_d = \frac{\bar{n}_{RU} \times s_{RU}}{\bar{T}_{dc} + \bar{x}_{seek} + \bar{x}_\ell + \bar{n}_{RU} \times \bar{x}_{RU}} \quad (37)$$

An upper bound to rebuild time can be obtained by setting $\bar{n}_{RU} = 1$, which is also the assumption made in Dholakia et al. 2008 [46]. In fact the number of consecutively transferred RUs with no intervening seeks can be derived as follows.

$$p_n = (1 - e^{-\lambda x_{RU}})(e^{-\lambda x_{RU}})^{n-1}, n \geq 1 \text{ hence } \bar{n}_{RU} = (1 - e^{-\lambda s_{RU}})^{-1}$$

In the case of ZBR outer disk tracks have have higher capacities and a small fraction of disk tracks are utilized for critical data, since this allows shorter seeks or short strocking. With a fraction U of disk capacity: C_d utilized rebuild time is:

$$T_{rebuild} = UC_d/b_d. \quad (38)$$

Dholakia et al. 2008 [46] estimates b_d in Eq. (13) as follows:

$$b_d = s_{req}/(1/r_{io} + s_{req}/t_d),$$

where r_{io} is the request rate and s_{req} is the request size.

A major shortcoming of most studies is the assumption that disks are fully occupied and disk requests are uniformly distributed over all disk cylinders. The analysis of seek distances in Thomasian et al. 2007 [212] and outlined in Section 12.1 can be modified to take into account only accesses to outer disks. A mapping of files onto disk cylinders and their access rates can be used to obtain more accurate estimates of seek times given the seek time characteristic, but such studies are precluded by striping which scatters data.

19 RAID Reliability Analysis

RAID5 disk arrays with $N + 1$ disks continue their operation without data loss but in degraded mode with a single disk failure. Denoting disk reliability versus time (t) as $r(t)$ (with $r(0) = 1$) the reliability of RAID5 at time t with no repair:

$$R_{RAID5}(t) = r^{N+1}(t) + (N + 1)(1 - r(t))r^N(t) = (N + 1)r^{N-1}(t) - Nr^N(t)$$

Generally the reliability for RAID(4+k) with $N + k$ disks with no repair is:

$$R_{RAID(4+k)} = \sum_{i=0}^k \binom{N+k}{i} r^{N+k-i}(t) (1-r(t))^i. \quad (39)$$

Due to its mathematical tractability the time to disk failure in Gibson 1992 [65] is approximated by the negative exponential distribution: $r(t) = e^{-\delta t}$, where δ is the disk failure rate.² The Weibull distribution, see e.g., Trivedi 2002 [228]), is a better fit and was utilized in Elerath and Schindler 2014 [51].

RAID5 reliability analysis is given in Section 5.4.1 in [65].³ A similar analysis in the context of mirrored disks is given by Example 8.34 in [228], where a surviving disk is being copied into a spare.

In addition to the $N + 1$ disks in RAID5 a spare disk is available so that rebuild processing can be started right away after a disk failure. The disk *Mean Time to Failure - MTTF* = $1/\delta$ and the RAID5 *Mean Time to Repair - MTTR* = $1/\mu$. There will be data loss if a second disk fails before rebuild is completed. A much more common cause of rebuild processing is the stalling of rebuild processing due to LSEs as discussed in Section 20.

The evolution of the system is modeled by a *Continuous Time Markov Chain - CTMC*, see e.g., Kleinrock 1975 [118] and Trivedi 2002 [228]. The CTMC has three states $S_i, i = 0, 2$, where i is the number of disks failed disks. We have the following transitions:

$$S_0 \xrightarrow{(N+1)\delta} S_1, \quad S_0 \xleftarrow{\mu} S_1, \quad S_1 \xrightarrow{N\delta} S_2$$

The system evolution is described by the following set of linear *Ordinary Differential Equations - ODEs*,

$$\frac{dP_0(t)}{dt} = -(N+1)\delta P_0(t) + \mu P_1(t), \quad \frac{dP_1(t)}{dt} = -(\delta + \mu)P_1(t) - (N+1)\delta P_0(t), \quad \frac{dP_2(t)}{dt} = N\delta P_1(t).$$

The *Laplace Stieltjes Transforms - LSTs* $L^*(s) = \int_0^\infty P(t)e^{-st} dt$ for the DOEs are given by Eq. (40)

$$\begin{aligned} s\mathcal{L}_0^*(s) - P_0(0) &= -(N+1)\delta\mathcal{L}_0^*(s) + \mu\mathcal{L}_1^*(s), & P_0(0) &= 1. \\ s\mathcal{L}_1^*(s) - P_1(0) &= -(\delta + \mu)\mathcal{L}_1^*(s) + (N+1)\mathcal{L}_0^*(s) & P_1(0) &= 0. \\ s\mathcal{L}_2^*(s) - P_2(0) &= N\delta\mathcal{L}_1^*(s) & P_2(0) &= 0. \end{aligned} \quad (40)$$

Solving for $\mathcal{L}_2^*(s)$ leads to

$$\mathcal{L}_Y^*(s) = s\mathcal{L}_2^*(s) = \frac{2\delta^2}{s^2 + ((2N+1)\delta + \mu)s + 2N\delta^2} = \frac{2\delta^2}{\zeta - \eta} \left(\frac{1}{s + \zeta} - \frac{1}{s + \eta} \right)$$

The reliability is the sum of probabilities that the system is functional.

²We are using δ here since we are reserving λ as the request rate in queueing systems.

³Out of print, but also not available at <https://www2.eecs.berkeley.edu/Pubs/Dissertations/>

$$R(t) = P_0(t) + P_1(t) = 1 - P_2(t) \text{ so that } f_Y(t) = -\frac{dR(t)}{dt} = \frac{dP_2(t)}{dt}.$$

$$R(t) = \frac{\zeta e^{\eta t} - \eta e^{\zeta t}}{\zeta - \eta} \text{ where: } \zeta, \eta = \frac{1}{2}[-(2N+1)\delta + \mu \pm \sqrt{\delta^2 + \mu^2 + 2(2N+1)\delta\mu}]. \quad (41)$$

Using RAID5 reliability $R(t)$ given by Eq. (41) and using the equation to obtain the expected value we have:

$$\text{MTTDL}_{\text{RAID5}} = \int_{t=0}^{\infty} R(t)dt = \frac{1}{\zeta - \eta} \left[-\frac{\zeta}{\eta} + \frac{\eta}{\zeta} \right] = -\frac{\zeta + \eta}{\zeta\eta} = -\frac{1}{\zeta} - \frac{1}{\eta} \quad (42)$$

Substitutions leads to the following equation:

$$\text{MTTDL} = \frac{(2N+1)\delta + \mu}{N(N+1)\delta^2} \approx \frac{\mu}{N(N+1)\delta^2} = \frac{\text{MTTF}^2}{N(N+1)\text{MTTR}}. \quad (43)$$

A simple method to derive Eq. (43) is to multiply the number of times the normal state: S_0 and the degraded state: S_1 are visited, before there is a transition to the failed state: S_2 . Given that the probability of an unsuccessful rebuild is $p_f = N\delta/(N\delta + \mu)$, then the probability of k successful rebuilds is:

$$p_k = (1 - p_f)^{k-1} p_f, k \geq 1 \text{ with mean } \bar{k} = 1/p_f = 1 + \mu/(N\delta) \approx \frac{\text{MTTDL}}{N \times \text{MTTR}}.$$

Chen et al. 1994 [32] generalized the formula to RAID(4+k), $k = 1, 2$ with N disks in total and parity group size G

$$\text{MTTDL}_{\text{RAID5}} \approx \frac{\text{MTTF}^2}{N(G-1)\text{MTTR}}, \quad \text{MTTDL}_{\text{RAID6}} \approx \frac{\text{MTTF}^3}{N(G-1)(G-2)\text{MTTR}^2}. \quad (44)$$

Generalizing the formula and setting $N = G$ (one parity group) we have:

$$\text{MTTDL}_{\text{RAID}(4+k)} \approx \frac{\text{MTTF}^{k+1}(k-1)!}{n!\text{MTTR}^k} \quad (45)$$

Chen's formula assumes that the repair rate remains fixed regardless of the number of failed disks, so that one disk is repaired at a time. Given N disks and with k failed disks we have the transitions.

$$S_{N-i} \rightarrow S_{N-(i+1)} : (N-i)\delta \quad S_{N-(i+1)} \leftarrow S_{N-i} : \mu$$

With two failed disks in RAID6 corresponding strips in both disks are reconstructed together. A repair rate proportional to the number of disks is postulated in Angus 1988. and furthermore the number of failed disks is allowed to exceed $n - k$ in Angus 1988 [10].

$$S_{N-i} \rightarrow S_{N-(i+1)} : (N-i)\delta \quad S_{N-(i+1)} \leftarrow S_{N-i} : i\mu$$

Using the previous notation the Angus MTTDL formula, which was shown to be more accurate against simulation results is as follows:

n	k	MTTF	Simul	Chen	S/C	Angus	S/C
10	10	2000	1.988E29	2.000E2	0.94	1.988E2	0.944
10	9	2000	4.488E4	4.444E4	1.010	4.467E4	1.005
10	8	1500	9.446E6	4.688E6	2.105	9.438E6	1.001
10	7	500	7.786E7	1.240E7	6.278	7.591E7	1.0126
10	6	200	6.407E7	2.511E7	25.513	6.441E7	0.9996

Table 9: Validation of Chen and Angus MTTDL formulas versus simulation.

$$MTTDL_{Angus} = \frac{MTTF^{n-k+1}}{k \binom{n}{k} MTTR^{n-k}} \times \sum_{i=0}^{n-k} \binom{n}{i} \left(\frac{MTTR}{MTTF}\right)^i \approx \frac{MTTF}{k \binom{n}{k}} \left(\frac{MTTF}{MTTR}\right)^{n-k}. \quad (46)$$

It is shown in Table 9 via simulation in Resch and Volvivski 2013 [176] that Chen's formula overestimates MTTDL by a factor $\approx (n-k)!$, but this is attributable to modeling assumptions. Setting $MTTR=1$ smaller values of MTTF are used for simulation efficiency.

Both CTMC models differ from the more accurate CTMC model for RAID6 where both RAID6 are rebuilt concurrently, i.e., the same transition rate applies for transitions $S_i \rightarrow S_0$, for $i = 1, 2$.

A RAID5 system is considered operational with no or one disk failures, but the two states differ substantially, e.g., the maximum read bandwidth is halved when a disk fails. Performability also defined a computation before failure is a better of reliability, see Trivedi 2002 [228]. Performability of four RAID1 variants discussed in Section 24 are derived in Thomasian and Xu 2008 [213].

In reliability modeling RAID5 can be substituted by a single component with the following reliability, where MTTDL is given by Eq. (43).

$$R_{RAID5}^{appr} = e^{-t/MTTDL} \quad (47)$$

RAID5 reliability using Eq. (43 and approximate MTTDL by Eq. (refeq:appr is compared in Figures 5.4a and 5.4b in Gibson 2002 [65].

The failure of a RAID5 with $N + 1$ disks due to a second disk failure is:

$$\delta_2 = \delta^2 \binom{N+1}{2} c MTTDL_{RAID5}.$$

where c is the correlation factor and $c > 1$ if disk failures are correlated.

19.1 RAID5/6 Reliability Analysis With Unrecoverable Errors

Based on the discussion in Dholakia et al. 2008 [46]. we extend the previous discussion to include the effect of unrecoverable sector failures in addition to disk failures on MTTDL.

We consider a CTMC with two states representing the number of failed disks and DF and UF states representing a data loss due to a disk failure (DF) and an unrecoverable sector failure (UF).

$$S_0 \rightarrow S_1 : N\delta \quad S_1 \rightarrow S_{UF} : \mu_1 P_{uf}^{(1)} \quad S_1 \rightarrow S_{DF} : (N-1)\delta \quad S_1 \leftarrow S_0 : \mu_1 (1 - P_{uf}^{(1)})$$

$P_{uf}^k, k = 1, 2$ are given by Eq. (49) for RAID5 and RAID6 arrays, respectively. The state transition matrix for RAID5 is given as follows.

$$\mathbf{Q} = \begin{pmatrix} -N\delta & N\delta & 0 & 0 \\ \mu(1 - P_{uf}^{(1)}) & -\mu - (N-1)\delta & (N-1)\delta & \mu P_{uf}^{(1)} \\ 0 & 0 & 0 & 0 \\ 0 & 0 & 0 & 0 \end{pmatrix}$$

Since there are no transitions from the DF and UF states, the submatrix Q_T representing states 0 and 1 is:

$$\begin{pmatrix} -N\delta & N\delta & 0 & 0 \\ \mu(1 - P_{uf}^{(1)}) & -\mu - (N-1)\delta & & \end{pmatrix}$$

The vector of the average time spent in the transient states before the Markov chain enters either one of the absorbing states DF and UF, is obtained as follows Trivedi 2002 [228]]

$$\tau_{Q_T} = \mathbf{P}_T(0) \text{ where } \tau = [\tau_0, \tau_1] \text{ and } \mathbf{P}_T(0) = [1, 0, 0]$$

Solving the above equations leads to

$$\tau_0 = \frac{(N-1)\delta + \mu}{N(N-1)\delta + \mu P_{uf}^{(1)}} \quad \tau_1 = \frac{1}{(N-1)\delta + \mu P_{uf}^{(1)}}$$

The MTTDL is given by

$$\text{MTTDL}_{RAID5} = \tau_0 + \tau_1 = \frac{(2N-1)\delta + \mu}{N\delta[(N-1)\delta + \mu P_{uf}^{(1)}]}. \quad (48)$$

Numerical results have shown that that RAID5 plus IDR attains the same MTTDL as RAID6. While IDR incurs longer transfers, this overhead is negligible compared to the extra disk access required by RAID6 with respect to RAID5. There is also the cost of an extra disk.

In the case of RAID6 the probability P_{ref} that a given segment of the failed disk cannot be reconstructed is upper-bounded by the probability that two or more of the corresponding segments residing in the remaining disks are in error. As segments residing in different disks are independent, the upper bound to P_{ref} is given by

$$P_{ref}^{UB} = \sum_{j=2}^{N-1} \binom{N-1}{j} P_{seg}^j (1 - P_{seg}^{N-1-j}) \approx \binom{N-1}{2} P_{seg}^2.$$

Given N_d segments per disk drive their reconstruction is independent of the reconstruction of the other disk segments. The probability that an unrecoverable failure occurs, because the rebuild of the failed disk cannot be completed is given by:

$$P_{uf}^r = 1 - (1 - P_{ref}^{UB})_d^n$$

It is assumed that rebuild time in the degraded and critical mode are exponentially distributed with rate μ_1 and μ_2 . Let $S_i, i = 0, 1, 2$ denote states the operating states of RAID6 with i failed disks, $calS_{DF}$ and S_{UF} failed states due to disk failure and unreadable sectors. We have the following transitions due to failures and repairs

$$\mathcal{S}_0 \rightarrow \mathcal{S}_1: N\delta \quad \mathcal{S}_1 \rightarrow \mathcal{S}_2: (N-1)\delta \quad \mathcal{S}_1 \rightarrow \mathcal{S}_{UF}: \mu_1 P_{uf}^{(2)} \quad \mathcal{S}_2 \rightarrow \mathcal{S}_{DF}: (N-2)\delta \quad \mathcal{S}_2 \rightarrow \mathcal{S}_{UF}: \mu_2 P_{uf}^{(2)}$$

$$\mathcal{S}_1 \leftarrow \mathcal{S}_0: \mu_1(1 - P_{uf}^{(r)}) \quad \mathcal{S}_2 \leftarrow \mathcal{S}_0: \mu_2(1 - P_{uf}^{(2)}).$$

Similarly to RAID5 we have the following submatrix \mathbf{Q}_T for states (0,1,2):

$$\tau \mathbf{Q}_T = \mathbf{P}_T(0) \text{ with } \mathbf{P}_T(0) = [1, 0, 0]$$

$$\tau_0 = \frac{\begin{pmatrix} -N\delta & N\delta & 0 \\ \mu_1(1 - P_{uf}^{(r)}) & -(N-1)\delta & -\mu(N-1)\delta \\ \mu_2(1 - P_{uf}^{(2)}) & 0 & -(N-2)\delta - \mu_2 \end{pmatrix}}{N\delta V}, \quad \tau_1 = \frac{(N-2)\delta + \mu_2}{V}, \quad \tau_2 = \frac{N-1}{V}$$

$$V = [(N-1)\delta + \mu P_{uf}^{(r)}][(N-2)\delta + \mu_2 P_{uf}^{(r)}] + \mu_1 \mu_2 P_{uf}^{(r)}(1 - P_{uf}^{(2)})$$

$$MTTDL_{RAID6} = \tau_0 + \tau_1 + \tau_2$$

Given $P_{uf}^{(r)} = P_{uf}^{(1)} = 0$ then $V = [(N-1)(N-2)\delta^2]$ It is to be noted that both failed disks are rebuild concurrently, but this is not the case with the Chen and Angus models.

20 Disk Scrubbing and IntraDisk Redundancy to Deal with Latent Sector Errors

The main cause of rebuild failures are *Latent Sector Errors - LSEs* rather than whole disk failures. *IntraDisk redundancy - IDR* in Dholakia et al. 2008 [46] and disk scrubbing are two less costly methods to deal with LSEs.

The probability of uncorrectable disk failures (P_{uf}) due segment errors is used in [46] to extend RAID5 reliability analysis in Section 19 to take into account LSEs.

IDR divides strips or SUs into segments of length $\ell = n + m$ sectors. There are n data and m checks sectors per segment. There are S bits per sector and the probability that a bit is in error is P_{bit} . Given that the probability of an uncorrectable sector error is P_s the probability that a segment is in error when no coding is applied ($m = 0$) is P_{seg}

$$P_S = 1 - (1 - P_{bit})^S, \quad P_{seg}^{none} = 1 - (1 - P_S)^\ell.$$

A single parity sector can be used to correct a single sector in error, since the sector in error is identified with a *Cyclic Redundancy Check - CRC*,

https://en.wikipedia.org/wiki/Cyclic_redundancy_check

so that the sectors in error can be identified.

Disk circa 2010 adopted 4096 B rather than 512 B sectors, but the section size $S = 512$ in the 2008 study. The *Error Correcting Code - ECC*

https://en.wikipedia.org/wiki/Error_correction_code

in the latter case is 100 rather 50 bytes with an efficiency of $4096/(4196) = 97.3\%$ versus $512/562 = 88.7\%$. More details about 4 KB sectors known as Advanced Format are given

below.

https://en.wikipedia.org/wiki/Advanced_Format

There are $n_d = C_d/(\ell S)$ segments on a disk with capacity C_d . The probability of an uncorrectable failure for a RAID(4 + k) with k failed disks, so that it is in critical mode:

$$P_{uf}^{(k)} = 1 - (1 - P_{seg})^{\frac{(N-k)C_d}{\ell S}} \quad (49)$$

Note that the exponent denotes the number of disk segments in critical rebuild mode.

Sector errors can be classified as independent and correlated. In the case of independent errors there is a probability P_s that a sector has an *Unrecoverable Failure - UF*. Correlated errors have an average burst length \bar{B} and there are \bar{I} successive error-free sectors on the average. Both are modeled with a geometric distribution:

$$a_j = P[I = j] = \alpha(1 - \alpha)\alpha^{j-1}, \text{ hence } \bar{I} = 1/\alpha$$

We also have $P[B = j] = b_j$ and $\bar{B} = \sum_{j \geq 1} j b_j$. Utilized in further discussions is the following parameter.

$$G_n \triangleq P[\text{burst_length} \geq n] = \sum_{j \geq n} b_j$$

The independent model is a special case of correlated model where

$$b_j = (1 - P_s)P_s^{j-1} \text{ and } \bar{B} = 1/(1 - P_s)$$

The probability P_s that an arbitrary sector has an unrecoverable error is:

$$P_s = \frac{\bar{B}}{\bar{B} + \bar{I}}$$

It follows

$$\alpha = \frac{P_s}{\bar{B}(1 - P_s)} \approx \frac{P_s}{\bar{B}} \text{ hence } P_s \leq \frac{\bar{B}}{\bar{B} + 1}$$

For independent errors we have:

$$P_{seg}^{none} = 1 - (1 - P_s)^\ell \approx \ell P_s, \quad P_{seg}^{none} \approx \left(1 + \frac{\ell - 1}{\bar{B}}\right) P_s \quad (50)$$

for bursty errors

$$P_{seg}^{none} = 1 - (1 - P_s)\left(1 - \frac{1}{\bar{B}}\right) \approx \left(1 + \frac{\ell - 1}{\bar{B}}\right) P_s \quad (51)$$

The probability that a segment is in error can be specified with the summation below, but only one term need to be considered for small P_s and the correlated model

$$P_{seg} = \sum_{i \geq 1} c_i P_s^i \quad P_{seg} = c_1 P_s + O(P_s^2)$$

20.1 Schemes to Implement IntraDisk Redundancy - IDR

Three IDR methods are proposed and evaluated in [46].

Reed-Solomon Check

RS - Reed-Solomon codes are discussed in coding theory textbooks in Section 1. An error occurs when over m bits among $\ell = n + m$ bits are in error.

$$P_{seg}^{RS} = \sum_{j=m+1}^{\ell} \ell P_s^j (1 - P_s)^{\ell-j} \approx \binom{\ell}{m+1} P_s^{m+1}. \quad (52)$$

In the case of a correlated model for small values of P_s .

$$P_{seg}^{RS} \approx \left[1 + \frac{1}{\bar{B}} \left((\ell - m - 1)G_{m+1} - \sum_{j=1}^m G_j \right) \right] P_s. \quad (53)$$

This is the best we can do since for a code with m parity symbols for a codeword of n symbols any m erasures can be corrected, but RS codes are computationally expensive.

$$P_{seg}^{RS} = \sum_{j=m+1}^{\ell} \binom{\ell}{j} P_s^j (1 - P_s)^{\ell-j} \approx \binom{\ell}{m+1} P_s^{m+1}. \quad (54)$$

In the case of correlated model for small values of P_s results in Appendix B are used to show:

$$P_{seg}^{RS} \approx \left[1 + \frac{(\ell - m - 1)G_{m+1} - \sum_{j=1}^m G_j}{\bar{B}} \right] P_s, \text{ where } \bar{B} = \sum_{j=1}^{\infty} G_j, \quad b_j = G_j - G_{j-1}. \quad (55)$$

Single Parity Check - SPC

The simplest coding scheme is one in which a single parity sector is computed by using the XOR operation on $\ell - 1$ data sectors to form a segment with ℓ sectors. The independent model yields:

$$P_{seg}^{SPC} = \sum_{j=2}^{\ell} \binom{\ell}{j} P_s^j (1 - P_s)^{\ell-j} \approx \frac{\ell(\ell-1)}{2} P_s^2 \quad (56)$$

In the case of correlated model for small values of P_s

$$P_{seg}^{SPC} \approx \left[1 + \frac{1}{\bar{B}} ((\ell - 2)G_2 - 1) \right] P_s. \quad (57)$$

Interleaved Parity Check - IPC

In this scheme $\ell - m$ contiguous sectors are placed in a rectangle with m columns. The XOR of the sectors in a column is the parity sector which is placed in an additional row. This scheme with ℓ/m sectors per interleave can correct a single error per interleave, but a segment is in error if there is at least one interleave with two uncorrectable segment errors.

An IPC scheme with m ($m \leq \ell/2$) interleaves per segment, i.e. ℓ/m sectors per interleave, has the capability of correcting a single error per interleave. Consequently, a segment is in error if there is at least one interleave in which there are at least two unrecoverable sector errors. Note that this scheme can correct a single burst of m consecutive errors occurring in a segment. However, unlike the RS scheme, it in general does not have the capability of correcting any m sector errors in a segment. The probability of an interleave error is then:

$$P_{interleave_error} = \sum_{j=2}^{\ell/m} \binom{\ell/m}{j} P_s^j (1 - P_s)^{\ell/m-j} \approx \frac{\ell(\ell-m)}{2m^2} P_s^2$$

$$P_{seg}^{IPC} = 1 - (1 - P_{interleave_error})^m \approx \frac{\ell(\ell-m)}{2m} P_s^2 \quad (58)$$

In the case of correlated model:

$$P_{seg}^{IPC} \approx \left[1 + \frac{1}{B} \left((\ell - m - 1)G_{m+1} - \sum_{j=1}^m G_j \right) \right] P_s \quad (59)$$

It follows $P_{seg}^{RS} \approx P_{seg}^{IPC}$, but of course IPC is preferable since it is easier to implement.

21 Effect of IDR on Disk Performance

The main focus in [46] is to study the effect of IDR on RAID5 reliability, but performance is also investigated using simulation and *IO Equivalents - IOEs* introduced in Hafner et al. 2004 [75].

$$IOE(k) = 1 + \frac{\text{time to transfer 4 KB}}{\text{average time per 4 KB}} = 1 + \frac{4 \text{ KB}/1024}{\text{Avg. media transfer rate in MB/sec}} \times \text{Avg IO/sec.} \quad (60)$$

Table 10: Results for IOE.

	10K PM	15K RPM	Units
IOs/sec.	250	333	IO/sec.
Avg. media transfer rate	53.25	62	MB/sec.
IOE for k KB	$1 + k/55$	$1 + k/48$	IOE

The approximation $IOE(k) = 1 + k/50$ is used in the study.

When a single-sector **A** is written using the IPC scheme, for example, it is written by a single I/O request also containing the corresponding intra-disk parity sector **PA**. The average length of an I/O request is minimized when the intra-disk parity sectors are placed in the middle of the segment. The analysis in Section 8.2 of the paper determines the increase in IOE as 8.5% for small and 3.6% for long writes

Errors	Independent	Correlated
None	5.2×10^{-9}	5×10^{-9}
RS	6.2×10^{-81}	2.5×10^{-12}
SPC	1.3×10^{-17}	8.5×10^{-14}
IPC	1.6×10^{-18}	$9.5 \times 2.5 \times 10^{-12}$

Table 11: Approximate P_{seg} for two error models

Scheme	Independent	Correlated
None	1.5×10^{-1}	1.5×10^{-1}
RS	2×10^{-73}	7.9×10^{-5}
SPC	4.3×10^{-10}	3.1×10^{-3}
IPC	6.1×10^{-11}	7.95×10^{-5}

Table 12: Approximate P_{uf} for RAID5 with $N = 8$.

The following parameters were used by the simulator: $1/\delta=500K$ hours, disk capacity $S = 300$ GB, $P_{bit} = 10^{-14}$, number of disks $N = 8/16$ for RAID5/6, rebuild time $1/\mu = 17.8$ hr, sector size $S = 512$ bytes, $\ell = 128$ sectors, $m = 8$ interleaves.

Both random number and trace-driven simulations results are reported in this study. FCFS scheduling is used in the study, but other policies such as SSTF, Look, C-Look are tried and shown to have a small effect on the relative performance due to IDR.

Numerical Results

SATA drives (see Section 20.3) in Jacobs et al. 2008 [104]) with disk capacity $C_d = 300$ GB, $P_{bit} = 10^{-14}$. so that 512 bytes sectors and $P_s = 4096 \times P_{bit} = 4.096 \times 10^{-11}$. The segment length was set to $\ell = 128$ sectors with $m = 8$ interleaving burst length distribution with at most 16 sector and $\bar{B} = 1.0291$ and

$$\underline{b} = [0.9812, 0.016, 0.0013(2), 0.0003(2), 0.00020.0001(2), 0, 0.0001, 0, 0.0001(2), 0, 0.0001(2)]$$

21.1 Comparison of Disk Scrubbing and IDR with IPC

The conclusions of quite complex analysis of disk scrubbing in Iliadis et al. [95] are summarized in this section and the analysis is used in comparing it with the IDR scheme.

Closed-form expressions were derived for operation with random, uniformly distributed I/O requests, for the probability of encountering unrecoverable sector errors, the percentage of unrecoverable sector errors that disk scrubbing detects and corrects, the throughput and the minimum scrubbing period achievable.

The probability of an error due to a write is P_w and writes constitute a fraction r_w of disk accesses with rate h . The probability of error in reading a sector without scrubbing is $P_e = r_w P_w$. The probability of sector failure for deterministic scrubbing and random (exponentially distributed) scrubbing period are:

$$P_s^{(det)} = [1 - (1 - e^{-hT_s})/(hT_s)]P_e \text{ and } P_s^{(exp)} = [hT_s/(1 + hT_s)]P_e,$$

where T_s denotes the mean scrub period. Given that $hT_s \ll 1$ we have the following approximations for deterministic and exponential scrubbing:

$$P_s^{(det)} \approx P_e h T_s \text{ and } P_s^{(exp)} \approx \frac{1}{2} P_s P_e h T_s$$

Deterministic scrubbing is preferable, since random scrubbing has double the value for P_s .

For heavy-write workloads and for typical scrubbing frequencies and loads, the reliability improvement due to disk scrubbing does not reach the level achieved by the IPC-based IDR

scheme, which is insensitive to the load. Note that IPC-based IDR for SATA drives achieves the same reliability as that of a system with no sector errors, with a small (about 6%) increase in capacity.

The penalty of disk scrubbing on I/O performance can be significant, whereas that of the IPC-based IDR scheme is minimal, but of course is some disk space overhead.

Given IOE(k) in Eq. (60) the maximum rate of read/write operations to the disk is:

$$\hat{\sigma}_{max} = [IOE(K)t_{seek}]^{-1} \quad (61)$$

Given a small write scenario with k sectors per chunk, S_D sectors per disk, with G_S sectors scrubbed a time, and $p = 1$ for RAID5 and $p = 2$ for RAID6

$$\sigma \leq \sigma_{max}(k, T_S) = \frac{\hat{\sigma}_{max}(k, T_S)}{1 + (1 + 2p)r_w} \quad (62)$$

The scrubbing T_S period should not be smaller than a critical value T_S^* given below:

$$T_S \geq T_S^* = \frac{S_D IOE(G_S)}{[1 + (1 + 2p)r_w] G_S IOE(k) [\sigma_{max}(k) - \sigma]} \quad (63)$$

In Figure 6 in [95] it is shown that in the area of practical interest, the reliability offered by scrubbing still inferior to that achieved by the intradisk redundancy scheme.

Iliadis et al. [95] argument that that IDR is preferable to disk scrubbing contradicts that of Schroeder et al. 2010 [187].

22 Combining Scrubbing with SMART and Machine Learning

SMART has been applied to predict HDD failures as discussed in Hughes et al. 2002 [93], Eckart et al. 2008 [50]. Once a disk is determined to be failing its contents are copied onto a spare with possibly occasional assist to restore unreadable segments using the RAID5 paradigm.

https://en.wikipedia.org/wiki/Self-Monitoring,_Analysis_and_Reporting_Technology

In monitoring disks with SMART there are 30 Attributes corresponding to different measures of performance and reliability Allen 2004 [3]. Attributes have a one-byte normalized value ranging from 1 to 253, e.g., SMART 187 is the number of read errors that could not be recovered using hardware ECC. If one or more of the Attribute values less than or equal to its corresponding threshold, then either the disk is expected to fail in less than 24 hours or it has exceeded its design or usage lifetime.

<https://www.backblaze.com/blog/hard-drive-smart-stats/> Western Digital *Network Attached Storage - NAS* HDDs are automatically given a warning label in Synology's *DiskStation Manager - DSM* after they were powered on for three years. This is also done Western Digital device *Analytics - WDDA* and Seagate's *IronWolf* is a similar offering.

https://en.wikipedia.org/wiki/Network-attached_storage

<https://arstechnica.com/gadgets/2023/06/clearly-predatory-western-digital-sparks-panic-anger-for-age-sha>

Nimble storage which is part of HPE has advertised predictive storage, which makes 86% of problems disappear. A 6-nines (99.9999%) availability is guaranteed over the installed base and 54% of problems resolved are determined to be outside storage.

<https://m.softchoice.com/web/newsite/documents/partners/hpe/Nimble-Six-Nine-White-Paper.pdf>

InfoSight developed by Nimble applies data science to identify, predict, and prevent problems across infrastructure layers.

https://en.wikipedia.org/wiki/Data_science

Machine Learning - ML methods are used by Murray et al. 2005 [148] to predicting HDD failures by monitoring internally the attributes of individual drives. An algorithm based on the multiple-instance learning framework and the naive Bayesian classifier (mi-NB) are specifically designed for the low false-alarm case. Other methods compared are *Support Vector Machines* - SVMs, unsupervised clustering, and non-parametric statistical tests (rank-sum and reverse arrangements).

https://en.wikipedia.org/wiki/Support_vector_machine

<https://www.section.io/engineering-education/clustering-in-unsupervised-ml/>

<https://www.ncbi.nlm.nih.gov/pmc/articles/PMC4754273/>

The failure-prediction performance of the SVM, rank-sum and mi-NB algorithm is considerably better than the threshold method currently implemented in drives, while maintaining low false alarm rates.

Goldszmidt 2012 [66] describes, characterizes, and evaluates D-FAD - Disk Failure Advance Detector of *Soon-To-Fail* - STF disks. The input to D-FAD is a single signal from every disk, a time series containing in each sample the *Average Maximum Latency* - AML and the output is an alarm according to a combination of statistical models. The parameters in these models are automatically trained from a population of healthy and failed disks ML techniques. Results from an *Hidden Markov Model* - HMM and a threshold (peak counter) were fused using logistic regression to sound alarms.

https://en.wikipedia.org/wiki/Hidden_Markov_model

https://en.wikipedia.org/wiki/Logistic_regression

When applied to 1190 production disks D-FAD predicted 15 out of 17 failed disks (88.2% detection rate), with 30 false alarms (2.56% false positive rate).

Amvrosiadis et al. 2012 [7] state that the goal of a scrubber is to minimize the time between the occurrence of an LSE and its detection/correction or *Mean Latent Error Time* - MLET, since during this time the system is exposed to the risk of data loss. In addition to reducing the MLET, a scrubber must ensure to not significantly affect the performance of foreground workloads.

Staggered scrubbing provides a lower MLET exploiting the fact that LSEs occur temporal and spatial bursts. Rather than sequentially reading the disk from beginning to end staggered scrubbing quickly probes different regions of the drive hoping that if a region has a burst of errors the scrubber will detect it quickly and then immediately scrub the entire region.

Staggered scrubbing potentially reduces scrub throughput and increase the impact on foreground workloads. At the time the articles was written there was no experimental evaluation that quantifies this overhead, and staggered scrubbing is currently not used in practice. The second design question is deciding when to issue scrub requests. The scrubbers employed in commercial storage systems today simply issue requests at a predefined rate, e.g. every r msec. Larger request sizes lead to more efficient use of the disk, but also have the potential of bigger impact on foreground traffic, as foreground requests that arrive while a scrub request is in progress get delayed

RAIDShield developed at EMC characterizes, monitors, and proactively protects against disk failures eliminating 88% of triple disk failures in RAID6, which constituted 80% of all RAID failures Ma et al. 2015 [133]. A method using the joint failure probability quantifies and predicts vulnerability to failure. Simulation shows that most vulnerable RAID6 systems can improve the coverage to 98% of triple errors.

The use of ML to make storage systems more reliable by detecting sector errors in HDDs and SSDs is explored by Mahdisoltani et al. 2017 [135] Exploration of a widerange of ML techniques shows that sector errors can be predicted ahead of time with high accuracy. Possible use cases for improving storage system reliability through the use of sector error predictors is provided The mean time to detecting errors can be greatly reduced by adapting the speed of a scrubber based on error predictions.

A scrub unleveling technique that enforces a lower rate scrubbing to healthy disks and a higher rate scrubbing to disks subject to LSEs is proposed by Jiang et al. 2019 [108]. A voting-based method is introduced to ensure prediction accuracy. Experimental results on a real-world field dataset have demonstrated that our proposed approach can achieve lower scrubbing cost together with higher data reliability than traditional fixed-rate scrubbing methods. Compared with the state-of-the-art, our method can achieve the same level of Mean-Time-To-Detection - MTTD with almost 32% less scrubbing.

The first experimental comparison of sequential versus staggered scrubbing in production systems determined that staggered scrubbing implemented with the right parameters can achieve the same (or better) scrub throughput as a sequential scrubber, without additional penalty to foreground applications. A detailed statistical analysis of I/O traces is used to define policies for deciding when to issue scrub requests, while keeping foreground request slowdown at a user-defined threshold. The simplest approach, based on idle waiting and using a fixed scrub request size outperforms more complex statistical approaches.

Scrubbing schemes to deal with LSEs have several limitations according to Zhang et al. 2020 [247]. (1) schemes use ML to predict LSEs, but only a single snapshot of training data for prediction; ignoring sequential dependencies between different statuses of a HDD over time. (2) accelerating scrubbing at a fixed rate based on the results of a binary classification model results in unnecessary increases in scrubbing cost; (3) naively accelerating scrubbing over full disks neglects partial high-risk areas; (4) they do not employ strategies to scrub these high-risk areas in advance based on I/O accesses patterns, in order to further increase the efficiency of scrubbing.

Tier-Scrubbing - TS scheme combines a *Long Short-Term Memory - LSTM* based *Adaptive Scrubbing Rate Controller - ASRC*, a module focusing on sector error locality to locate high-risk areas in a disk, and a piggyback scrubbing strategy to improve the reliability of a storage system. Realistic datasets and workloads evaluated from two data centers demonstrate that TS can simultaneously decreases *Mean-Time-To-Detection - MTTD* by about 80% and scrubbing cost by 20%, compared to a state-of-the-art scrubbing scheme.

Disk fault detection models based on SMART data with ML algorithms require a large amount of disk data to train the models, but the small amount of training data in traditional ML algorithms greatly increases the risks of overfitting or weak generalization, which weaken the performance of the model and seriously affect the reliability of the storage systems.

A novel *Small-Sample Disk Fault Detection - SSDFD* optimizing method, with synthetic data using *Generative Adversarial Networks - GANs* [67]. is proposed in Wang 2022 [232] is The proposed approach utilizes GAN to generate failed disk data conforming to the failed disk data

distribution and expands the dataset with the generated data, then the classifiers are trained. Disk SMART attributes vary with the usage and are time-related; LSTM is adopted since it is good at learning the characteristics of time series data as the GAN generator to fit the distribution of SMART data, and use the multi-layer neural network as the discriminator to train the GAN-model to generate realistic failed disk data. With sufficient generated failed disk data samples, ML algorithms can detect disk faults more precisely than before with the small original failed disk data samples.

23 Undetected Disk Errors and Silent Data Corruption - SDC

Bairavasundaram et al. 2007 [14] is a major study revealing interesting aspects of *Undetected Disk Errors - UDEs* or LSEs. The following observations were made: (1) a high degree of temporal locality between successive LSE occurrences; (2) the vast majority of disks developed relatively few errors during first three years, but these few errors can cause significant data loss if not detected proactively by disk scrubbing.

Silent Data Corruption - SDC manifests itself as UDEs. The causes of UDEs and their effects on data integrity is discussed by Hafner et al. 2008 [77]. Techniques to address the problem at various software layers in the I/O stack and solutions that can be integrated into the RAID subsystem are discussed at:

https://en.wikipedia.org/wiki/Data_corruption.

UDE types are *Undetectable Write/Read Errors - UWEs/UREs*. UWEs are in the form of dropped or phantom writes and off-track or misdirected writes resulting in stale data. UREs are in the form of *Error Correcting Code - ECC* miscorrects or off-track reads, which result in reading of stale or corrupted data.

Presented in this work are technologies for addressing data corruption problems caused by UDEs, as well as other causes of data corruption. Technologies are divided into classes depending on the software layer and the type of problem.

Checking at middleware or application software layers: Some file systems checksum 4-8 KB data chunks and store them separately. When the data chunk is read the checksum is recomputed and compared. A mismatch indicates corruption of either the data or the checksum, but the former is more likely because of its larger size.

This method was utilized by ZFS Karlsson 2006 [114] and the *IRON - Internal ROBustNess* file system Prabhakaran et al. 2005 [169], The IRON file system prototype which incurs minimal time and space overheads via in-disk checksumming, replication, and parity is shown to greatly enhance file system robustness.

Detection of Errors by the Storage System: Errors introduced along the datapath between the storage system and the application may not be detected. This class has several subclasses with respect to different powers of detection and correction with associated performance impacts and performance/cost tradeoffs.

By itself data and parity scrubbing cannot detect UDEs. A parity scrub provides an additional step beyond a data scrub.

Data scrubbing. A data scrub in addition to reading all of the data blocks recomputes the parity and compares this computed parity with the stored parity on disk. A mismatch implies a data corruption error. Data scrubs and parity scrubs do not always provide for recovery, and a comparison does not always provide a guarantee that no data corruption has occurred.

Metadata options. When metadata is colocated with data and metadata contains checksums, a read of the data and metadata can detect data corruption errors, especially those introduced by firmware, software, or the memory bus. When the metadata contains the data address, a read can detect off-track writes but only at the offset target location, where data was incorrectly overwritten. These methods are usually combined with a data scrub to enhance its effectiveness as discussed in Sundaram 2006 [194].

https://atg.netapp.com/wp-content/uploads/2018/08/TECH_ONTAP-Private_Lives_of_Disk_Drives.pdf

SCSI Write Verify Disk Command. This command rereads data after it is written to ensure that it was written correctly. This works for dropped write errors but cannot necessarily detect off-track writes, because the same possibly incorrect track is accessed. This is an obvious performance impact, since a full disk rotation is required. This method has a simple recovery algorithm which rewrites the data to the same or a different location on disk.

Verification handled by fresh data in write cache When the data needs to be evicted from the cache, the disk is first read and compared with the cache copy and the eviction occurs only if the data compare is correct. This has the same simple recovery algorithm as the write-verify approach.

Idle Read After Write - IRAW proposed by Riedel and Riska 2008 [177]. is an improvement over *Read After Write - RAW* to reduce this performance penalty. The idea is to retain the written content in the disk cache and verify it once the disk drive becomes idle. Trace-driven evaluation of IRAW shows its feasibility and that disk idleness can be utilized for WRITE verification with minimal effect on user performance.

Metadata as checksum or version number The second copy of the metadata is stored in memory for fast comparison and access, but must be flushed to disk to maintain detection capabilities after system crashes.

Metadata stored as RAID It then has a locality of reference that can be used to mitigate some of the disk I/O overheads of separate locations. The advantages of this approach are lower I/O and bandwidth penalties for most operations; the disadvantage is potential loss of detection under certain failure scenarios.

SDCs may go undetected until a system or application malfunction occurs. A major problem with SDC is that data errors propagate during data rebuild. Developed in Li and Shu 2010 [128] a reconstruction method in the presence of silent data corruption. This method outperforms others when periodic validation is carried out.

24 Mirrored and Hybrid Disk Arrays Description and Reliability Comparison

Mirrored disks are classified as RAID1 in Patterson et al. [159] Chen et al. 1994 [32]. *Basic Mirroring - BM* is an early form of mirroring, which was utilized in Tandem (now part of HP) NonStop SQL system as duplexed disk Tandem 1987 [197] and by EMC's (now Dell/EMC) Symmetrix disk array with capability to emulate IBM drives.

https://en.wikipedia.org/wiki/EMC_Symmetrix

Four mirrored disk organizations including BM are described and their reliability and performance analyzed in Thomasian and Blaum 2006, and Thomasian and Xu 2008 [211, 213]. Hybrid disk arrays which store XORs of multiple disks instead of just mirroring are described and evaluated in Thomasian and Tang 2012 [218]

Most performance studies of RAID1 are carried out in the context of BM organization. Mirroring provides the opportunity to reduce disk access time for read requests by accessing the disk one of k disks in k -way replication, which provides the lower seek distance and hence time assuming that the position of disk arms is known to OS. Derived in Gray and Bitton 1988 [72] is the expected seek distance with k -way replication for reads and writes, which are the minimum and maximum of k uniformly distributed seek distances.

$$E[\text{min of } k\text{-way seeks}] \approx \frac{C}{2k+1}, \quad E[\text{max of } k\text{-way seeks}] \approx C(1 - I_k), \quad \text{where: } I_k = \frac{2k}{2k+1} \frac{2k-2}{2k-1} \cdots \frac{2}{3}.$$

Loads across disk pairs can be balanced via striping at the higher level in the hierarchical RAID0/1, where RAID0 is at the higher level and RAID1 at the lower level. The load due to read requests to disk pairs is balanced via uniform routing (with equal probabilities) or round-robin routing. In what follows the latter is shown to exhibit shorter waiting times under simplifying queueing assumptions.

With Poisson arrivals of disk requests the latter improves response time, since the arrival process to each disk is the sum of two exponential interarrivals or Erlang-2, which has a *Coefficient of Variation* - $CV = 1/2 < 1$ for Poisson arrivals Kleinrock 1975 [118]. The mean waiting time on a GI/M/1 queue with Erlang-2 arrivals and exponential service time with mean $\bar{x} = 1/\mu$ is:

$$W_{GI/M/1} = \frac{\sigma \bar{x}}{1 - \sigma} \quad \text{with } \sigma = \mathcal{A}^*(\mu - \mu\sigma), \quad \text{where } \mathcal{A}^*(s) = \left[\frac{2\lambda}{s + 2\lambda} \right]^2$$

$$\sigma^2 - (1 + 4\rho)\sigma + 4\rho^2 = 0, \quad \sigma = \frac{1}{2}(1 + 4\rho - \sqrt{1 + 8\rho})$$

A smaller CV does not insure a smaller mean waiting time $W_{GI/M/1}$ which can be shown by a counterexample given in Thomasian 2014b [221].

RAID1 is especially suited in doubling disk bandwidth for random disk accesses in OLTP, while RAID5 incurs SWP. RAID1 seems to be less efficient than RAID5 in writing large blocks, which can be carried out as full stripe writes, but this can be done in parallel on striped RAID 0/1 arrays as well.

When one of two of disk pairs in BM fails the load of the surviving disk is doubled. This may lead to overload leading to high queueing delays and this led to novel RAID1 configurations starting with *Interleaved Declustering - ID* in the case of Teradata *Data Base Computer* -

Primary Disks				Secondary Disks			
D_1	D_2	D_3	D_4	D_5	D_6	D_7	D_8
A	B	C	D	A'	B'	C'	D'
E	F	G	H	E'	F'	G'	H'
I	J	K	L	I'	J'	K'	L'
M	N	O	P	M'	N'	O'	P'

Figure 21: RAID0/1 with $N = 8$ disks.

DBC/1012.

https://en.wikipedia.org/wiki/DBC_1012

Thomasian and Blaum 2006 and Thomasian and Xu 2008 [211, 213]:

Basic Mirroring - BM: Also known as duplexing this is the simplest form of replication, where the same data appears at both disks. RAID0/1 is a striped array with $M = N/2$ pairs of mirrored disks. When a disk fails BM has the worst performance in terms of unbalanced disk loads, i.e., the read load of the surviving disk is doubled. Up to M disk failures can be tolerated as long as they are not pairs. According to Table 13 BM has the highest reliability among the four RAID1 organizations considered here. This is because the probability that the second disk failures that may lead to data loss by being a pair of the first failed disk is lowest.

Interleaved Declustering - ID: Teradata DBC/1012 database machine partitioned its N disks into c clusters with $n = N/c$ disks per cluster as shown in Figure 23. Each disk has a primary and a secondary area. The data in primary area is partitioned and placed onto $n - 1$ secondary areas in the same cluster. A failed disk results in $n/(n - 1)$ load increase at the $n - 1$ surviving disks in a cluster. Two disk failure in a cluster will lead to data loss. The setting $c = N/2$ or $n = 2$ is tantamount to BM.

Group Rotate Declustering - GRD: There are two mirrored RAID0 arrays with $M = N/2$ disks or RAID1/0, but strips on the right side are rotated with respect to the strips on the left side as shown in Figure 22 Chen and Towsley 1996 [35]. When a disk on the left side fails its load is evenly distributed over the disks on the right side. Two disk failures on one side will lead to data loss.

Chained Declustering: The primary data on the i^{th} disk is replicated on the secondary area of the $i + 1^{st} \bmod(N)$ disk as shown in Figure 24 Hsiao and DeWitt 1990 [85]. Similarly to ID primary and secondary data can be placed in outer or inner cylinders, or upper and lower disk tracks when there are an even number of tracks per cylinder. Two successive disk failures leads to data loss, but the reliability is lower than BM since there are twice as many data loss opportunities as in BM: when following the i^{th} disk failure the $i \pm 1 \bmod(N)$ disk fails.

The maximum number of disk failures that can be tolerated without data loss for mirroring with $N = 2M$ disks is $I = M$, but $I = c$ for the ID organization. Setting $r = r(t)$ to simplify notation RAID1 reliability expressions can be expressed as follows:

Primary Disks				Secondary Disks			
D_1	D_2	D_3	D_4	D_5	D_6	D_7	D_8
A	B	C	D	A'	B'	C'	D'
E	F	G	H	H'	E'	F'	G'
I	J	K	L	K'	L'	I'	J'
M	N	O	P	N'	O'	P'	M'

Figure 22: Group Rotate Declustering with $N = 8$ disks.

Cluster 1				Cluster 2			
D_1	D_2	D_3	D_4	D_5	D_6	D_7	D_8
A	B	C	D	E	F	G	H
b_3	a_1	a_2	a_3	f_3	e_1	e_2	e_3
c_2	c_3	b_1	b_2	g_2	g_3	f_1	f_2
d_1	d_2	d_3	c_1	h_1	h_2	h_3	g_1

Figure 23: Interleaved Declustering with $N = 8$ disks, $c = 2$ clusters, and $n = 4$ disks per cluster. Capital letters denote primary data and small letters subsets of secondary data.

$$R_{RAID}(N) = \sum_{i=0}^I A(N, i) r^{N-i} (1-r)^i. \quad (65)$$

$A(N, 0) = 1$ by definition and $A(N, i) = 0$ for $i > M$.

In the case of BM up to M disk failures can be tolerated, as long as one disk in each pair survives:

$$A(N, i) = \binom{M}{i} 2^i, \quad 0 \leq i \leq M. \quad (66)$$

In the case of ID with c clusters and $n = N/c$ disks per cluster, we can have only one disk failure per cluster.

$$A(N, i) = \binom{c}{i} n^i, \quad 0 \leq i \leq c. \quad (67)$$

In the case of GRD up to M disks can fail as long as they are all on one side.

$$A(N, i) = 2 \binom{M}{i}, \quad 0 \leq i \leq M. \quad (68)$$

The expression for $A(N, i)$ for CD is derived in Thomasian and Blaum 2006 [211]:

$$A(N, i) = \binom{N-i-1}{i-1} + \binom{N-i}{i}, \quad 1 \leq i \leq M. \quad (69)$$

Hybrid disk arrays combine mirroring with parity coding. LSI RAID has disks holding the XOR of neighboring disks Wilner 2001 [236].

D_1	D_2	D_3	D_4	D_5	D_6	D_7	D_8
$\frac{1}{2}A$	$\frac{1}{2}B$	$\frac{1}{2}C$	$\frac{1}{2}D$	$\frac{1}{2}E$	$\frac{1}{2}F$	$\frac{1}{2}G$	$\frac{1}{2}H$
$\frac{1}{2}h$	$\frac{1}{2}a$	$\frac{1}{2}b$	$\frac{1}{2}c$	$\frac{1}{2}d$	$\frac{1}{2}e$	$\frac{1}{2}f$	$\frac{1}{2}g$

Figure 24: Chained declustering with $N = 8$ disks. Primary (resp. secondary) blocks are in capital (resp. small) letters. The read load is evenly distributed among the primary and secondary copies.

$$D_A, (D_A \oplus D_B), D_B, (D_B \oplus D_C), D_C, (D_C \oplus D_D), D_D, (D_D \oplus D_A)$$

Three disk failures can be tolerated as long as the middle disk is not a data disk.

SSPIRAL proposed in Amer et al. 2008 [12] is a generalization to three disks participating in parities as follows:

$$D_A, D_B, D_C, D_D, (D_A \oplus D_B \oplus D_C), (D_B \oplus D_C \oplus D_D), (D_C \oplus D_D \oplus D_A), (D_D \oplus D_A \oplus D_B)$$

Up to four disk failures can be tolerated as long as it is not a data disk and the parities it participates in.

A minor correction to enumerations used in SSPIRAL paper to obtain reliability expressions is made in Thomasian and Tang 2012 [218].

Mirrored pairs in Tandem computers came with two processors cross-connected to both disks, instead of dedicated processor/disk pairs. Guven that R_c and R_d are the CPU and disk reliability, the former configuration has a higher reliability.

$$R_{cross-connected} = 1 - (1 - R_c R_d)^2 \approx 2R_c R_d - 4R_c^2 R_d^2, \quad R_{dedicated} = [1 - (1 - R_c)^2][1 - (1 - R_d)^2] \approx 4R_c R_d$$

24.1 Shortcut Method to Compare the Reliability of Mirrored Disks and RAID(4+k)

We provide a simple method to compare the reliability of various RAID configurations rather than plotting disk reliability $R(t)$ versus t . As in Thomasian 2006 [210] this is accomplished by expressing disk reliability as $r = 1 - \epsilon$, e.g., for MTTF=10⁶ hours or 114 years, a good approximation for relatively short time (t_s)

$$R(t_s) = e^{-\delta t_s} \approx 1 - \delta t_s \text{ after three years } R(3) = 1 - 3/114 = 0.975, \text{ hence } \epsilon = 0.025.$$

RAID with n -way replication fails with n disk failures and this is indicated by the power n in the reliability expression (we use $\bar{r} = 1 - r$. In other words the number of failures tolerated is $n - 1$)

$$R_{n-way} = 1 - (1 - r)^n = 1 - \bar{r}^n = 1 - \epsilon^n$$

The expressions for the RAID1 configurations are as follows:

$$R_{BM} \approx r^N + N r^{N-1} \bar{r} + \binom{N}{2} r^{N-2} (\bar{r})^2 \approx 1 - 0.5N\epsilon^2. \quad (70)$$

For GRD the reliability expression can be written directly, since it is as if we have two logical disks each comprising $M = N/2$ disks.

$$R_{GRD} = 2r^{N/2} - r^N \approx 1 - 0.25N^2\epsilon^2. \quad (71)$$

$$R_{ID} \approx r^N + c\left(\frac{N}{c}\right)r^{N-1}\bar{r} + \binom{c}{2}\left(\frac{N}{c}\right)^2r^{N-2}(\bar{r})^2 = 1 - 0.5N\left(\frac{N}{c} - 1\right)\epsilon^2. \quad (72)$$

We only need the first three terms in the reliability expression to obtain R_{CD} . With two disk failures there are N configurations leading to data loss:

$$A(N, 2) \approx \binom{N}{2} - N = 0.5N(N - 3)$$

$$R_{CD} \approx r^N + Nr^{N-1}\bar{r} + 0.5N(N - 3)r^{N-2}(\bar{r})^2 = 1 - N\epsilon^2. \quad (73)$$

Reliability of RAID5 and RAID(4+k) is given as R_k . In the case of RAID5 we have:

$$R_{RAID5} = r^N + N\bar{r}r^{N-1} = (1 - \epsilon)^N + N\epsilon(1 - \epsilon)^{N-1} \approx 1 - 0.5N(N - 1)\epsilon^2$$

$$R_{RAID(4+k)} \approx 1 - \binom{N}{k+1}\epsilon^{k+1} + \binom{N}{k+2}\epsilon^{k+2} - \dots \quad (74)$$

A summary of results of shortcut reliability analysis results in [218] are given in Table 13.

RAID5	BM	CD	GRD	ID	RAID6	LSI	RAID7	SSP
	$\frac{163}{2808}$	$\frac{379}{8408}$	$\frac{3}{88}$	$\frac{61}{1688}$	$\frac{73}{1688}$	$\frac{82}{1058}$	$\frac{533}{8408}$	$\frac{701}{8408}$
0.2688^{-1}	0.5828^{-1}	0.4518^{-1}	0.3758^{-1}	0.3638^{-1}	0.4358^{-1}	0.7818^{-1}	0.6358^{-1}	0.83458^{-1}
$\binom{N}{2}\epsilon^2$	$\frac{N\epsilon^2}{2}$	$N\epsilon^2$	$\frac{N(N-1)\epsilon^2}{4}$	$\frac{N(N-c)\epsilon^2}{2c}$	$\binom{N}{3}\epsilon^3$	$\left(\binom{N}{3} - \frac{N}{2}\right)\epsilon^3$	$\binom{N}{4}\epsilon^4$	$\frac{1}{5}\binom{N}{4}\epsilon^4$

Table 13: MTDLs as a ratio and a fraction of the MTTF (δ^{-1}) and the first term in asymptotic reliability expression with ϵ denoting the unreliability of a single disk and the power is the minimum number of disk failures leading to data loss.

RAID6 results apply to EVENODD, X-code, and RDP, all three of which are 2DFT.

Hybrid disk arrays which combine replication and parity coding provide a higher reliability at the same redundancy level. RAID1 provides 2-way, LSI RAID 3-way, and SSPIRAL 4-way replication. The update penalty is proportional to the number of ways.

25 Reliability Analysis of Multilevel RAID Arrays

Two multilevel RAID disk arrays are considered in this section: mirrored RAID5 (RAID1/5) and RAID5 consisting of mirrored disks (RAID5/1). RAID1/0 and RAID0/1 was discussed in the previous section. Note that the number of disks is the same in both cases, but one configuration provides higher reliability than the other and this is verified with the shortcut reliability analysis method in Thomasian 2006 [210].

25.1 Reliability of Mirrored RAID5 - RAID1/5 Reliability

Consider mirroring of RAID5 arrays and no repair via mirroring, from one side to the other. If more than one disk on each side fails, that side is considered failed although the remaining disks are intact.

$$R_{RAID1/5} = 2R_5(t) - R_5^2(t)$$

Substituting R_{RAID5} given by Eq. (refeq:RAID5t):

$$R_{RAID1/5} = 2\left[\frac{\zeta e^{\eta t} - \eta e^{\zeta t}}{\zeta - \eta}\right] - \left[\frac{\zeta e^{\eta t} - \eta e^{\zeta t}}{\zeta - \eta}\right]^2 = \quad (75)$$

$$2\frac{\zeta e^{\eta t} - \eta e^{\zeta t}}{\zeta - \eta} - \frac{\zeta^2 e^{2\eta t} + \eta^2 e^{2\zeta t} - 2\eta\zeta e^{(\eta+\zeta)t}}{(\zeta - \eta)^2}$$

$$MTTDL_{mirrored/RAID5} = \frac{1}{\zeta - \eta} \left[-2\frac{\zeta}{\eta} + \frac{\eta}{\zeta}\right] - \frac{1}{(\zeta - \eta)^2} \left[-2\frac{\zeta^2}{\eta} + 2\frac{\eta^2}{\zeta} + 2\frac{\eta\zeta}{\eta + \zeta}\right]$$

RAID5 reliability can be expressed as a single component whose MTTF equals the MTTDL as was given by Eq. (47).

$$R_{RAID15}^{appr}(t) = 2R_5^{appr}(t) - [R_5^{appr}(t)]^2$$

$$MTTDL_{RAID15}^{appr} = \frac{1.5\mu}{N(N+1)\delta^2} = \frac{1.5MTTF^2}{N(N+1)MTTR}$$

25.2 Reliability of RAID5 Consisting of Mirrored Disks - RAID5/1

An approximate expression for mirrored RAID5 MTTDL was given in Xin et al. 2003 [240]. The contents of a failed disk are recovered by its mirror, but otherwise by invoking the RAID5 paradigm

$$MTTDL_{RAID5/1} \approx \frac{\mu^3}{4N(N-1)\delta^4} = \frac{MTTF^4}{4N(N-1)MTTR^3}$$

A rigorous method to derive RAID5/1 MTTDL using the shortest path reliability model is presented in Iliadis and Venkatesan 2015b [98]. The state tuples (x, y, z) indicate that there are x pairs with both devices in operation, y pairs with one device in operation and one device failed, and z pairs with both devices failed. With D devices on each side and failure rate δ and repair rate μ we have the following state transitions leading to *Data Loss - DL*:

$$\begin{aligned}
& (D, 0, 0) \xrightarrow{2D\delta} (D-1, 1, 0), \quad \xleftarrow{\mu} (D-1, 1, 0) \\
& (D-1, 1, 0) \xrightarrow{\delta} (D-1, 0, 1), \quad (D-1, 0, 1) \xleftarrow{2\mu} (D-1, 1, 0) \\
& (D-1, 1, 0) \xrightarrow{2(D-1)\delta} (D-2, 2, 0), \quad (D-2, 2, 0) \xleftarrow{2\mu} (D-1, 1, 0) \\
& (D-1, 0, 1) \xrightarrow{2(D-1)\delta} (D-2, 1, 1), \quad (D-2, 1, 1) \xleftarrow{\mu} (D-1, 0, 1) \\
& (D-2, 2, 0) \xrightarrow{2\delta}, \quad (D-2, 1, 1) \xleftarrow{\mu} (D-2, 2, 0) \\
& D_2, 1, 1) \xrightarrow{\delta} DL
\end{aligned}$$

Taking into account that $\delta \ll \mu$ we get the following end-to-end probabilities for the upper and lower paths.

$$\begin{aligned}
P_u &\approx \frac{\delta}{\mu} \times \frac{2(D-1)\delta}{2\mu} \times \frac{\delta}{2\mu} = \frac{(D-1)\delta^3}{2\mu^3} \\
P_{ell} &\approx \frac{2(D-1)\delta}{\mu} \times \frac{\delta}{\mu} \times \frac{\delta}{2\mu} = \frac{(D-1)\delta^3}{\mu^3} \\
P_{DL} = P_u + P_{\ell} &\approx \frac{3(D-1)\delta^3}{2\mu^3}
\end{aligned}$$

It is argued that the MTTDL is a product of two first device failures and the expected number of first device failure events:

Given that $MTTDL \approx E[T]/P_{DL}$, where $E[T] = 1/(N\delta)$. It follows that $MTTDL \approx 1/(N\delta P_{DL})$ and noting that $N = 2D$ we obtain:

$$MTTDL_{RAID(5/1)}^{(approx)} \approx \frac{\mu^3}{3D(D-1)\delta^4} = \frac{MTTF^4}{D(D-1)MTTR^3} \quad (76)$$

25.3 Shortcut Reliability Analysis to compare RAID1/5 and RAID5/1

That RAID5/1 is more reliable than RAID1/5 as shown by the shortcut reliability analysis in Thomasian 2006 [210]. We consider RAID with N disks and denote disk reliability with r .

$$R_{RAID1/5} = 1 - [1 - R_{RAID5}]^2 = 1 - [R^N + Nr^{N-1}(1-r)]^2 \quad (77)$$

The reliability of RAID5 with mirrored disks can be expressed as:

$$R_{RAID5/1} = NR_{RAID1}^{N-1} - (N-1)R_{RAID}^N = N[1 - (1-r)^2]^{N-1} - (N-1)[1 - (1-r)^2]^N \quad (78)$$

For all values on N it is easy to show from the above equations that $RAID_{5/1} > RAID_{1/5}$, e.g., for $N = 3$ we have

$$R_{RAID5/1} - R_{RAID1/5} = 6r^2(1-r)^4 > 0$$

Setting $r = 1 - \epsilon$ in the above equations and retaining only the lowest power of ϵ we have:

$$R_{RAID1/5} \approx 1 - \frac{1}{4}N^2(N-1)\epsilon^4 \quad R_{RAID5/1} \approx 1 - \frac{1}{2}N(N-1)\epsilon^4.$$

It is easy to see that $R_{RAID5/1} > R_{RAID1/5}$.

25.4 AutoRAID Hierarchical Array

AutoRAID is a two level memory hierarchy with two disks organized as RAID1 holding hot data and cold data with an RAID5/LSA organization Wilkes et al. 1996 [235]. Data is initially written onto RAID1 and as RAID1 disks fill their contents are moved to RAID5/LSA.

AutoRAID assumes that part of data that resides on RAID1 is active at any time and the working set changes slowly. Whole *Relocation Blocks* - RBs are promoted to RAID1 when they are updated.

26 Simulation Studies for Reliability Evaluation

The use of simulation in computer and network performance analysis dates back to late 1950s. An early application to study network delays is reported in [117], who in addition to a pseudo-random number generator used a builtin radio-active decay random number generator, which was found not to be random (personal communication from Prof. L. Kleinrock, 6/4/2022).

https://en.wikipedia.org/wiki/Radioactive_decay

The RAIDframe simulator could also be used for rapid prototyping for disk arrays [39]. RAIDframe was developed at CMU to assist in the implementation and evaluation of new RAID architectures. DiskSim with its origin at Univ. of Michigan Worthington et al. 1994 [238] was further developed at CMU's PDL, refer to Section 21.

The authors of Section refsec:DEH argue why they did not use HP's Pantheon disk array simulator:

<http://shiftright.com/mirrors/www.hpl.hp.com/research/ssp/papers/PantheonOverview.pdf>

or the DiskSim simulator developed at CMU's PDL.

<https://www.pdl.cmu.edu/DiskSim/index.shtml>

DiskSim relies on Dixtrac automated disk drive characterization, which provides disk specifications until 2007.

<https://www.pdl.cmu.edu/Dixtrac/index.shtml>

<https://www.pdl.cmu.edu/DiskSim/diskspecs.shtml>

Hsu and Smith 2004 [86] is a comprehensive study dealing with disk performance, whose abstract is as follows:

“In this paper, we use real server and personal computer workloads to systematically analyze the true performance impact of various I/O optimization techniques, including read caching, sequential prefetching, opportunistic prefetching, write buffering, request scheduling, striping, and short-stroking. We also break down disk technology improvement into four basic effects, faster seeks, higher RPM, linear density improvement, and increase in

track density and analyze each separately to determine its actual benefit. In addition, we examine the historical rates of improvement and use the trends to project the effect of disk technology scaling. As part of this study, we develop a methodology for replaying real workloads that more accurately models I/O arrivals and that allows the I/O rate to be more realistically scaled than previously. We find that optimization techniques that reduce the number of physical I/Os are generally more effective than those that improve the efficiency in performing the I/Os. Sequential prefetching and write buffering are particularly effective, reducing the average read and write response time by about 50% and 90%, respectively. Our results suggest that a reliable method for improving performance is to use larger caches up to and even beyond 1% of the storage used. For a given workload, our analysis shows that disk technology improvement at the historical rate increases performance by about 8% per year if the disk occupancy rate is kept constant, and by about 15% per year if the same number of disks are used. We discover that the actual average seek time and rotational latency are, respectively, only about 35% and 60% of the specified values. We also observe that the disk head positioning time far dominates the data transfer time, suggesting that to effectively utilize the available disk bandwidth, data should be reorganized such that accesses become more sequential.”

In what follows several simulation based studies are discussed.

26.1 Simulation Study of a Digital Archive

Digital archives require stronger reliability measures than RAID to avoid data loss from device failure. Multi-level redundancy coding is used to reduce the probability of data loss from multiple simultaneous device failures Wildani et al. 2009 [234]. This approach handles failures of one or two devices efficiently, while still allowing the system to survive rare-events, i.e., larger-scale failures of four or more devices.

The uber/super-parity is calculated from all user data in all disklets belonging to a stripe in the uber-group using another erasure code. The uber-parity can be stored on NVRAM or always powered-on disks to offset write bottlenecks, while still keeping the number of active devices low. The calculations of failure probabilities determined that the addition of uber/super-parities allows the system to absorb many more disk failures without data loss. Adding uber-groups negatively impacts performance when these groups need to be used for a rebuild. Since rebuilds using uber parity occur rarely, they impact system performance minimally. Robustness against rare events can be achieved for under 5% of total system cost.

26.2 Simulation of Hierarchical Reliability

Hierarchical RAID - HRAID was described in Thomasian 2006 [209] and evaluated in Thomasian et al. 2012 [219]. There are N Storage Nodes - SNs, where each SN has a DAC - Disk Array Controller with a cache serving M disks. HRAID(k/ℓ) provides recovery against k SN failures and ℓ disk failures at each node, which means k (resp. ℓ) strips out of M strips per stripe (at each SN) are dedicated to inter-SN (resp. intra-SN) check strips. Data and inter-SN check strips are protected by intra-SN check strips. It can be said HRAID k/ℓ is k -Node-Failure Tolerant and ℓ DFT Hierarchical RAID is shown in Figure 25.

Parities are rotated from row-to-row and SN to SN to ensure that Q parities cover all SN strips for inter-SN rebuild. The P parity is used for intra-SN rebuild due to a local disk failure and they cover data and Q parity strips (as stated earlier).

Node 1				Node 2				Node 3				Node 4			
$D_{1,1}^1$	$D_{1,2}^1$	$P_{1,3}^1$	$Q_{1,4}^1$	$D_{1,1}^2$	$P_{1,2}^2$	$Q_{1,3}^2$	$D_{1,4}^2$	$P_{1,1}^3$	$Q_{1,2}^3$	$D_{1,3}^3$	$D_{1,4}^3$	$Q_{1,1}^4$	$D_{1,2}^4$	$D_{1,3}^4$	$P_{1,4}^4$

Figure 25: HRAID1/1 with $N = 4$ nodes, $M = 4$ disks per node. P is the intra-SN and Q the inter-SN parity. Only the first stripe on all 4 SNs is shown in the figure.

Intra-SN rebuild is carried out by restriping (Rao et al. 2011 [172]) so that we may have the following progression [214]:

$$RAID7 \rightarrow RAID6 \rightarrow RAID5 \rightarrow RAID0 \rightarrow Data_Loss.$$

InterSN rebuild is carried by overwriting Q strips.

Three options for HRAID operation are considered.

I. Intra-SN but no Inter-SN Redundancy: There are N independent SNs which are RAID($4 + \ell$) disk arrays. This option serves as a baseline in reliability comparisons comparisons.

Option II: Inter-SN Redundancy and Rebuild Processing: Inter-SN rebuild processing is invoked on demand and for rebuild.

Option III: Inter-SN Redundancy, but no Rebuild Processing: Rebuild may not be possible due to limited interconnection network bandwidth. In the case of SNs considered failed due to the failure of more than ℓ failed disks but no controller failures, operation continues in degraded mode with on-demand reconstruction via inter-SN redundancy, until data loss detected. This is strictly done to determine the MTDDL, since the system can continue operation .

Given that u is a uniformly distributed pseudo-random numbers in the range $(0, 1)$, it can converted to (negative) exponential distribution to determine the time to next failures. Given u exponentially distributed random numbers can be obtained as follows.

$$F(t) = 1 - e^{-\delta t} = u \text{ leads to } t = (-1 / \sum_{\forall i} \delta_i) \times \ln(1 - u) \text{ or just } t = -\text{MTTF} \times \ln(u).$$

$\sum_{\forall i} \delta_i$ is the sum of the failures rates of all components.

More complex methods for obtaining distributions are available. The accuracy of simulation results is specified by the confidence interval at a given confidence level. The two topics are discussed in Chapters 5 and 6 in Lavenberg 1983 [124].

Procedure: Hierarchical RAID Simulator to Determine MTDDL

- Inputs:** N : The number of SNs.
 M : The number of disks per SN.
 $D = N \times M$: Total number of disks.
 k : Internode redundancy level ($k = 0$ for Option I).
 ℓ : Intranode redundancy level, $\ell = 0$ for RAID0, else RAID($4 + \ell$).
 δ : Disk failure rate, $\delta = 10^{-6}$ and $\text{MTTF} = 1/\delta = 10^6$ hours.
 γ : Controller failure rate, multiple of δ).

Outputs (with initializations):

$F_{cd} = 0/1$ data loss occurred due to controller/disk failure.

$N_c = 0$: number of failed controllers.

Initialize SN/controller state: $C[n] = 1, \forall n$.

Initialize number of failed disks at n^{th} SN: $F[n] = 0, \forall n$.

Simulation Variables: $Clock = 0$: Simulation time initialized.

State 0: Failed. State 1: Operational.

$C[0 : N - 1]$ the state of controllers. $Disks[0 : N - 1, 0 : M - 1]$ the state of $D = N \times M$ disks.

$(Disks[n, m] = 1, \forall n, \forall m)$. /* initial disk states*/

$F[0 : N - 1]$ # of failed disks at node n Ω : Failure rate for a given configuration.

T_{NF} : Time to next failure.

$N_c = 0$: Number of failed controllers.

$N_n = 0$: Number of failed nodes for to controller and $> \ell$ disk failures

$N_d = 0$: number of failed disks.

u_i : i^{th} uniformly distributed pseudo-random variable in $(0, 1)$.

Simulation steps:

Step_1: Total failure rate since all failures exponential: $\Omega = (N - N_c)\gamma + (D - N_d)\delta$.

Compute time to next failure and increment $Clock$:

$T_{NF} = (-1/\Omega)\ln(u_1)$,

$Clock += T_{NF}$. /* advance simulation clock */

Step_2: Probability a controller failed: $p = (N - N_c)\gamma/\Omega$.

If $u_2 \leq p$ then controller failure: goto Step 4.

Else disk failure: goto Step 4.

Step_3: Determine failed controller: $n = \lfloor N \times u_3 \rfloor$.

If $C[n] = 0$ then regenerate u_3 and recompute n ,

else $\{ C[n] = 0, N_c ++, N_n ++, D[n, m] = 0, 0 \leq m \leq M - 1,$

$t = M - F[n]$ disk inaccessible, so $N_d = N_d + t. \}$

If $N_n > k$ then $\{F_{cd} = 0, \text{goto Step 6}\}$, else goto Step_1.

Step_4: $t = \lfloor D \times u_4 \rfloor$. /* index of failed disk */

SN number: $n = \lfloor t/M \rfloor$;

Disk number: $m = \text{mod}(t, M)$.

If $Disks[n, m] == 0$ (disk already failed) resample u_4 and recompute n and m ,

/* disks attached to failed controller are considered failed */

else $\{ Disks[n, m] == 0, N_d ++, F[n] ++ \}$.

If $F[n] \leq \ell$ goto Step_1.

else $\{ C[n]=0, t = M - F[n], N_d = N_d + t, N_n ++ \}$.

If $N_n \leq k$ then go to Step_1, else $F_{cd} = 1$.

Step_5: Return($Clock, F_{cd}, N_c, N_{df}$).

The simulation is repeated to obtain confidence intervals at a sufficiently high confidence level.

It is shown by the shortcut reliability analysis method Thomasian 2006 [210] and results based on the above simulation in Thomasian et al. 2012 [219] that a higher MTTDL is attained by associating higher reliability at the intra-SN rather than inter-SN level. For example, given three check strips P, Q, R, then P and Q can be used for as intra-SN and R for inter-SN recovery. This is contradictory to the two preferred configurations for IBM's Intelligent Bricks project described in Wilcke et al. 2006 [233],

(1) 1DFT (RAID5) at the the node level and 2NFT at the node level provides 40-75% storage efficiency.

(2) 0DFT in bricks and 3NFT at brick level provides 50-75% storage efficiency.

26.3 Proteus Open-Source Simulator

The Proteus open-source simulator developed at *Storage Systems Research Center - SSRC at U. Calif. at Santa Cruz - UCSC* can be used to predict the risk of data loss in many disk array configurations: mirrored disks, all RAID levels, and two-dimensional arrays Kao et al. 2013 [113]. Proteus was used to learn that there is no measurable difference between values obtained assuming deterministic versus exponential repair times, which are used in Markov chain modeling, which was an issue raised in RAID5 reliability analysis in Gibson 1992 [65].

26.4 CQSIM_R Tool Developed at AT&T

CQSIM_R is a tool suited for predicting the reliability of large scale storage systems Hall 2016 [79]. It includes direct calculations based on an only-drives-fail failure model and an event-based simulator for predicting failures. These are based on a common combinatorial framework for modeling placement strategies.

CQSIM_R models common storage systems, including replicated and erasure coded designs. New results, such as the poor reliability scaling of spread-placed systems and a quantification of the impact of data center distribution and rack-awareness on reliability, demonstrate the tools' usefulness. Analysis and empirical studies show the tool's soundness, performance, and scalability.

26.5 SIMedc Simulator for Erasure Coded Data Centers

The discrete-event SIMedc simulator for the reliability analysis of erasure-coded data centers was developed at *Chinese Univ. of Hong-Kong - CUHK* by Zhang et al. 2019 [248]. SIMedc reports reliability metrics of an erasure-coded data center based on data center topology, erasure codes, redundancy placement, and failure/repair patterns of different subsystems based on statistical models or production traces.

Simulation is accelerated via importance sampling assisted by uniformization which is discussed in Section 30.5. It is shown that placing erasure-coded data in fewer racks generally

improves reliability by reducing cross-rack repair traffic, even though it sacrifices rack-level fault tolerance in the face of correlated failures.

27 Reliability Modeling Tools

Analytic and simulation software packages developed to assess the reliability, availability, and serviceability of computer systems are surveyed in Johnson and Malek 1988 [109]. Provided are the application of the tool, input, models, and model solution methods.

In what follows we discuss three reliability modeling tools: ARIES at UCLA in Subsection 27.1, SAVE at IBM Research in Subsection 27.2, SHARPE at Duke Univ. in Subsection 27.3.

27.1 Automated Reliability Interactive Estimation System - ARIES Project at UCLA

Triple Modular Redundancy - TMR with the voter outputting the majority outcome until a unit fails was an early proposal to achieve high reliability. The system continues operation until two units disagree. Assuming the voter hardware is less complex than its input units and hence its contribution to system failure is negligible, so we voter reliability to one. Given the unit reliabilities: $r(t) = e^{-\delta t}$.

$$R_{TMR}(t) = r^3(t) + 3r^2(t)(1 - r(t)) = 2e^{-3\delta t} - 3e^{-2\delta t}, \text{MTTF}_{TMR} = \int_0^{\infty} R_{TMR}(t)dt = \frac{5}{6\delta}$$

Note that $MTTF_{TMR} < R_{simplex} = 1/\delta$, but TMR reliability exceeds that of a single unit for $(0, t_m)$, where t_m the mission time can be determined as follows:

$$3e^{-2\delta t_m} - 2e^{-3\delta t_m} > e^{-\delta t_m} \text{ so that } t_m < \frac{\ln(2)}{\delta}$$

TMR/Simplex is a TMR variant that continues its operation after failure with a single unit according to a hypoexponential distribution with parameters 3δ and δ Trivedi 2002 [228].

$$R_{TMR/Simplex}(t) = 1.5e^{-\delta t} - 0.5e^{-3\delta t} \text{ sum of MTTFs for 2 phases of operation: } MTTF_{TMR/Simplex} = \frac{1}{3\delta}$$

Application of Shortcut Method to Reliability Comparison

We apply the shortcut method in Thomasian 2006 [210] to the problem at hand for a small t_s .

$$R_{TMR/Simplex}(t_s) = 1.5e^{-\delta t_s} - 0.5e^{-3\delta t_s} \approx 1.5(1 - \delta t_s + 0.5(\delta t_s)^2 - \dots) - 0.5(1 - 3\delta t_s + 0.5(3\delta t_s)^2 - \dots) =$$

We also compare TME/Simplex with TMR and its observed that TMR/Simplex is more reliable

$$R_{TMR} = 3e^{-2\delta t_s} - 2e^{-3\delta t_s} \approx 3(1 - 2\delta t_s + 0.5(2\delta t_s)^2 + \dots) - 2(1 - 3\delta t_s + 0.5(3\delta t_s)^2 + \dots) = 1 - 3(\delta t_s)^2$$

An example of a reliability expression derived for a particular system is that of a hybrid k -out-of- n system with n components energized (with failure rate λ) and m components deenergized (with failure rate μ) Mathur and Avizienis [138], which is given in Example 3.32 in Trivedi 2002 [228].

Aries is a unifying method for analyzing closed systems Ng and Avizienis 1980 [152]. In closed systems no new spares can be introduced as in the case for space-borne computers. The parameters used in this study are:

N	initial number of modules in the active configuration.
D	number of degradations allowed in the active configuration
S	number of spare modules.
Ca	coverage for recovery from active module failures.
Cd	coverage for recovery from spare module failures.
λ	failure rate of active modules.
μ	failure rate of spare modules
\mathbf{Y}	sequence of allowed degradations of the active configuration.
\mathbf{CY}	coverage vector for transitions into degraded configuration.

Table 14: Parameters used in Ng and Avizienis 1970 [152]

The reliability of a closed fault-tolerant system has a reliability function of the form:

$$R(t) = \sum_{\forall i} A_i e^{-\sigma_i t} \quad (79)$$

The analysis is based on the eigenvalues of the CTMC representing the failure of system components and its recovery by using spares. Repeated roots are not considered.

Let S_i indicate a nonfailed state and σ_i the failure rate at that state. A_i can be expressed as a function of state parameters can be quite complex. The MTFE easily follows from Eq. 79

$$\text{MTFF} = \int_{t=0}^{\infty} R(t) dt = \sum_{\forall i} \frac{A_i}{\sigma_i}.$$

For closed systems $R(t)$ given by Eq. (79) has a specific form.

$$R(t) = X(t) \mathcal{A} W(t) \quad (80)$$

$$X(t) = (e^{-Y[0]\lambda t}, \dots, e^{-Y[D]\lambda t}) \text{ with } Y[0] = N \quad \text{and } W(t) = (1, e^{-\mu t}, \dots, e^{-S\mu t}),$$

$$\mathcal{A} = \begin{pmatrix} A_{S,0}^0 & \cdots & A_{S,0}^D \\ \vdots & \ddots & \vdots \\ A_{S,S}^0 & \cdots & A_{S,S}^D \end{pmatrix} \quad (81)$$

Two more parameters used for modeling repairable systems are the number of repairman or repair facilities (M) and the repair rate of one repairman (Ψ)

27.2 System Availability Estimator - SAVE Project at IBM Research

An early and influential reliability modeling effort at IBM is Bouricius et al. 1971 [25]. The coverage factor (c) which is the probability that the system can successfully recover from a failure is defined in this study. An example of such calculations is the probability of encountering LSEs in RAID5 with and without IDR or disk scrubbing Iliadis et al. [95].

The processors of a duplex systems fail with rate δ and the coverage factor is c according to Example 8.35 in Trivedi 2002 [228]. Given that S_i is a state with i failed disks we have the following transitions:

$$S_0 \xrightarrow{2\delta c} S_1, \quad S_0 \xrightarrow{2\delta(1-c)} S_2, \quad S_0 \xleftarrow{\mu} S_1, \quad S_1 \xrightarrow{\delta} S_2. \quad (82)$$

The SAVE project was started in Steve Lavenberg's Systems Modeling and Analysis Dept. at IBM Research in mid-1985. The effort first dealt with analytical reliability modeling techniques, along the lines adopted in ARIES and SHARPE Blum et al. 1994 [23].

Adopting simulation as an alternative to analysis for reliability estimation led to unified framework for simulating Markovian models of highly dependable systems Goyal et al. 1992 [69], This is because realistic system models are often not amenable to analysis using conventional analytic or numerical methods as discussed in Section 30. Straightforward simulations is too costly since failures are rare. Techniques for fast simulation of models of highly dependable systems are reviewed in Nicola et al. 2001 [154]. Importance sampling is one such method and when it works well it can reduce simulation run lengths by several orders of magnitude.

The following example is provided in this study: (1) two sets of processors with four processors per set, (2) two sets of controllers with two controllers per set, (3) four clusters of disks each consisting of four disks. The multiprocessors are connected to all controllers. The pair of controllers have two connections to disk clusters. In a disk cluster, data are replicated so that one disk can fail without affecting the system. The ID organization for mirrored disks in Section 24 is utilized.

When a processor fails it has a 0.01 probability of causing another processor to fail. Each unit in the system has two failure modes which occur with equal probability. The repair rates for mode 1 and 2 failures are 1 and 0.5 hour, respectively. The failure rates in hour⁻¹ are 1/1000 for processors, 1/20,000 for controllers, and 1/60,000 for disks. The repair rates (per hour) are 1 for all mode 1 failures and 1/2 for all mode 2 failures.

Efficient simulation techniques for estimating steady-state quantities in models of highly dependable computing systems with general component failure and repair time distributions are developed in Nicola et al. 1993 [153]. The regenerative method of simulation for steady state estimation can be used when the failure time distributions are exponentially distributed. A splitting technique is used for importance sampling to speed up the simulation of rare system failure events during a cycle. Experimental results show that the method is effective in practice.

27.3 Symbolic Hierarchical Automated Reliability and Performance Evaluator - SHARPE

SHARPE is a reliability and performance modeling tool was developed at Duke Univ. by Sahner, Trivedi and Puliafito 1996 [180]. Several generations of Trivedi's students have contributed to SHARPE.

Parameter	Definition
n	number of storage devices
c	amount of data stored on each device
r	replication factor
k	spread factor of data placement scheme
b	reserved rebuild bandwidth per device
$1/\lambda$	mean time to failure of a storage device
U	amount of user data stored in the system ($U = nc/r$)
$1/\mu$	time to read data amount c at rate b ($1/\mu = c/b$)

Table 15: Systems parameters with derived parameters below the line.

<https://sharpe.pratt.duke.edu/>

Section 5.4 titled “Imperfect Fault Coverage and Reliability” in Trivedi 2002 [228] provides a good discussion of the topic and some formulas derived in Ng and Avizienis [152]. Section 8.5 titled “Markov Chains with Absorbing States” discusses a technique used in Sharpe as discussed in Appendix II. Hierarchical reliability modeling is discussed in Chapter 16 in Trivedi and Bobbio 2017 [229]. The mathematics behind SHARPE is covered in Appendix II.

28 Reliability Analysis at IBM Zurich Research Lab - ZRL

Earlier work on reliability of storage systems at ZRL dealt with a comparison of different *Intra-Disk Redundancy - IDR* methods on reducing the effect of LSEs on disk failures in Dholakia et al. [46]. Other topics studied at ZRL are discussed below:

28.1 System Reliability Metrics

Most redundancy schemes have been evaluated via the MTTDL metric, which has been proven useful for assessing tradeoffs, for comparing reliability schemes and for estimating the effect of the various parameters on system dependability.

That MTTDL derivations based on CTMC models provide unrealistically high reliability estimates by Elerath and Schindler 2014 [51] is refuted by Iliadis and Venkatesan 2015 [97] by showing that MTTDL equations that account for latent sector errors and scrubbing operations yield satisfactory results.

In the context of distributed and cloud storage systems the magnitude of lost data is as important as the frequency of data loss. A general methodology to obtain the EAFDL metric analytically, in conjunction with the MTTDL metric, for various redundancy schemes and for the Weibull and Gamma real-world distributions Trivedi 2002 [228] is provided in this study.

It is shown that the declustered placement scheme offers superior reliability in terms of both metrics. The parameters used in the study are summarized in Table 15.

At any point the system is either in normal or rebuild mode, which starts immediately after a failure. Deferring rebuild has its advantages, since some disk failures are due to transient server failures and are resolved by restarting servers. Following a first-device failure, rebuild operations and subsequent device failures may occur, which eventually lead the system either to *Data Loss - DL* with probability P_{DL} or back to the original normal mode by restoring all replicas with

D_1	D_2	D_3	D_4	D_5	D_6
A	A	K	K	.	.
B	B	L	L	.	.
C	C
D	D
E	E
F	F
G	G
I	I
J	J

D_1	D_2	D_3	D_4	D_5	D_6
A	A	B	C	D	E
B	F	G	H	I	J
C	K	K	L	.	.
D	D
E	E
F	F
G	G
I	I
J	J

Figure 26: Clustered and declustered data placement with six devices with degree of replication $r = 2$.

probability $1 - P_{DL}$. Typically, rebuild time is negligible compared to the time between failures: $E[T] = 1/(n\delta)$. Given that the expected number of first-device failures until data loss occurs is $1/P_{DL}$. It follows:

$$MTTDL \approx \frac{E(T)}{P_{DL}} \quad (83)$$

Let H denote the amount in data loss when data loss occurs and U is the amount of stored user data. EAFDL is then the normalized data lost per MTTDL:

$$EAFDL = \frac{E[H]}{MTTDL \cdot U} \quad (84)$$

Define Q as follows: $Q = H$ if DL and $Q = 0$ if no DL. Given $E(Q)$ we can determine EAFDL as follows:

$$E(Q) = P_{DL} \cdot E(H), \text{ hence: } EAFDL = \frac{E(Q)}{E(T)U} \quad (85)$$

28.2 Clustered versus Declustered Data Placements

To justify the EAFDL measure consider clustered and declustered data placements. In *Clustered Placement - CP* the k blocks on a device are replicated in another device, while in *Declustered Placement - DP* the k blocks are distributed over k blocks as shown in Figure 26.

In both cases two node failures will lead to data loss, but two node failures with DP result in a lower data loss than CP. Expressions for MTTDL and EAFDL derived in Iliadis and Venkatesan 2014 [96] are as follows:

$$MTTDL \approx \begin{cases} \left(\frac{b}{\delta c}\right)^{r-1} \frac{1}{n\delta} & \text{for CP} \\ \left(\frac{b}{2\delta c}\right)^{r-1} \frac{(r-1)!}{n\delta} \prod_{e=1}^{r-2} \left(\frac{n-e}{r-e}\right)^{r-e-1} & \text{for DP} \end{cases}$$

$$EAFDL \approx \begin{cases} \left(\frac{\delta c}{b}\right)^{r-1} \lambda & \text{for CP} \\ \left(\frac{2\delta c}{b}\right)^{r-1} \frac{\delta}{(r-1)!} \prod_{e=1}^{r-1} \left(\frac{r-e}{n-e}\right)^{r-e} & \text{for DP} \end{cases}$$

Analytical reliability expressions for the symmetric, clustered, and declustered data placement schemes are derived in Iliadis 2022 [102], where it is demonstrated that the employment of lazy rebuild results in a reliability degradation of orders of magnitude. The degradation of MTTDL due to sector errors is observed in all cases, those that apply lazy rebuild, and those that

do not. By contrast there is no degradation for the EAFDL. It is also shown that the declustered data placement scheme offers superior reliability.

The adverse effect of LSEs on the MTTDL and the EAFDL reliability metrics is evaluated in Iliadis 2023 [103]. A theoretical model is developed, and closed-form expressions for the metrics of are derived. Highly reliable storage devices with a very small ratio for mean time to repair ($1/\mu$) to mean time failure ($1/\lambda$), expressed as:

$$\mu \int_0^{\infty} F_{\lambda}(t) [1 - F_X(t)] dt \ll 1 \quad \text{with} \quad \frac{\lambda}{\mu} \ll 1$$

The MTTDL and EAFDL are obtained analytically for (i) the entire range of bit error rates; (ii) the symmetric, clustered, and declustered data placement schemes; and (iii) arbitrary device failure and rebuild time distributions under network rebuild bandwidth constraints. For realistic values of sector error rates the MTTDL degrades, while EAFDL remains practically unaffected. In the range of typical sector error rates and for very powerful erasure codes, EAFDL degrades as well. It is also shown that the declustered data placement scheme offers superior reliability. The actual probability of data loss in the case of correlated symbol errors is smaller than that obtained assuming independent symbol errors and of the same order of magnitude.

28.3 Performance Analysis of a Tape Library System at ZRL

An analytical model to evaluate the performance of a tape library system is presented in Iliadis et al. 2016 [99]. The analysis takes into account the number of cartridges and tape drives as well as different mount/unmount policies to determine the mean waiting time for tapes. The accuracy of the model is confirmed by validation against measurements. Earlier work on this topic is also reviewed.

A tape library consists of tape drives, robot arms, a storage rack for the tape cartridges, and a cartridge control unit. To serve a request, a robot arm fetches the appropriate tape cartridge from the storage rack and delivers it to a free tape drive. The tape drive control unit mounts the tape, positions the head to the desired file and then transfers its data. To free a tape drive, a robot arm unmounts the tape cartridge and returns it to the storage rack. Tape read/write requests contain the cartridge id, the position of the data block in the cartridge, and its size. Requests submitted for cartridges are queued and served according to a scheduling policy. The hierarchical scheduling algorithm ensuring fairness and avoiding starvation is as follows:

Upper level: Cyclic or round-robin scheduling among the queues (mounting cartridges).

Lower level: A FCFS policy for serving requests within a queue (reading from a mounted cartridge).

When all requests for a cartridge are served (exhaustive service), and there are still pending requests at some other, non-mounted cartridge, an unused cartridge is unmounted and another cartridge with pending requests is mounted. If, however, there are no other pending requests to any other non-mounted cartridge, the cartridge can either remain mounted in anticipation of future requests or be unmounted so as to save time when future requests arrive for other non-mounted cartridges. Two mount/unmount policies deployed in this context are:

Parameter	Values	Definition
c	3200	number of cartridges
d	32	number of tape drives
a	1,2	number of arms
R	5 s (fixed)	robot transfer time
t_L	24 s (fixed)	load ready time
\bar{t}_R	59 s	mean rewind time
\bar{t}_U	24 s	unload ready time
s_{max}	118 s	maximum seek time
\bar{Q}	843 MB	mean request size
\bar{Q}^2	2.8 GB	standard deviation
b_w	360 MB/s	bandwidth
n	100	# cartridges per tape drive
M	20 s (fixed)	mount time $M = R + t_L$
\bar{U}	88 s	mean unmount time ($\bar{U} = \bar{t}_R + t + U + R$)
\bar{t}_T	2.34	mean transfer time ($t_T = \bar{Q}/b_w$)

Table 16: Parameter values according to Table II in Iliadis et al. 2021 [101].

Always-Unmount (AU): A tape cartridge is immediately unmounted upon completion of all pending requests for it in anticipation of the next request arriving for another non-mounted cartridge.

Not-Unmount (NU): A tape cartridge remains mounted upon completion of all pending requests for it in anticipation of the next request arriving for this same currently mounted, but idle cartridge.

The performance analysis of the resulting polling system relies on state-dependent queues Takagi 1986 [195] Parameters considered in this study are given in Table 16 based on IBM 2021 [94].

Predicting the performance of a tape library system is key to efficiently dimensioning it, possibly in the context of multi-tiered storage systems that include tape libraries. The effect of two mount/unmount policies was analytically assessed. For light loads, the AU - Always-Unmount policy yields a mean delay that is lower than that of the NU - Not-Unmount policy, with the difference becoming negligible as the load increases. The effect of the number of robot arms was assessed by means of simulation shows that given fast robot arms multiple arms do not provide a significant performance improvement, but multiple arms may be necessary to attain higher availability. The analysis has been extended in Iliadis et al. 2021 [101]

29 Flash Solid State Drives - SSDs

Flash SSDs which are fast, nonvolatile, consume less power than HDDs are replacing them for high performance applications as their prices are dropping. https://en.wikipedia.org/wiki/Hard_disk_drive

https://en.wikipedia.org/wiki/Flash_memory

Flash SSDs are classified according to the cell type, i.e., number of bits per cell: SLC (single), MLC (multiple-2), TLC (triple), QLC (quad), PLC (penta). There is a rapid drop in *Program/Erase* - *P/E* cycles as the cell size is decreased from 5 nanometer-nm to 1nm (Fig. 1 in

Jaffer et al. 2022 [106] and given in Table 17.

<https://blocksandfiles.com/2019/08/07/penta-level-cell-flash/>

Cell type	SLC (1 bit)	MLC (2 bits)	TLC (3 bits)	QLC (4 bits)	PLC (5 bits)
5Xnm	11,00	10,000	2,500	800	400
3Xnm	10,000	5,000	1,250	350	175
2Xnm	7,500	3,000	750	150	75
1Xbn	5,000	1,500	500	70	35

Table 17: P/E cycles for varying number of bits-per-cell as cell size is varied. The number for PLC are estimated.

To summarize (10 QLC WOM-v(2,4) can store 2 logical bits per cell. (20 MLC drives also store 2 logical bits per cell. (3) Without WOM-v coding, MLC drive has better endurance than QLC drive.

A comparison of flash SSDs and HDDs from several viewpoints is presented in Table 18. Flash storage is discussed in more detail in Section 2.3.20 in Thomasian 2021 [224].

Performance-wise SSDs outperform HDDs. For example., Huawei OceanStor Dorado 18000 V6, set a new peak for SPC-1 Benchmark performance in Oct. 2020, achieving 21,002,561 SPC-1 IOPS according to *Storage Performance Council - SPC*:

<https://e.huawei.com/en/products/storage/all-flash-storage/dorado-8000-18000-v6>

HDDs led in price-performance with the SPC-2 benchmark in March 2017.

<https://www.spcresults.org>.

Rebuild times for HDDs and SSDs are given in Table 19.

https://www.theregister.com/2016/05/13/disak_versus_ssd RAID_rebuild_times/

The one and four TB drives just differ in the number of platters, but are based on the same technology, Seagate 18 TB drives with 564 MB/s transfer rate takes about nine hours to read, which is due to the fact that disk transfer rates have not kept up with disk capacities. The Seagate dual actuator HDDs area is a partial solution doubling transfer rate from 6 to 12 Gb/s.

<https://www.tomshardware.com/news/seagate-launches-2nd-gen-dual-actuator-hdds-18-tb>

<https://www.storagereview.com/news/seagate-exos-2x18>

The much higher bandwidth provided by Flash SSDs is a better solution.

In spite of problems such as “flash wear” Flash SSDs are much more reliable than HDDs. Counting the AFRs - Annual Failure Rates of Backblaze’s drives; HDDs had a 10.56% AFR, while SSDs had just 0.58% AFR.

<https://www.backblaze.com/blog/backblaze-hard-drive-stats-q1-2021/>

This makes higher levels of redundancy less of a consideration for SSDs. Given the superior

Device & Year	Capacity (GB)	Cost (\$)	Cost/MB	Random Access Latency/Bandwidth	Seq'l Access Bandwidth	Device Scan (s)
HDD'08	0.1	2K	200	28/0.28	1.2	83
HDD'10	1000	300	0.0003	8/0.98	80	12,500
SSD'10	00	2000	0.02	0.026/300	700	143

Table 18: Comparison of HDDs and SSDs (latency in msec, bandwidth in MB/s) Athanassoulis et al. 2010 [11]

RAID	Capacity TB	Seq'l Write MB/sec	Rebuild time Minutes
Disk-1/2/3	0.72/1/4	80/115/460	15/145/580
FlashMax III	2.2	1,400	26
Intel D3600	2	1,500	22
Micron 9100	3.2	1,500	27
Intel DC 3608	4	3,000	22

Table 19: Minimum rebuild times for disks and flash SSDs. Capacity in TB times 1000 divided by Seq'l write in MB/s yields rebuild time in seconds

performance of SSDs with respect to HDDs hybrid arrays are of no interest, unless SSD capacities are exceeded in which SSDs may cache HDD data Yu et al. 2012 [246]. Conversely increasing SSDs sizes allow them to hold large databases, but a portion of the database can be supplemented with disks. Indexing structures support on flash SSDs is discussed in Fevgas et al. 2020 [54].

Flash wear can be reduced by first writing into *Storage Class Memory - SCM*, before being downloaded in large chunks to Flash SSD to reduce wear.

Evolving SCMs are discussed in Freitas and Wilcke 2008 [57]

HDDs still provide less costly storage per GB, but NAND Flash technology is progressing rapidly yielding higher capacity chips at lower cost.

<https://www.intel.com/content/www/us/en/products/docs/memory-storage/solid-state-drives/ssd-vs-hdd.html>

The disk/flash crossover is discussed in this work.

<https://blocksandfiles.com/2023/02/15/pure-the-disk-flash-crossover-event-is-closer-than-you-think/> and the Purestorage CEO projected in 2023 that no disk drives will be sold after 2028.

<https://blocksandfiles.com/2023/05/09/pure-no-more-hard-drives-2028/>

Data updates in SSDs are carried out by writing a new copy, as in LFS, rather than overwriting old data, marking prior copies of data invalidated. Writes are performed in units of pages, similarly to disks, even if data to be written is smaller. Space is reclaimed in units of multipage erasing, which necessitates copying of any remaining valid pages in the block before reclamation.

The efficiency of the cleaning process greatly affects performance under random workloads; *Write Amplification factor - WAF* defined as the ratio of the amount of data an SSD controller writes in relation to the amount of data that the host's flash controller writes reduces application throughput. A nearly-exact closed-form solution for write amplification under greedy cleaning for uniformly-distributed random traffic is presented in Desnoyers 2014 [42] and validated using simulation.

Log-Structured File System for Infinite Partition is a scheme eliminates garbage collection in flash SSDs Kim et al 2022 [116]. The scheme separates *Logical Partition Size - LPS* from the physical storage size and the LPS is large enough so that there is no lack of free segments during SSD's lifespan, allowing the filesystem to write the updates in append-only fashion without reclaiming the invalid filesystem blocks. The metadata structure of the baseline filesystem, so that it can efficiently handle the storage partition with 2^{64} sectors. Interval mapping minimizes the memory requirement for the *Logical Block Address - LBA-to-PBA* translation in *Flash Translation Layer - FTL*.

FTL is a hardware and software layer is part of flash memory controllers.

https://en.wikipedia.org/wiki/Flash_memory_controller

FTL's role is to emulate a block-type peripheral such as HDDs.

The effect of Flash memories on transaction performance has been investigated using simulation and measurement studies. NoFTL allows for native Flash access and integrates parts of the FTL functionality into the DBMS yielding significant performance increase and simplified I/O stack Hardock et al. 2013 [81]. A Flash emulator integrated with a DBMS (Shore-MT) demonstrate a performance improvement of ≈ 3.7 -fold under various TPC workloads.

Performance evaluation of the write operation in flash-based SSDs is reported in Bux 2009 [29]. Performance of greedy garbage collection in flash-based SSDs by Bux and Iliadis 2010 [30]. Scheduling and performance modeling and optimization by Bux et al. 2012 [31]. The complicating factor in flash SSDs is write performance which is analyzed in Desnoyers 2014 [42].

Flash SSD storage is available from PureStorage, Dell/EMC, NetApp, Fungible, Oracle (Exadata), etc. Flash SSDs outperform HDDs in power consumption 3-fold (2-5 watts) versus (6-15 watts). From a TCO viewpoint SSDs will be preferred when they are less than 5-fold expensive than HDDs per GB.

<https://www.intelice.com/ssd-or-hdd-hard-drives/>

Vastdata is a Flash SSD-based storage system which adopts LSA, but does not provide block storage, which takes any data, like a file or database entry, and divides it into blocks of equal sizes.

<https://vastdata.com/whitepaper>

<https://vastdata.com/blog/providing-resilience-efficiently-part-ii>

Since SSDs play an important role in data centers their failures affect the stability of storage systems and cause additional maintenance overhead. The *Multi-View and Multi-Task Random Forest - MVTRF* scheme described in [249] is a scheme to predict SSD failures based on multi-view features extracted from both long and short-term monitoring of SSD data. MVTRF can simultaneously predict the type of failure it is and when it will occur. These are useful for handling SSD failures. MVTRF has been evaluated on the large-scale Tencent data centers showing its high failure prediction accuracy and improves precision by 46.1% and recall by 57.4% on average compared with the existing schemes.

https://en.wikipedia.org/wiki/Precision_and_recall

29.1 Write-Once Memory - WOM Codes to Enhance SSD Lifetimes

Increased storage density is achieved with higher bits per cell, but is accompanied by order of magnitude lower P/E cycles, which decreases the number of times the SSD can be rewritten and their lifetime.

Write-Once Memory - WOM codes are one way of improving drive lifetime. i.e., rewrite on top of pre-existing data without erasing previous data. WOM codes alter the logical data before it is physically written, thus allowing the reuse of cells for multiple writes. On every consecutive write, zeroes may be overwritten with ones, but not vice versa Yaakobi et al. 2012 [245]. A WOM(x,y) code encodes a code word of x bits into a code word of y bits

WOM increases the total logical data that can be written on the physical medium before requiring an erase operation. Traditional WOM codes are not scalable and only offer up to 50% increase in total writable logical data between any two erase operations. Simple and highly

v(3,4)	v(2,4)	v(1,4)
D111,V15,G2	D11,V15,G5	D1,V15,-
D110,V14,G2	D10,V14,G5	D0,V14,G14
D101,V13,G2	D01,V13,G5	D1,V13,G13
D100,V12,G2	D00,V12,G5,G4	D0,V12,G12
D011,V11,G2	D11,V11,G4	D1,V11,G11
D010,V10,G2	D10,V10,G4	D0,V10,G10
D001,V09,G2	D01,V09,G4,G3	D1,V09,G09
D000,V08,G2	D00,V08,G3	D0,V08,G08
D111,V07,G1,G1	D11,V07,G3	D1,V07,G07
D110,V06,G1	D10,V06,G3,G2	D0,V06,G06
D101,V05,G1	D01,V05,G2	D1,V05,G05
D100,V04,G1	D00,V04,G2	D0,V04,G4
D011,V03,G1	D11,V03,G2,G1	D1,V03,G3
D010,V02,G1	D10,V02,G1	D0,V03,G2
D001,V01,G1	D01,V01,G1	D1,V02,G1
D000,V00,G0	D00,V00,G0	D0,V01,-

Table 20: Voltage-based codes for encoding 3,2,1 bits into 16 voltage levels. D=data,V-voltage level,G-generation, shared sates have two generations.

efficient family of generic WOM codes that could be applied to any N-Level cell drive, The focus of Jaffer et al. [106] is QLC drives. The application of coding at various levels is given in Table 20.

Microbenchmarks and trace-driven simulation shows that WOM-v codes can reduce erase cycles 4.4-11.1-fold with minimal performance overheads. The increase in the total logical writable data before an erase is 50-375%. The total logical writable data between two erase operations may be increased by up to 500% by the choice of internal ECC.

29.2 Predictable Microsecond Level Support for Flash

Barroso et al. 2017 [16] discuss the issue of lack of support for microsecond (μs) scale events. It is argued that disk accesses are in milliseconds (ms) and the CPU accesses its registers, cache and even main memory in nanoseconds (ns) (refer to Table 21). The emerging Flash memory access times which are in μs are not adequately supported by the interface (refer to Table 22).

Nanosecond events	Microsecond events	Millisecond events
register file: 1-5 ns	datacenter networking $O(1 \mu s)$	disk $O(10)$ ms
cache accesses:4-30 ns	new NVM memory $O(1 \mu s)$	low-end-flash $O(1)$ ms
memory access 100 ns	high end flash $O(10 \mu s)$ GPU/accelerator $O(10 \mu s)$	wide area networking $O(10)$ ms

Table 21: Events and their latencies based on [16].

SSD performance is inherently non-deterministic due to the internal management activities such as the garbage collection, wear leveling, and internal buffer flush.

https://en.wikipedia.org/wiki/Wear_leveling

I/O Determinism interface is a host/SSD co-designed flash array with predictable latency which does not sacrifice aggregate bandwidth Li et al. 2023 [126]. Minimal changes to the *NonVolatile Memory Express - NVMe* interface and flash firmware was required to achieve near

Flash	225K instructions=O(100μs)
Fast Flash	20K instruction=O(10μs)
bf New NVM memory	2K instructions =O(1μs)
DRAM	500 instructions = O(100ns-1μs)

Table 22: # instructions between I/O events based on [16]. Data in bold is for unavailable new memories based on trace analysis.

ideal latencies.

https://en.wikipedia.org/wiki/NVM_Express

29.3 Differential RAID for SSDs

Diff-RAID design takes into account the fact that flash memories have very different failure characteristics from HDDs, i.e., the *Bit Error Rate - BER* of an SSD increases with more writes Balakrishnan et al. 2010 [15].

By balancing writes evenly across the array, RAID schemes wear together at similar rates, making all devices susceptible to data loss at the same time. Diff-RAID reshuffles the parity distribution on each drive replacement to maintain an age differential when old devices are replaced by new ones,

Diff-RAID distributes parity blocks unevenly masking higher BERs on aging SSDs while: (1) Retaining the low overhead of RAID5. (2) Extending the lifetime of commodity SSDs. (3) Alleviating the need for expensive error correction hardware.

For a workload consisting only of random writes, the relative aging rates of devices for a given parity assignment. Let $a_{i,j}$ represent the ratio of the aging rate of the i^{th} device to that of the j^{th} device, and p_i and p_j the percentages of parity allotted to the respective devices, then:

$$a_{i,j} = \frac{p_i(n-1) + (100 - p_i)}{p_j(n-1) + (100 - p_j)}. \quad (86)$$

Consider $n = 4$ SSDs and 50% of the parity at the first device and the rest evenly distributed over three disks, so that (70, 10, 10, 10) Using the above formula the aging rate of the first device is twice that of the others.

$$(70 \times 3 + 100 - 70) / (10 \times 3 + 100 - 10) = 240 / 120 = 2$$

After numerous replacements the ages of remaining devices at replacement time converge to (5750, 4312.5, 2875, 1437.5). The implementation of device replacement can be accomplished via rebuild processing, while maintaining the same parity layout.

A simulator to evaluate Diff-RAID's reliability by using BERs from 12 flash chips showed that it is more reliable than RAID5 by orders of magnitude.

29.4 Fast Array of Wimpy Nodes - FAWN

FAWN was a project at CMU's PDL combined low-power nodes with flash cluster storage providing fast and energy efficient processing of random queries in a *Key Value - KV* store.

https://en.wikipedia.org/wiki/Key%E2%80%93value_database

Andersen et al. 2022 [9]. FAWN-KV begins with a log-structured per-node datastore to serialize writes and make them fast on flash. KV-stores store retrieves and manages associative arrays using a dictionary or hash table. FAWN uses replication between cluster nodes to provide reliability and strong consistency. The FAWN prototype with 1000 queries/Joule demonstrated a significant potential for I/O-intensive workloads In 2011 4-year-old FAWN nodes delivered over an order of magnitude more queries per joule (watt×second) than disk systems.

<https://en.wikipedia.org/wiki/Joule>

29.5 Distributed DRAM-based Storage - RAMCloud

The crossover point for at which the more costly DRAM will replace disks is explored in Gibson 1992 [65]. Plotted in 1992 Graph 2.1(a) and 2.1(b) give 2010 and 2020 as optimistic and pessimistic crossover points.

RAMCloud is a distributed storage system keeping all data in DRAM offering exceptionally low latency for remote accesses, e.g., small reads completed in less than $10 \mu s$ in a 100,000 node datacenter Ousterhout et al. 2015 [155]. RAMCloud's 1 PB or more storage supports Web applications, via a single coherent key-value store. an associative array where each key is associated with one and only one value in a collection. RAMCloud maintains backup copies of data on HDDs to ensure high durability and availability. Memory prices per GB= $2^{30} \approx 10^9$ bytes which are dropping are given here <https://thememoryguy.com/dram-prices-hit-historic-low/> NAND prices are lower than DRAM, but Flash is slower than DRAM.

30 Conclusions

We discussed the reliability analysis of various RAID configurations, most notably RAID5 w/o and with IDR, analyzing reliability models via numerical methods and discrete-event simulation. We have mentioned but not delved into fast simulation methods such as importance sampling for reliability modeling.

We presented the performance analysis of RAID5 disk arrays implemented as HDDs in normal, degraded and rebuild modes is presented using the M/G/1 queueing model. Performance analysis of F/J queues arising in degraded mode operation and VSM for rebuild processing are discussed.

There has been significant increase in bandwidths used at hyperscalar *Data Storage Centers DSCs*, i.e., 100 Gb/s.

<https://www.nextplatform.com/2019/08/18/the-future-of-networks-depends-on-hyperscalers-and-big-clouds/>

Two important issues are Interconnection network reliability Goyal and Rajkumar 2020 [70] and performance Rojas-Cessa 2017 [178] (Part III - Data Center Networks). “The design space for large, multipath datacenter networks is large and complex, and no one design fits all purposes. Network architects must trade off many criteria to design cost-effective, reliable, and maintainable networks, and typically cannot explore much of the design space.” Condor enables a rapid, efficient design cycle Schlinker et al. 2015 [184].

Interested readers should follow advances in the field by following relevant trade magazines and conferences mentioned in this article.

In conclusion there is a need to increase the knowledge of computer scientists and engineers in stochastic processes and operations research techniques by expanding the curriculum. Steps

in this direction are proposed in Hardin 2102 [80], SEFI 2013 [192].

Appendix I: Transient Analysis of State Probabilities in Markov Chains

This section summarizes the review paper by de Souza and Gail 2000 [43]. Considered are time-homogeneous, finite-state CTMCs. The state-space is $\mathbf{S} = \{s_i, i = 1, \dots, M\}$ and the infinitesimal generator:

$$\mathbf{Q} = \begin{pmatrix} -q_{1,1} & q_{1,2} & \dots & q_{1,M} \\ q_{2,1} & -q_{2,2} & \dots & q_{2,M} \\ \vdots & \vdots & \ddots & \vdots \\ q_{M,1} & q_{M,2} & \dots & -q_{M,M} \end{pmatrix}$$

Due to time homogeneity:

$$\Pi_{i,j}(t) = P\{X(t'+t) = s_j | X(t') = s_i\}$$

The backward and forward Kolmogorov equations according to Kleinrock 1975 [118]:

$$\Pi'(t) = \mathbf{Q}\Pi(t) \text{ and } \Pi'(t) = \Pi(t)\mathbf{Q}. \quad (87)$$

where the state probabilities for CTMC are

$$\underline{\pi}(t) = [\pi_1(t), \dots, \pi_M(t)], \text{ where } \pi_i(t) = P\{X(t) = s_i\}$$

Methods to obtain transient solutions to finite state CTMCs are as follows:

30.1 Solutions Based on ODEs

A simple method for solving ODEs is dividing the time interval $(0, t)$ to n subintervals of length h and then approximating the derivative at the point $(y(nh), nh)$ with the difference $[y((n+1)h) - y(nh)]/h$ which can be applied to Eq. (87). A better approximation to the derivative using Euler's single step method is the two-step method

$$y'(t_n) = \frac{y(t_{n+1}) - y(t_{n-1}))}{2h} + O(h^2) \quad (88)$$

Applying Eq. 88 to Eq. (87) we have:

$$\Pi(t) = \Pi(t - 2h) + 2h\Pi'(t - h)$$

Generally, there is the Taylor series expansion

$$y(t+h) = y(t) + hy'(t) + \frac{h^2}{2}y''(t) + \frac{h^3}{3!}y'''(t) + \dots \quad (89)$$

The ODE of interest is $\Pi'(t) = \mathbf{Q}\Pi(t)$:

$$\Pi^{(n)}(t) = \mathbf{Q}^n\Pi(t)$$

Similarly to Eq. (89)

$$\Pi(t+h) = \left[\mathbf{I} + h\mathbf{Q} + \frac{h^2}{2!}\mathbf{Q}^2 + \frac{h^3}{3!}\mathbf{Q}^3 + \dots \right] \Pi(t) \quad (90)$$

30.2 Solutions Based on the Exponentials of a Matrix

Eq. (87) has the solution

$$\Pi(t) = e^{\mathbf{Q}t} \text{ where } e^{\mathbf{Q}t} = \sum_{n=0}^{\infty} \frac{(\mathbf{Q}t)^n}{n!} \quad (91)$$

One method to compute $\Pi(t)$ is as follows:

$$\Pi(t) = \sum_{n=0}^N \mathbf{F}_n(t) + \mathbf{E}(N) \quad (92)$$

where $\mathbf{E}(N)$ is a matrix which represent the error introduced by truncation at N . $\mathbf{F}_n(t)$ is defined by the recursion:

$$\mathbf{F}_n(t) = \mathbf{F}_{n-1}(t) \mathbf{Q} \frac{t}{n}. \quad (93)$$

Instead of calculating $\Pi(t)$ it is more efficient to calculate:

$$\Pi(t) = \sum_{n=0}^N \mathbf{F}_n(t) + \mathbf{E}(N) \text{ where } \mathbf{F}_n(t) = \mathbf{F}_{n-1}(t) \mathbf{Q} \frac{t}{n}$$

A related approach is to quantize time, such that $t = nh$ and apply Eq. (91).

Another simple approach is to perform a similarity transformation of \mathbf{Q} . Assuming that all the eigenvalues of \mathbf{Q} are distinct, or more generally that \mathbf{Q} is diagonalizable, \mathbf{Q} can be written as:

$$\mathbf{Q} = \mathbf{V} \mathbf{\Lambda} \mathbf{V}^{-1} \quad (94)$$

where $\mathbf{\Lambda}$ is a diagonal matrix with the M eigenvalues λ_i of \mathbf{Q} and \mathbf{V} holds the eigenvectors.

$$\begin{aligned} \Pi(t) &= \sum_{n=0}^{\infty} \mathbf{Q}^n \frac{t^n}{n!} = \mathbf{V} \left[\sum_{n=0}^{\infty} \mathbf{\Lambda}^n \frac{t^n}{n!} \right] \mathbf{V}^{-1} \\ \mathbf{V} e^{\mathbf{\Lambda}t} \mathbf{V}^{-1} &= \mathbf{V} \text{diag}\{e^{\lambda^1 t}, \dots, e^{\lambda^M t}\} \mathbf{V}^{-1} \end{aligned} \quad (95)$$

The problem of finding $\Pi(t)$ reduces to the problem of finding the eigenvalues and eigenvectors of \mathbf{Q} . Note that the matrix \mathbf{Q} has an eigenvalue equal to 0, and so the corresponding eigenvector gives the steady state solution ($t \rightarrow \infty$). Furthermore, the convergence to the steady state solution is determined by the subdominant eigenvalue of \mathbf{Q} .

30.3 Laplace Transform Methods

Applying the LT to the backward Kolmogorov equation in Eq (87) we obtain:

$$[s\mathbf{I} - \mathbf{Q}]\Pi^*(s) = \mathbf{I} \quad (96)$$

the LT of $\Pi(t)$ is $\Pi^*(s)$ and therefore

$$s\Pi^*(s) - \Pi(0) = s\Pi^*(s) - \mathbf{I} \text{ is the LT of } P_i'(t)$$

$$\Pi^*(s) = \frac{1}{s} \left[\mathbf{I} - \frac{\mathbf{Q}}{s} \right]^{-1} = \sum_{n=0}^{\infty} \frac{\mathbf{Q}^n}{s^{n+1}} \text{ inverting } \Pi(t) = \sum_{n=0}^{\infty} \frac{\mathbf{Q}^n}{n!} = e^{\mathbf{Q}t} \quad (97)$$

30.4 Krylov Subspace Method

This method is not discussed.

30.5 Uniformization or Randomization

This method is described in Grassman 1991 [71] and de Souza and Gail 1996 [44]. For the CTMC \mathcal{X} for the finite space \mathcal{S} and generator \mathbf{Q} let $\Lambda \geq \max\{q_{i,i}\}$. Define the matrix $\mathbf{P} = \mathbf{I} + \mathbf{Q}/\Lambda$, which is stochastic by choice of Λ . From Eq. (91) we have:

$$\pi(t) = \pi(0) \sum_{n=0}^{\infty} e^{-\lambda t} \frac{(\Lambda t)^n}{n!} \mathbf{P}^n \quad (98)$$

This equation can be evaluated recursively

$$\mathbf{v}(n) = \pi(0) \mathbf{P}^n \text{ and noting that } \mathbf{v}(n) = \mathbf{v}(n-1) \mathbf{P}. \quad (99)$$

The reader is also referred to Section 8.6 ‘‘Solution Techniques’’ in Trivedi 2002 [228].

Appendix II: The Mathematics Behind SHARPE Reliability Modeling Package

Section 4.7.2 in [180] considers a CTMC with $m = 2$ non-absorbing and $n = 2$ absorbing states, states with no transitions to other states Trivedi 2002 [228]. In the case of RAID5 failures there are two failure states during rebuild: failure due a second disk failure or unreadable sector as discussed in Section 20. The infinitesimal generator matrix with the states indexed as $(0 : m - 1)$ and $(m : m + n - 1)$ is given as:

$$\mathbf{Q} = \begin{pmatrix} -(\gamma + \lambda) & \gamma & \lambda & 0 \\ \beta & -(\beta + \delta + \mu) & \mu & \delta \\ 0 & 0 & 0 & 0 \\ 0 & 0 & 0 & 0 \end{pmatrix}$$

Differential equations and respective LSTs are as follows where $\alpha = \pi(0) = \{\alpha_0, \alpha_1, \alpha_2, \alpha_3\}$ denotes the initial state vector.

$$\begin{aligned} \frac{d\pi_0(t)}{dt} &= -(\gamma + \lambda)\pi_0(t) + \beta\pi_1(t), & sL_0^*(s) - \alpha_0 &= -(\gamma + \lambda)L_0^*(s) + \beta L_1^*(s) \\ \frac{d\pi_1(t)}{dt} &= -(\beta + \delta + \mu)\pi_1(t) + \gamma\pi_0(t), & sL_1^*(s) - \alpha_1 &= -(\beta + \delta + \mu)L_1^*(s) + \gamma L_0^*(s) \\ \frac{d\pi_2(t)}{dt} &= \lambda\pi_0(t) + \mu\pi_1(t), & sL_2^*(s) - \alpha_2 &= \gamma L_0^*(s) + \mu L_1^*(s) \\ \frac{d\pi_3(t)}{dt} &= \delta\pi_1(t), & sL_3^*(s) - \alpha_3 &= \delta L_1^*(s) \end{aligned}$$

Let $\mathbf{L}^* = (L_0^*, \dots, L_{m-1}^*)$ and \mathbf{T} the upper $m \times m$ upper left hand corner of generator matrix \mathbf{Q} , we have:

$$s\mathbf{L}^* - \alpha = \mathbf{L}^*\mathbf{T} \Rightarrow \mathbf{L}^* = \alpha(s\mathbf{I} - \mathbf{T})^{-1}$$

We now have the LST to the transient distribution functions for nonabsorbing states We define \mathbf{T}_i to be the $m \times 1$ vector that is transpose of $(q_{1i}, q_{2i}, \dots, q_{mi})$ so

$$sL^2(s) = \alpha_2 + \mathbf{L}T_2 = \alpha_2 + \alpha(s\mathbf{I} - \mathbf{T})^{-1}T_2$$

For the absorbing state L_i^* we have:

$$\mathbf{L}_i^*(s) = \frac{1}{s} \left(\alpha_i + \alpha(s\mathbf{I} - \mathbf{T})^{-1} \right) \mathbf{T}_i,$$

The real work is inverting the LST using partial fraction expansion:

$$\mathbf{P}(s) = \frac{1}{s} \left(\alpha(s\mathbf{I} - \mathbf{T})^{-1} \mathbf{T}_i \right)$$

Vector $\mathbf{X}(s)$ is defined as

$$\mathbf{X}(s) = (s\mathbf{I} - \mathbf{T})^{-1} \mathbf{T}_i \text{ then } (s\mathbf{I} - \mathbf{T}) \mathbf{X}(s) = \mathbf{T}_i$$

Applying Cramer's rule ⁴ the i^{th} element of \mathbf{X} is

$$X_i(s) = \frac{N_i(s)}{D(s)} \text{ where } D(s) = \det(\mathbf{I} - \mathbf{T})$$

$N_i(s)$ is the determinant of the matrix obtained by replacing the i^{th} column by the vector \mathbf{T}_i . Given the column vector \mathbf{X}

$$P(s) = \frac{1}{s} (\alpha \mathbf{X}(s)) = \frac{\sum \alpha_i N_i(s)}{sD(s)}$$

To invert $P(s)$ we need to carry out a partial fraction expansion. The zero root of the denominator yields the steady state solution. Given $D(s) = \det(s\mathbf{I} - \mathbf{T})$ eigenvalues of \mathbf{T} are given as sorted list of the roots" $(s_1, s_2, \dots, s_{m+1})$, where root s_k may occur d_k times. Then after determining a_k we have the inversion:

$$P^*(s) = \sum_{k=1}^{m+1} \frac{a_k}{(s - s_k)^{d_k}} \Rightarrow F(t) = \sum_{k=1}^{m+1} \frac{a_k}{(d_k - 1)!} t^{d_k - 1} e^{s_k t}$$

This solution yields transient state probabilities. However, the number and types of matrix manipulations make the algorithm unstable for some CTMCs Purely numerical algorithms for computing the transient probabilities are more stable. Use is made of Eq. (91) discussed in Section 30.

$$\pi(t) = \pi(0)e^{\mathbf{Q}t} \text{ given } q \geq \max_i |q_{ii}| e^{\mathbf{Q}t} = \sum_{i=0}^{\infty} \frac{(\mathbf{Q}t)^i}{i!}$$

$$\pi(t) = \sum_{k=1}^{\infty} \theta(k) e^{-qt} \frac{(qt)^k}{k!}$$

where $\theta(0) = \pi(0)$, $\mathbf{Q}^* = \frac{\mathbf{Q}}{q} + \mathbf{I}$ and $\theta(k) = \theta(k-1)\mathbf{Q}^*$

Incidentally hierarchical performance modeling for queueing networks in Thomasian and Bay 1986 [199] is incorporated into SHARPE.

⁴https://en.wikipedia.org/wiki/Cramer's_rule

Abbreviations

BIBD - Balanced Incomplete Block Design, **CTMC** - Continuous Time Markov Chain, **DAC** - Disk Array Controller, **DAR** - Disk Adaptive Redundancy, **DRC** - Degraded Read Cost, **EAFDL** - Expected Annual Fraction of Data Loss, **EB** - exabyte= 10^{18} , **FBA** - Fixed Block Architecture. **F/J** - Fork/Join, **FSQ** - Fair Share Queueing, **GB** - gigabyte= 10^9 , **HDFS** - Hadoop Distributed File System, **IOPS** - Input/Output Per Second, **IDR** - Intra-Disk Redundancy, **IPC** - Interleaved Parity Check, **KB** - kilobyte= $10^3 = 2^{10}$, **kDFT** - k Disk-Failure Tolerant, **LRC** - Local Redundancy Code. **LSE** - Latent Sector Error, **LST** - Laplace Stieltjes Transform, **MDS** - Maximum Distance Separable, **MB** - megabyte= 10^6 , **MTTD** - Mean Time to Detection, **MTTF** - Mean Time To Failure, **MTTR** - Mean Time To Repair, **MTTDL** - Mean Time To Data Loss, **NRC** - Normalized Repair Cost, **NRP** - Nearly Random Permutations, **NVMeoF** - NVMe[®]over Fabrics (NVMe-oF™), **NVRAM** - Non-Volatile Random Access Memory, **ODE** - Ordinary Differential Equation, **OLTP** - OnLine Transaction Processing, **PB** - petabyte= 10^{15} , **PCM** - Permanent Customer Model, **PDF** - Probability Distribution Function, **PDL** - Parallel Data Laboratory, **PUE** - Power Usage Effectiveness, **RAID** - Redundant Array of Inexpensive/Independent Disks, **RDP** - Rotated Diagonal Parity, **RMW** - Read-Modify Write, **RPM** - Rotations Per Minute, **RS** - Reed-Solomon (code). **RU** - Rebuild Unit, **SATF** - Shortest Access Time First, **SDC** - Silent Data Corruption, **SPC** - Single Parity Check, **SPTF** - Shortest Processing Time First, **SSD** - Solid State Disk, **SU** - Stripe Unit, **SWP** - Small Write Penalty, **TCO** - Total Cost of Ownership, **UDE** - Undetected Disk Errors, **UPS** - Uninterruptible Power Supply, **VSM** - Vacationing Server Model, **TB** - terabyte= 10^{12} , **XOR** - eXclusive OR, **ZB** - zettabyte= 10^{21} , **ZBR** - Zoned Bit Recording, **ZLA** - Zero Latency Access. **ZRL** - Zurich Research Lab (IBM)

References

- [1] [1] J. Abate, H. Dubner, S. B. Weinberg. 1968. Queueing analysis of the IBM 2314 disk storage facility. *Journal of the ACM* 15, 4 (1968), 577-589.
- [2] [2] M. Abd-El-Malek, W. V. Courtright II, C. Cranor, G. R. Ganger, J. Hendricks, A. J. Klosterman, M. P. Mesnier, M. Prasad, B. Salmon, R. R. Sambasivan, S. Sinnamohideen, J. D. Strunk, E. Thereska, M. Wachs, J. J. Wylie. 2005. Ursa Minor: Versatile Cluster-based Storage. In *Proc. 4th USENIX File and Storage Technologies - FAST 2005*, 69-72.
- [3] [3] B. Allen. 2004. Monitoring Hard Disks with SMART LINUX *Journal*, January 1, 2004. <https://www.linuxjournal.com/article/6983>
- [4] [4] G. A. Alvarez, W. A., Burkhard, G. Cristian. 1997. Tolerating multiple failures in RAID architectures with optimal storage and uniform declustering. In *Proc. 24th Ann'l Int'l Symp. Computer Architecture - ISCA'97*, pp. 62-72.
- [5] [5] G. A. Alvarez, W. A., Burkhard, L. J. Stockmeyer, F. Christian. 1998 Declustered disk array architectures with optimal and near optimal parallelism. In *Proc. 25th Int'l Symp. Computer Architecture, ISCA'98*, pp. 119-120.
- [6] [6] A. Amer, D. D. E. Long, E. L. Miller, J. F. Pâris, T. J. E. Schwarz: Design issues for a shingled write disk system. In *Proc. 26th IEEE Symp. on Massive Storage Systems and Technologies, MSST 2010*: 1-12

- [7] [7] G. Amvrosiadis, A. Oprea, B. Schroeder. 2012. Practical scrubbing: Getting to the bad sector at the right time. In Proc. 42nd IEEE/IFIP Dependable Systems and Networks, DSN 2012, 1-12.
- [8] [8] D. Anderson, J. Dykes, E. Riedel. 2003. More Than an Interface - SCSI vs. ATA. In Proc. 2nd USENIX Conference on File and Storage Technologies - FAST 2003, pp. 245-257.
- [9] [9] D. G. Andersen, J. Franklin, M. Kaminsky, A. Phanishayee, L. Tan, V. Vasudevan. 2011. FAWN: A Fast Array of Wimpy Nodes Commun. ACM, 54, 7 (2011), 101-109.
- [10] [10] J. E. Angus. On computing MTBF for a k-out-of-n: G Repairable System. IEEE Trans. on Reliability 37, 3 (1988), 312-313.
- [11] [11] M. Athanassoulis, A. Ailamaki, S. Chen, P. B. Gibbons, R. Stoica. 2010. Flash in a DBMS: Where and how? IEEE Data Engineering Bulletin 33, 4 (2010), 28-34.
- [12] [12] A. Amer, T. J. E. Schwarz, J. F. Paris, D. D. E. Long. 2008. Increased reliability with SSPiRAL data layouts. In Proc. 17th IEEE/ACM Int'l Symp. on MASCOTS 2008, 189-198.
- [13] [13] R. H. and A. C. Arpaci-Dusseau. 2018. Operating Systems: Three Easy Pieces. <https://pages.cs.wisc.edu/~remzi/OSTEP/>
- [14] [14] L. N. Bairavasundaram, G. R. Goodson, S. Pasupathy, J. Schindler. 2007. An analysis of Latent Sector Errors in disk drives. In Proc. Int'l Conf. on Measurements and Modeling of Computer Systems, SIGMETRICS'07, 289-300.
- [15] [15] M. Balakrishnan, A. Kadav, V. Prabhakaran, D. Malkhi. 2010. Differential RAID: Rethinking RAID for SSD reliability, ACM Trans. on Storage 6, 2 (July 2010), Article No. 4.
- [16] [16] L. Barroso, M. Marty, D. Patterson, P. Ranganathan. 2017. Attack of the killer micro-seconds. Commun. ACM 60, 4 (2017), 48-54.
- [17] [17] J. Basak and R. Katz. 2015. RAID-Cube: The Modern Datacenter Case for RAID. EECS Dept. UC Berkeley. Technical Report NO. UCB/EECS-2015-4.
<https://www2.eecs.berkeley.edu/Pubs/TechRpts/2015/EECS-2015-4.pdf>
- [18] [18] M. Blaum and R. M. Roth. On lowest density MDS codes. IEEE Transactions on Information Theory 45, 1 (Jan 1999), 46-59.
- [19] [19] M. Blaum, J. Brady, J. Bruck, J. Menon, A. Vardy. 2002. The EVENODD code and its generalizations. In High Performance Mass Storage and Parallel I/O: Technologies and Applications, H. Jin, T. Cortes, and R. Buyya, eds, Wiley, 2002, 187-208.
- [20] [20] M. Blaum. A Short Course on Error-Correcting Codes, 2009.
<https://arxiv.org/abs/1908.09903>
- [21] [21] M. Blaum, J. L. Hafner, S. Hetzler. 2013. Partial-MDS codes and their application to RAID type of architectures. IEEE Trans. Information Theory 59, 7 (2013), 4510-4519.

- [22] [22] J. Blomer, M. Kalfane, M. Karpinski, R. Karp, M. Luby, D. Zuckerman 1995. An XOR-based erasure-resilient coding scheme. Technical Report TR-95-048, Int'l Computer Science Institute.
- [23] [23] A. M. Blum, A. Goyal, P. Heidelberger, S. S. Lavenberg, M. K. Nakayama, P. Shahabuddin. 1994. Modeling and analysis of system dependability using the system availability estimator. In Proc. 24th IEEE Ann'l Int'l Symp. on Fault-Tolerant Computing Systems, FTCS 1994, 137-141.
- [24] [24] D. Borthakur. 2007. The Hadoop Distributed File System: Architecture and Design. Technical Report Apache Software Foundation 2007.
http://svn.apache.org/repos/asf/hadoop/common/tags/release-0.16.3/docs/hdfs_design.pdf
- [25] [25] W. G. Bouricius, W. C. Carter, D. C. Jessep, P. R. Schneider, A. B. Wadia. 1971. Reliability modeling for fault-tolerant computers. IEEE Trans. Computers 20, 11 (1971), 1306-1311.
- [26] [26] O. J. Boxma and J. W. Cohen. 1991. The M/G/1 queue with permanent customers. IEEE J. Selected Areas in Communications - JSAC 9, 2 (1991), 179-184.
- [27] [27] E. Brewer. 2016. Spinning disks and their cloudy future. In Proc. 14th USENIX Conf. on File and Storage Technologies - FAST 2016.
- [28] [28] E. Brewer, L. Ying, L. Greenfield, R. Cypher, T. Ts'o. 2016. Disks for Data Centers White paper for FAST 2016 <https://storage.googleapis.com/pub-tools-public-publication-data/pdf/44830.pdf>
- [29] [29] W. Bux. 2009. Performance evaluation of the write operation In flash-based solid-state drives IBM Research Report Zurich RZ 3757 (#99767), Nov. 2009/
- [30] [30] W. Bux and I. Iliadis. 2010. Performance of greedy garbage collection in flash-based solid-state drives. Performance Evaluation 67, 11, (2010), 1172-1186.
- [31] [31] W. Bux, X.-Y. Hu, I. I. Iliadis, R. Haas. 2012. Scheduling in flash-based solid-state Drives - performance modeling and optimization. In Proc. 20th IEEE/ACM Int'l Symp. on MASCOTS 2012, 459-468.
- [32] [32] P. M. Chen, E. K. Lee, G. A. Gibson, R. H. Katz, D. A. Patterson. 1994. RAID: High-performance, reliable secondary storage. ACM Computing Survey 26, 2 (1994), 145-185.
- [33] [33] R. Chen and L. Xu. 2020. Practical performance evaluation of space optimal erasure codes for high-speed data storage systems. SN Computer Science 1, 1 (2020), 54.
- [34] [34] S. Chen and D. F. Towsley. 1993. The design and evaluation of RAID 5 and parity striping disk array architectures. J. Parallel Distributed Computing - JPDC 17, 1-2 (1993), 58-74.
- [35] [35] S. Chen and D. F. Towsley. 1996. A performance evaluation of RAID architectures. IEEE Trans. Computers 45, 10, (Oct. 1996), 1116-1130.

- [36] [36] A. Cidon, S. M. Rumble, R. Stutsman, S. Katti, J. K. Ousterhout, M. Rosenblum. 2013. Copysets: Reducing the frequency of data loss in cloud storage. USENIX Ann'l Tech. Conf. - ATC 2013: 37-48
- [37] [37] D. Colarelli and D. Grunwald. 2002. Massive arrays of idle disks for storage archives. In Proc. ACM/IEEE Conf. on Supercomputing - SC'02, 2002, 56.1-56.11. Baltimore, MD: November 2002, 56.1-56.11.
- [38] [38] P. Corbett, B. English, A. Goel, T. Gracanac, S. Kleiman, J. Leong, and S. Sankar. 2004. Row-diagonal parity for double disk failure correction. In Proc. 3rd USENIX Conf. on File and Storage Technologies - FAST 2004, 1-14.
- [39] [39] W. V. Courtright II, G. Gibson, M. Holland, L. N. Reilly, J. Zelenka. 1997. RAID-frame: A Rapid Prototyping Tool for RAID Systems Technical Report CMU-CS-97-142. 1997.
<https://www.pdl.cmu.edu/PDL-FTP/RAID/CMU-CS-97-142.pdf>
- [40] [40] H. A. David and H. N. Nagaraja, 2003. Order Statistics, 3rd ed., Wiley 2003.
- [41] [41] J. Dean and L. A. Barroso. 2013 The tail at scale. Commun. ACM 56, 2 (Feb. 2013), 74-80.
- [42] [42] P. Desnoyers, 2014. Analytic Models of SSD write performance. ACM Trans. on Storage 10, 2 (2014), 8:1-8:25.
- [43] [43] E. de Souza e Silva and H. R. Gail. 2000. Transient solutions for Markov chains. In: W.K. Grassmann (ed), Computational Probability. Int'l Series in Operations Research & Management Science, vol 24. Springer 2000.
- [44] [44] E. de Souza e Silva and H. R. Gail. 1996. The uniformization method in performability analysis. IBM Research Report RC 20383, Yorktown Heights, NY, 1996.
- [45] [45] P. J. Denning. 1967. Effects of scheduling on file memory operations. In Proc. AFIPS Spring Joint Computing Conf. 1967, 9-21.
<https://denninginstitute.com/pjd/PUBS/Starting.html>
- [46] [46] A. Dholakia, E. Eleftheriou, X.-Y. Hu, I. Iliadis, J. Menon, K. K. Rao. 2008. A new intra-disk redundancy scheme for high-reliability RAID storage systems in the presence of unrecoverable errors. ACM Trans. on Storage 4, 1 (2008), 1:1-1:42.
- [47] [47] A. G. Dimakis, K. Ramchandran, Y. Wu, C. Suh. 2011. A survey on network codes for distributed storage, Proc. IEEE 99, 3 (March 2011), 476-489.
- [48] [48] B. T. Doshi. 1985. An M/G/1 queue with variable vacations. In Modeling Techniques and Tools for Performance Analysis'85, N. Abu et Ata (ed.)m North Holland, pp, 67-81.
- [49] [49] R. Durstenfeld. 1964. Algorithm 235: Random permutation. Commun. ACM, 7, 7 (1964), 420.

- [50] [50] B. Eckart, X. Chen, X. He, S. L. Scott. 2008. Failure prediction models for proactive fault tolerance within storage systems. In Proc. 16th IEEE/ACM Int'l Symp. on MASCOTS 2008, 1-8.
- [51] [51] J. G. Elerath and J. Schindler. 2014. Beyond MTDDL: A closed-form RAID 6 reliability equation. ACM Trans. on Storage 10, 2, (March 2014), Article 7.
- [52] [52] B. Fan, W. Tantisiriroj, L. Xiao, G. Gibson. 2009. DiskReduce: RAID for data-intensive scalable computing. In Proc. 4th Petascale Data Storage Workshop - PDSW, 2009.
- [53] [53] T. Feldman and G. Gibson. 2013. Shingled Magnetic Recording: Areal density increase Requires new data management. ;login USENIX Magazine 38, 3, 2013, 22-30.
- [54] [54] Fevgas, L. Akritidis, P. Bozanis, Y. Manolopoulos. Indexing in flash storage devices: a survey on challenges, current approaches, and future trends. VLDB Journal 29, 1 (2020), 273–311.
- [55] [55] L. Flatto and S. Hahn. 1984: Two parallel queues created by arrivals with two demands: I. SIAM J. Applied Mathematics 44 (1984), 1041-1053.
- [56] [56] C. Fleiner, R. B. Garner, J. L. Hafner, K. K. Rao, D. R. Kenchammana-Hosekote, W. W. Wilcke, J. S. Glider. 2006 Reliability of modular mesh-connected intelligent storage brick systems. IBM J. Research & Development 50, 2-3, (2006), 199-208.
- [57] [57] F. F. Freitas and W. W. Wilcke. 2008. Storage-class memory: The next storage system technology. IBM J. Research and Development 52, 4-5 (2008), 439-448.
- [58] [58] D. A. Ford, R. J. T. Morris, A. E. Bell: Redundant Arrays of Independent Libraries (RAIL): The StarFish tertiary storage system. Parallel Computing 24, 1 (1998), 45-64.
- [59] [59] D. Ford, F. Labelle, F. I. Popovici, M. Stokely, V.-A. Truong, L. Barroso, C. Grimes, S. Quinlan. 2010. Availability in Globally Distributed Storage Systems. In Proc. 9th USENIX Symp. on Operating System Design and Implementation, OSDI 2010, 61-74.
- [60] [60] G. Fu, A. Thomasian, C. Han, S. W. Ng. 2004. Rebuild strategies for redundant disk arrays. In Proc. NASA/IEEE MSST'04: 12th NASA Goddard, 21st IEEE Conf. on Mass Storage and Technologies, MSST 2004.
- [61] [61] G. Fu, A. Thomasian, C. Han, S. W. Ng. 2004. Rebuild strategies for clustered RAID. In Proc. Int'l Symp. on Performance Evaluation of Computer and Telecomm. Systems, SPECTS 2004, 598-607.
- [62] [62] E. Fujiwara. 2006. Code Design for Dependable Systems Theory and Practical Applications. Wiley-Interscience, 2006.
- [63] [63] G. R. Ganger, B. L. Worthington, R. U. Hsu, Y. N. Patt. Disk subsystem load balancing: Disk striping vs. conventional data placement In Proc. Hawaii Int'l Conf. on System Sciences, HICSS 1993, 40-49.
- [64] [64] L. Georgiadis, C. Nikolaou, A. Thomasian. 2004. A fair workload allocation policy for heterogeneous systems. J. Parallel Distributed Computing - JPDC 64, 4 (2004), 507-519.

- [65] [65] G. A. Gibson. 1992. Redundant Disk Arrays: Reliable, Parallel Secondary Storage Systems. The MIT Press 1992.
- [66] [66] M. Goldszmidt. 2012. Findings Soon-to-Fail Disks in a haystack. In Proc. 4th USENIX Workshop Hot Topics in Storage and File Systems, HotStorage 2012, 5 pages.
- [67] [67] I. J. Goodfellow, J. Pouget-Abadie, M. Mirza, B. Xu, D. Warde-Farley, S. Ozair, A. C. Courville, Y. Bengio. 2014. Generative adversarial nets. In Proc. Advances in Neural Information Processing Systems 27: Annual Conf. on Neural Information Processing Systems 2014, 2672–2680.
- [68] [68] P. Gopalan, C. Huang, H. Simitci, S. Yekhanin. 2012 IEEE Trans. Information Theory, 58, 11 (Nov. 2012), 6925-6934.
- [69] [69] A. Goyal, P. Shahabuddin, P. Heidelberger, V. F. Nicola, P. W. Glynn. 1992. A unified framework for simulating Markovian models of highly dependable systems. IEEE Trans. Computers 41, 1 (1992), 36-51.
- [70] [70] N. K. Goyal and S. Rajkumar (2020): Interconnection Network Reliability Evaluation: Multistage Layouts. Wiley, 2020.
- [71] [71] W. Grassmann. 1991. Finding transient solutions in Markovian event systems through randomization. In Stewart, W. J., ed., Numerical Solution of Markov Chains, pages 357–371. Marcel Dekker 1991.
- [72] [72] D. Bitton, J. Gray: Disk shadowing. In Proc. 14th Int’l Conf. on Very Large Data Bases - VLDB 1988: 331-338
- [73] [73] J. Gray, B. Horst, M. Walker: Parity striping of disk arrays: Low-cost reliable storage with acceptable throughput. In Proc. 16th Int’l Conf. on Very Large Data Bases, VLDB 1990, 148-161.
- [74] [74] J. Gray and P. J. Shenoy. 2000. Rules of thumb in data engineering. In Proc. 16th Int’l Conf. on Data Engineering - ICDE 2000: 3-10
- [75] [75] J. L. Hafner, V. Deenadhayalan, T. Kanungo, K. K. Rao, 2004. Performance metrics for erasure codes in storage systems. IBM Research Report RJ 10321, 2004.
- [76] [76] J. L. Hafner, V. Deenadhayalan, K. K. Rao, J. A. Tomlin. 2005. Matrix methods for lost data reconstruction in erasure codes. In Proc. 4th USENIX Conf. on File and Storage Technologies - FASR 2005, 183-196.
- [77] [77] J. L. Hafner, V. Deenadhayalan, W. Belluomini, K. Rao. 2008. Undetected disk errors in RAID arrays. IBM J. Research and Development 52, 4-5 (July 2008): 413-425.(July 2008).
- [78] [78] M. Hall. 1986. Combinatorial Theory, Second Ed., Wiley-Interscience, New York, NY.
- [79] [79] R. J. Hall. 2016. Tools for predicting the reliability of large scale storage systems. ACM Trans. on Storage 12, 4 (2016), 24.1-24.30.

- [80] [80] J. R. Hardin, A. Holder, J. C. Beck, K. Furman, A. Hanna, D. Rader, C. Rego. 2012. Recommendations for an undergraduate curriculum at the interface of operations research and computer science. *INFORMS Trans. on Education* 12, 3 (2012), 117-123.
- [81] [81] S. Hardock, I. Petrov, R. Gottstein, A. P. Buchmann. 2013. NoFTL: Database Systems on FTL-less flash storage . In *Proc. VLDB Endow.* 6, 12, (2013), 1278-1281.
- [82] [82] L. Hellerstein, G. A. Gibson, R. M. Karp, R. H. Katz, D. A. Patterson. 1994: Coding techniques for handling failures in large disk arrays. *Algorithmica* 12, 2/3 (1994), 182–208.
- [83] [83] J. L. Hennessey and D. A. Patterson: *Computer Architecture: A Quantitative Approach*, 6th ed. Morgan-Kaufmann Publisher 20197.
- [84] [84] M. Holland, G. A. Gibson, D. P. Siewiorek. 1994. Architectures and algorithms for on-line failure recovery in redundant disk arrays. *Distributed Parallel Databases* 2, 3 (1994), 295-335.
- [85] [85] H.-I. Hsiao and D. J. DeWitt. 1990. Chained declustering: A new availability strategy for multiprocessor database machines. In *Proc. 6th IEEE Int’l Conf. on Data Eng. - ICDE’90*, 456-465.
- [86] [86] W. W. Hsu and A. J. Smith. 2004. The performance impact of I/O optimizations and disk improvements. *IBM J. Res. Dev.* 48, 2 (2004), 255-289.
- [87] [87] W. W. Hsu, A. J. Smith, H. C. Young. 2005. The automatic improvement of locality in storage systems. *ACM Trans. Computer Systems* 23, 4 (Nov. 2005), 424-473.
- [88] [88] Y. Hu, L. Cheng, Q. Yao, P. C. Lee, W. Wang, W. Chen. 2021 Exploiting combined locality for wide-stripe erasure coding in distributed storage. In *Proc. USENIX File and Storage Technologies - FAST 2021*.
- [89] [89] C. Huang and L. Xu, 2005. STAR: An efficient coding scheme for correcting triple storage node failures. In *Proc. 4th USENIX Conf. on File and Storage Technologies - FAST 2005*, 197-210.
- [90] [90] C. Huang, M. Chen, J. Li. 2007. Pyramid codes: Flexible schemes to trade space for access efficiency in reliable data storage systems. In *Proc. 6th IEEE Int’l Symp. on Network Computing and Applications, NCA 2007*: 79-86.
- [91] [91] C. Huang, H. Simitci, Y. Xu, A. Ogus, B. Calder, P. Gopalan, J. Li, S. Yekhanin. 2012 Erasure Coding in Windows Azure Storage. In *Proc. USENIX Ann’l Tech. Conf. ATC 2012*: 15-26.
- [92] [92] C. Huang. 2013. Tutorial on erasure coding for storage applications, Part 2, Tutorial. *FAST-2013: 11th Usenix Conf. File and Storage Technologies*, 2013.
- [93] [93] G. Hughes, J. Murray, K. Kreutz-Delgado, C. Elkan. 2002. Improved disk drive failure warnings. *IEEE Trans. on Reliability* 51, 3 (2002), 350-357.
- [94] [94] IBM TS4500 Tape Library, Systems Hardware Data Sheet. <https://www.ibm.com/downloads/cas/KXYRJYW1>

- [95] [95] I. Iliadis, R. Haas, X.-Y. Hu, E. Eleftheriou. 2011, Disk scrubbing versus Intradisk Redundancy for RAID storage systems. *ACM Trans. on Storage* 7, 2 (2011), 5:1-5:42.
- [96] [96] I. Iliadis and V. Venkatesan, 2014. Expected annual fraction of data loss as a metric for data storage reliability. In *Proc. 22nd IEEE/ACM Int'l Symp. on MASCOTS 2014*: 375–384.
- [97] [97] I. Iliadis and V. Venkatesan. 2015. Rebuttal to "Beyond MTDDL: A closed-form RAID-6 reliability equation. *ACM Trans. on Storage* 11, 2 (2015), 9:1-9:10..
- [98] [98] I. Iliadis and V. Venkatesan. 2015b An efficient method for reliability evaluation of data storage systems, In *Proc. 8th Int'l Conf. on Communication Theory, Reliability, Quality of Service, CTRQ 2015*: 6-12.
- [99] [99] I. Iliadis, Y. Kim, S. Sarafijanovic, V. Venkatesan. 2016. Performance Evaluation of a Tape Library System. In *Proc. 24th IEEE/ACM Int'l Symp. on MASCOTS 2016*. 59-68.
- [100] [100] I. Iliadis, 2019. Data Loss in RAID-5 and RAID-6 storage systems with latent errors *Int'l Journal on Advances in Software* 12, 3/4, 2019.
<http://www.iariajournals.org/software/>
- [101] [101] I. Iliadis, L. Jordan, M. A. Lantz, S. Sarafijanovic. 2021. Performance evaluation of automated tape library systems. In *Proc. 28th IEEE/ACM Int'l Symp. on MASCOTS 2016*, 1-8.
- [102] [102] I. Iliadis. 2022. Effect of lazy rebuild on reliability of erasure coded storage systems. In *Proc. CTRQ 2022: 15th Int'l Conf. on Communication Theory*.
https://www.iaria.org/conferences2022/filesCTRQ22/CTRQ_70005.pdf
- [103] [103] I. Iliadis. 2023. Reliability evaluation of erasure-coded storage systems with latent errors. *ACM Trans. on Storage* 19, 1, (2023), 4:1-4:47.
- [104] [104] B. L. Jacob, S. W. Ng, D. T. Wang. 2008. *Memory Systems: Cache, DRAM, Disk*. Morgan Kaufmann Publishers 2008.
- [105] [105] D. M. Jacobson and J. Wilkes. 1991. Disk scheduling algorithms based on rotational position. Technical Report HPL–CSP–91–7rev. March 1991.
<https://pages.cs.wisc.edu/~remzi/Courses/838/Fall2001/Papers/hp-sched.pdf>
- [106] [106] S. Jaffer, K. Mahdavian, B. Schroeder. 2022. Improving the Endurance of Next Generation SSD's using WOM-v Codes. *ACM Trans. Storage* 18, 4 (2022), 29:1-29:32.
- [107] [107] W. Jiang, C. Hu, Y. Zhou, A. Kanevsky. 2008. Are disks the dominant contributor for storage failures? A comprehensive study of storage subsystem failure characteristics. *ACM Trans. on Storage* 4, 3 (2008), 7:1-7:25.
- [108] [108] T. Jiang, P. Huang, K. Zhou. 2019. Scrub unleveling: Achieving high data reliability at Low scrubbing cost. In *Proc. 2019 Design, Automation & Test in Europe Conf. & Exhibition - DATE, 2019*, 1403-1408.

- [109] [109] A. M. Johnson Jr. and M. Malek, 1988. Survey of software tools for evaluating reliability, availability, and serviceability. *ACM Computing Surveys* 20, 4 (1988), 227-269.
- [110] [110] N. L. Johnson, S. Kotz, N. Balakrishnan. 1995. *Continuous Univariate Distributions, Vol. 2. 2nd Ed. Wiley Series in Probability and Statistics* 1995.
- [111] [111] S. Kadekodi, F. Maturana, S. Athlur, A. Merchant, K. V. Rashmi, G. R. Ganger. 2022. Tiger: Disk-adaptive redundancy Without placement restrictions. In *Proc. 16th USENIX Symp. Operating Systems Design and Implementation- OSDI 2022*, 413-429.
- [112] [112] S. Kadekodi, S. Silas, D. Clausen, A. Merchant. 2023. Practical design considerations for wide Locally Recoverable Codes - LRCs. In *Proc. 21st USENIX Conf. on File and Storage Technologies - FAST 23*, pages=(1-16).
- [113] [113] H.-W. Kao, J.-F. Paris, T. J. E. Schwarz, D. D. E. Long: A flexible simulation tool for estimating data loss risks in storage arrays. In *Proc. 29th Symp. on Mass Storage Systems Technology, MSST 2013*: 1-5.
- [114] [114] P. Karlsson. 2006. *Solaris 10 Features In-depth: Containers and ZFS*. http://uk.sun.com/sunnews/events/2006/mar/javauk06/presentations/Peter_Karlsson_Containers_ZFS.pdf
- [115] [115] D. R. Kenchamma-Hosekote, D. He, J. L. Hafner. 2007. REO: A generic RAID Engine and Optimizer. In *Proc. 5th USENIX Conf. on File and Storage Technologies, FAST 2007*, 261-276
- [116] [116] J. Kim, M. Kim, M. D. Tehseen, J. Oh, Y. Won, 2022. IPLFS: Log-structured file system without garbage collection. In *Proc. USENIX Ann'l Tech. Conf. - ATC 2022*, 739-754
- [117] [117] L. Kleinrock. 1964. *Communication Nets: Stochastic Message Flow and Delay*. McGraw-Hill 1964 (Dover 1972).
- [118] [118] L. Kleinrock. 1975. *Queueing Systems, Vol. I: Theory*. Wiley-Interscience 1975.
- [119] [119] L. Kleinrock. 1976. *Queueing Systems, Vol. II: Applications*. Wiley-Interscience 1976.
- [120] [120] H. Kobayashi, B. L. Mark, W. Turin. 2014. Cambridge Univ. Press, 2014.
- [121] [121] O. Kolosov, G. Yadgar, M. Liram, I. Tamo, A. Barg. On fault tolerance, locality, and optimality in locally repairable codes. In *Proc. USENIX Annual Technical Conference - ATC 2018*, 2018, 865-877.
- [122] [122] S. Kotz and S. Nadarajah. 2000. *Extreme Value Distributions: Theory and Applications*. Imperial College Press, London 2000.
- [123] [123] T Lahiri, M.-A. Neimat, S. Folkman. 2013. Oracle TimesTen: An In-Memory Database for Enterprise Applications. *IEEE Data Eng. Bull.* 36(2): 6-13 (2013)

- [124] [124] S. S. Lavenberg, ed. 1983. *Computer Performance Modeling Handbook*. Academic Press 1983.
- [125] [125] J. F. Lawless. 2003. *Statistical Models and Methods for Lifetime Data*, 2nd ed. Wiley, 2003.
- [126] [126] H. Li, M. L. Putra, R. Shi, F. I. Kurnia, X. Lin, J. Do, A. I. Kistijantoro, G. R. Ganger, H.i S. Gunawi. 2023. Extending and programming the NVMe I/O determinism interface for Flash Arrays. *ACM Trans. on Storage* 19, 1 (2023), 5:1-5:33.
- [127] [127] M. Li, J. Shu, W. Zheng. 2009. GRID codes: Strip-based erasure codes with high fault tolerance for storage systems. *ACM Trans. Storage* 4, 4 (2009), 15:1-15:22.
- [128] [128] M. Li and J. Shu. 2010. Preventing silent data corruptions from propagating during data reconstruction. *IEEE Trans. Computers* 59, 12 (2010),: 1611-1624.
- [129] [129] P. J. Meaney, L. A. Lastras-Montano, V. K. Papazova, E. Stephens, J. S. Johnson, L. C. Alves, J. A. O'Connor, W. J. Clarke. 2012. IBM zEnterprise redundant array of independent memory subsystem. *IBM Journal of Research and Development* 56, 1 (2012), 4:1-4:12.
- [130] [130] S. M. A. Mohamed and Y. Wang. 2021. A survey on novel classification of deduplication storage systems *Distributed and Parallel Databases* 39, 101 (March 2021), 201–230.
- [131] [132] S. Lin, C. Zhang, D. Wang, J. Liu. 2009. Reliability analysis for Full-2 Code. In *Proc. 10th Int'l Symp. Pervasive Systems, Algorithms, and Networks: 2009*, 454-459.
- [132] [133] C. R.Lumb and R. Golding. 2004. D-SPTF: Decentralized request distribution in brick-based storage systems. *SIGOPS Operating System Review* 38, 5 (Oct. 2004), 37–47.
- [133] [134] A. Ma, R. Traylor, F. Dougliis, M. Chamness, G. Lu, D. Sawyer, S. Chandra, W. Hsu. 2015 RAIDShield: Characterizing, Monitoring, and Proactively Protecting Against Disk Failures. *ACM Trans. on Storage* 11, 4 (2015), Article 17.
- [134] [135] F. J. MacWilliams, N. J. A. Sloane. 1977. *The Theory of Error-Correcting Codes*. North Holland, 1977.
- [135] [136] F. Mahdisoltani, I. A. Stefanovici, B. Schroeder. 2017. Proactive error prediction to improve storage system reliability. In *Proc. USENIX Ann'l Technical Conf. ATC 2017*, 391-402
- [136] [137] C. Maltzahn; E. Molina-Estolano; A. Khurana; A. J. Nelson; S. A. Brandt; S. Weil . 2010. Ceph as a scalable alternative to the Hadoop Distributed File System". ;login *USENIX Magazine*, 35 (4), 2010, 38-49.
- [137] [138] S. Maneas, K. Mahdavian, T. Emami, B. Schroeder. 2021. Reliability of SSDs in enterprise storage Systems: A large-scale field study. *ACM Trans. on Storage* 17, 1 (2021), 3:1-3:27.

- [138] [139] F. P. Mathur and A. Avizienis. 1970. Reliability analysis and architecture of a hybrid-redundant digital system: Generalized triple modular redundancy with self-repair. In Proc. AFIPS Spring Joint Computing Conf. 1970, 375-383.
- [139] [140] B. McNutt. 1994. Background data movement in a log-structured disk subsystem. IBM J. Research & Development 38, 1 (1994), 47-58.
- [140] [141] B. McNutt. 2002. The Fractal Structure of Data Reference - Applications to the Memory Hierarchy. Advances in Database Systems 22, Kluwer 2002.
- [141] [142] J. Menon and J. Cortney. 1993. The architecture of a fault-tolerant cached RAID controller. In Proc. 20th Ann'l Int'l Symp on Computer Architecture, ISCA 1993, 76-86.
- [142] [143] J. Menon. 1994 Performance of RAID5 disk arrays with read and write Caching. Distributed Parallel Databases 2, 3 (1994), 261-293.
- [143] [144] J. Menon. 1995. A performance comparison of RAID-5 and log-structured arrays. In Proc. 4th Int'l Symp. on High Performance Distributed Computing, HPDC 1995, 167-178
- [144] [145] J. Menon and L. J. Stockmeyer. 1998. An age threshold algorithm for garbage collection in log-structured arrays and file systems. IBM Research Report RJ 10120, Almaden Research Center, May 1998. Abridged version in *High Performance Computing Systems and Applications*, J. Schaefer, ed. Kluwer Academic Publishers, 119-132).
<https://www.cstheory.com/stockmeyer@sbcglobal.net/agerj.pdf>
- [145] [146] A. Merchant and P. S. Yu. 1996. Analytic modeling of clustered RAID with mapping based on nearly random permutation. IEEE Trans. Computers 45, 3 (1996), 367-373.
- [146] [147] R. Micheloni, L. Crippa, A. Marelli. 2010. Inside Flash NAND Memories Springer 2010.
- [147] [148] R. R. Muntz and J. C. S. Lui. 1990. Performance analysis of disk arrays under failure. In Proc 16th Int'l Conf. on Very Large Data Bases, VLDB 1990, 162-173.
- [148] [149] J. Murray, G. Hughes, K. Kreutz-Delgado. 2005. Machine learning methods for predicting failures in hard drives: a multiple-instance application. The Journal of Machine Learning Research 6, 783-816
- [149] [150] R. D. Nelson and A. N. Tantawi. 1988. Approximate Analysis of Fork/Join Synchronization in Parallel Queues. IEEE Trans. Computers 37, 6, (1988), 739-743.
- [150] [151] L. A. Newberg and D. Wolf. 1994. String layouts for a redundant array of inexpensive disks. Algorithmica 12, 2/3 (1994), 209-224.
- [151] [152] S. W. Ng and R. L. Mattson. 1994. Uniform parity group distribution in disk arrays with multiple failures. IEEE Trans. Computers 43, 4 (1994), 501-506.
- [152] [153] Y. W. Ng and A. Avizienis. 1980. A Unified Reliability Model for Fault-Tolerant Computers. IEEE Trans. Computers 29, 11 (1980), 1002-1011.

- [153] [154] V. F. Nicola, M. K. Nakayama, P. Heidelberger, A. Goyal. 1993. Fast simulation of highly dependable systems with general failure and repair processes. *IEEE Trans. Computers* 42, 12 (1993), 1440-1452.
- [154] [155] V. F. Nicola, P. Shahabuddin, M. K. Nakayama. 2001. Techniques for fast simulation of models of highly dependable systems. *IEEE Trans. Reliability* 50, 3 (2001), 246-264.
- [155] [156] J. K. Ousterhout, A. Gopalan, A. Gupta, A. Kejriwal, C. L. Behnam Montazeri, D. Ongaro, S. J. Park, H. Qin, M.I Rosenblum, S. M. Rumble, R. Stutsman, S. Yang. 2015. The RAMCloud storage system. *ACM Trans. Computer Systems* 33, 3, (2015), Article 7
- [156] [157] M. Ovsianikov, S. Rus, D. Reeves, P. Sutter, S. Rao, J. Kelly. 2013. The Quantcast file System. In *Proc. VLDB Endowment* 6, 11 (2013), 1092-1101.
- [157] [158] J. F. Paris and T. J. Schwarz. 2021. Three dimensional RAID arrays with fast repairs. In *Proc. Int'l Conf. on Electrical, Computer and Energy Technologies, ICECET 2021*.
- [158] [159] C.-I. Park. 1995. Efficient placement of parity and data to tolerate two disk failures in disk array systems. *IEEE Trans. Parallel and Distributed Systems* 6, 11 (Nov. 1995), 1177-1184.
- [159] [160] D. A. Patterson, G. A. Gibson, R. H. Katz. 1988. A case for Redundant Arrays of Inexpensive Disks (RAID). In *Proc. ACM SIGMOD Int'l Conf. on Management of Data, SIGMOD 1988*, 109-116.
- [160] [161] J. Paulo and J. Pereira. 2014. A survey and classification of storage deduplication systems. *ACM Computing Surveys* 47, 1 (2014), 11.1-11:30.
- [161] [162] H.-O. Peitgen, H. Jürgens, D. Saupe. 2004. *Chaos and Fractals: New Frontiers of Science* 2nd Ed., Springer 2004.
- [162] [163] W. F. Piepmeier. 1975. Optimal balancing of I/O requests to disks, *Commun. ACM* 18,9 (Sept. 1975), 524-527
- [163] [164] J. S. Plank. 1997. A tutorial on Reed-Solomon coding for fault-tolerance in RAID-like systems. *Software Practice & Experience* 27, 9, (1997), 995-1012.
- [164] [165] J. S. Plank. 2005. Erasure codes for storage applications, Tutorial, 4th Usenix Conf. File and Storage Technologies, FAST 2005.
- [165] [166] J. S. Plank and Y. Ding. 2005. Note: Correction to the 1997 tutorial on Reed-Solomon coding. *Software Practice & Experience* 35, 2 (2005), 189-194.
- [166] [167] J. S. Plank. 2013. Tutorial on erasure coding for storage applications, Part 1, Tutorial. 11th Usenix Conf. File and Storage Technologies, FAST 2013.
- [167] [168] J. S. Plank, M. Blaum, J. L. Hafner. 2013. SD codes: Erasure codes designed for how storage systems really fail. In *Proc. 11th USENIX Conf. on File Storage Technologies, FAST 2013*, 95–104 Removed but available at:
<http://web.eecs.utk.edu/~jplank/plank/papers/FAST-2013-SD.pdf>

- [168] [169] J. S. Plank and M. Blaum. 2014. Sector-Disk (SD) erasure codes for mixed failure modes in RAID systems. *ACM on Trans. Storage* 10, 1 (2014), 4:1-4:17.
- [169] [170] V. Prabhakaran, L. N. Bairavasundaram, N. Agrawal, H. S. Gunawi, A. C. and R. H. Arpaci-Dusseau. 2005. IRON file systems. In *Proc. 20th ACM Symp. on Operating Systems Principles, SOSP 2005*.
- [170] [171] K. K. Ramakrishnan, P. Biswas, R. Karedla. 1992. Analysis of file I/O traces in commercial computing environments. In *Proc. SIGMETRICS'92/Performance'92 Proc. ACM Joint Conf.*, 78-90.
- [171] [172] R. Ramakrishnan and J. Gehrke. 2002. *Database Management Systems, 3rd Ed.* McGraw-Hill, 2002.
- [172] [173] K. K. Rao, J. L. Hafner, R. A. Golding. 2011. Reliability for networked storage nodes. *IEEE Trans. Dependable and Secure Computing* 8, 3 (2011), 404-418.
- [173] [174] K. V. Rashmi, N. B. Shah, D. Gu, H. Kuang, D. Borthakur, K. Ramchandran. 2013. A solution to the network challenges of data recovery in erasure-coded distributed storage systems: A study on the Facebook warehouse cluster. In *Proc. 5th USENIX Workshop on Hot Topics in Storage and File Systems, HotStorage 2013*. 1–5.
- [174] [175] K. V. Rashmi, M. Chowdhury, J. Kosaian, I. Stoica, K. Ramchandran. 2016. EC-Cache: Load-Balanced, Low-Latency Cluster Caching with Online Erasure Coding. In *Proc. OSDI 2016*: 401-417
- [175] [176] A. L. N. Reddy, J. A. Chandy, P. Banerjee. 1993. Design and evaluation of gracefully degradable disk arrays. *J. Parallel Distributed Computing - JPDC* 17, 1-2 (1993), 28-40.
- [176] [177] J. Resch and I. Volvivski. 2013. Reliability models for highly fault-tolerant storage systems. arxiv.org/abs/1310.4702.
- [177] [178] A. Riska and E. Riedel. 2003. It's not fair - Evaluating efficient disk scheduling. In *Proc. 11th MASCOTS 2003*. 288-295.
- [178] [179] R. Rojas-Cessa. 2017. *Interconnections for Computer Communications and Packet Networks*. CRC Press, 2017.
- [179] [180] M. Rosenblum and J. K. Ousterhout, 1992. The design and implementation of a log-structured file system. *ACM Trans. Computing Systems*, 10, 1 (1992), 26-52.
- [180] [181] R. A. Sahner, K. S. Trivedi, A. Puliafito. 1996. *Performance and Reliability Analysis of Computer Systems: An Example-Based Approach Using the SHARPE Software Package*, Kluwer 1996.
- [181] [182] F. G. Sanchez. 2007. *Modeling of Field and Thermal Magnetization Reversal in Nanostructured Magnetic Materials*. PhD thesis, Autonomous Univ. of Madrid 2007. <http://www.fgarciasanchez.es/thesisfelipe.pdf>

- [182] [183] M. Sathiamoorthy, M. Asteris, D. S. Papailiopoulos, A. G. Dimakis, R. Vadali, S. Chen, D. Borthakur: XORing elephants: Novel erasure codes for big data. In Proc. VLDB Endow. 6, 5 (2103), 325-336.
- [183] [184] K. Sayood. 2017. Introduction to Data Compression, 5th Ed. MKP Publishers, 2017.
- [184] [185] B. Schlinker, R. N. Mysore, S. Smith, J. C. Mogul, A. Vahdat, M. Yu, E. Katz-Bassett, M. Rubin. 2015. Condor: Better topologies through declarative design. In Proc. ACM SIGCOMM 2015,: 449-463
- [185] [186] J. Schindler, S. Shete, K. A. Smith. 2011: Improving throughput for small disk requests with Proximal I/O. IN Proc. File and Storage Technologies, FAST 2011: 133-147.
- [186] [187] B. Schroeder and G. A. Gibson. 2007. Understanding disk failure rates: What does an MTTF of 1,000,000 hours mean to you? ACM Trans. on Storage 3, 3 (2007), 8:1-8:31.
- [187] [188] B. Schroeder, S. Damouras, P. Gill. 2010. Understanding latent sector errors and how to protect against them. ACM Trans. on Storage 6, 3 (2010), 9:1-9:23.
- [188] [189] B. Schroeder, A. Merchant, R. Lagisetty. 2017. Reliability of NAND-Based SSDs: What field studies tell us. Proceedings IEEE 105, 9 (Sept. 2017), 1751-1769.
- [189] [190] T. J. E. Schwarz and W. A. Burkhard. 1996. Almost Complete Address Translation (ACATS) disk array declustering, In Proc. 8th IEEE Symp. on Parallel and Distributed Processing - SPDP 1996, pp. 324-331.
- [190] [191] T. J. E. Schwarz, J. Steinberg, W. A. Burkhard. 1999. Permutation Development Data Layout - PDDL disk array declustering. In Proc 5th IEEE Symp. on High Performance Computer Architecture - HPCA'99, pp. 214-217.
- [191] [192] T. J. E. Schwarz, A. Amer, T. M. Kroeger, E. L. Miller, D. D. E. Long, J.-F. Pâris. 2016. RESAR: Reliable Storage at Exabyte Scale. In Proc. 24th IEEE/ACM Int'l Symp. on MASCOTS 2016, 211-220.
- [192] [193] SEFI - European Soc. Eng. Education. 2013. A framework for mathematics curricula in engineering education: A report of the mathematics working group. 2013. <http://sefibenvwh.cluster023.hosting.ovh.net/wp-content/uploads/2017/07/Competency-based-curriculum-incl-ads.pdf>
- [193] [194] A. J. Smith. 1985. Disk cache-miss ratio analysis and design considerations. ACM Trans. Computer Systems 3(3): 161-203 (1985).
- [194] [195] R. Sundaram. The Private Lives of Disk Drives, Tech OnTap, NetApp, Inc. 2006, http://www.netapp.com/go/techontap/mat1/sample/0206tot_resiliency.htm
- [195] [196] H. Takagi. 1986. Analysis of Polling Systems., MIT Press, 1986.
- [196] [197] H. Takagi. 1991. Queueing Analysis: A Foundation of Performance Evaluation : Vacation and Priority Systems, Part 1 North Holland 1991.

- [197] [198] Tandem Database Group. 1987. NonStop SQL: A distributed, high-performance, high-availability implementation of SQL In High Performance Transaction Systems. D. Gawlick, M. Haynie, A. Reuter (editors). Springer 1987. Also Tandem Technical Report 87.4 , April 1987.
- <https://www.hpl.hp.com/techreports/tandem/TR-87.4.pdf>
- [198] [199] A. J. Thadhani. 1981. Interactive user productivity. IBM Systems Journal, 20, 4 (1981), 407-423.
- [199] [200] A. Thomasian and P. F. Bay. 1986. Analytic Queueing Network Models for Parallel Processing of Task Systems. IEEE Trans. Computers 35, 12 (Dec. 1986), 1045-1054.
- [200] [201] A. Thomasian and J. Menon. 1994. Performance analysis of RAID5 disk arrays with a vacationing server model for rebuild mode operation. In Proc. 10th Int'l Conf. on Data Eng., ICDE 1994, 111-119.
- [201] [202] A. Thomasian and A. N. Tantawi. 1994/ Approximate solutions for M/G/1 fork/join synchronization. In Proc. 26th Conf. on Winter Simulation - WSC 1994, 361-368
- [202] [203] A. Thomasian: Rebuild Options in RAID5 Disk Arrays. In Proc. 7th IEEE Symp. on Parallel and Distributed Processing, SPDP 1995: 511-518.
- [203] [204] A. Thomasian and J. Menon. 1997. RAID5 Performance with distributed sparing. IEEE Trans. Parallel Distributed Systems 8, 6 (June 1997), 640-657.
- [204] [205] A. Thomasian. 2005. Reconstruct versus Read-Modify Writes in RAID. Information Processing Letters - IPL 93, 4 (2005), 163-168.
- [205] [206] A. Thomasian, B. A. Branzoi, C. Han. 2005 Performance evaluation of a heterogeneous disk array architecture. In Proc. 13th Int'l Symp. on Modeling, Analysis, and Simulation of Computer and Telecomm. Systems, MASCOTS 2005, 517-520
- [206] [207] A. Thomasian and C. Liu: Comment on "Issues and Challenges in the Performance Analysis of Real Disk Arrays". IEEE Trans. Parallel Distributed Systems 16, 11 (2005), 1103-1104.
- [207] [208] A. Thomasian. 2005b: Clustered RAID arrays and their access costs. Comput. J. 48, 6 (2005), 702-713.
- [208] [209] A. Thomasian and G. Fu. 2006. Anticipatory disk arm placement to reduce seek time. Computer Systems: Science & Engineering 21, 3, (May 2006), 173-182.
- [209] [210] A. Thomasian: Multi-level RAID for very large disk arrays. ACM SIGMETRICS Perform. Evaluation Review, 33, 4 (2006), 17-22.
- [210] [211] A. Thomasian. 2006. Shortcut method for reliability comparisons in RAID. J. Systems & Software 79, 11 (2006), 1599-1605.
- [211] [212] A. Thomasian and M. Blaum. 2006. Mirrored Disk Organization Reliability Analysis. IEEE Trans. Computers 55, 12 (2006), 1640-1644.

- [212] [213] A. Thomasian, G. Fu, C. Han. 2007. Performance of two-disk failure-tolerant disk arrays. *IEEE Trans. Computers* 56, 6 (2007), 799-814.
- [213] [214] A. Thomasian and J. Xu: Reliability and performance of mirrored disk organizations. *Computer Journal* 51, 6 (2008), 615-629.
- [214] [215] A. Thomasian and M. Blaum. 2009. Higher reliability redundant disk arrays: Organization, operation, and coding. *ACM Trans. Storage* 5, 3 (2009), 7:1-7:59.
- [215] [216] A. Thomasian. 2011. Survey and analysis of disk scheduling methods. *ACM SIGARCH Computer Architecture News* 39, 2 (2011), 8-25.
- [216] [217] A. Thomasian and J. Xu. 2011. X-code double parity array operation with two disk failures. *Information Processing Letters* 111, 12 (2011), 568-574.
- [217] [218] A. Thomasian and J. Xu 2011b. Data Allocation in Heterogeneous Disk Arrays. In *Proc. 6th Int'l Conf. on Networking, Architecture, and Storage, NAS 2011*: 82-91.
- [218] [219] A. Thomasian and Y. Tang. 2012. Performance, reliability, and performability of a hybrid RAID array and a comparison with traditional RAID1 arrays. *Cluster Computing* 15, 3 (2012), 239-253.
- [219] [220] A. Thomasian, Y. Tang, Y. Hu. 2012. Hierarchical RAID: Design, performance, reliability, and recovery. *J. Parallel Distributed Computing - JPDC* 72, 12 (2012), 1753-1769.
- [220] [221] A. Thomasian. 2014. Analysis of fork/join and related queueing systems. *ACM Computing Surveys* 47, 2 (2014), 17:1-17:71.
- [221] [222] A. Thomasian, 2014. Performance Evaluation of Computer Systems. *Computing Handbook*, 3rd ed. (Vol. 1) 2014: Chapter 56: 1-50.
- [222] [223] A. Thomasian. 2018. Mirrored and hybrid disk arrays: Organization, scheduling, reliability, and performance. *CoRR abs/1801.08873* (2018).
<https://arxiv.org/pdf/1801.08873.pdf>
- [223] [224] A. Thomasian. 2018. Vacationing server model for M/G/1 Queues for rebuild processing in RAID5 and threshold scheduling for readers and writers. *Information Processing Letters - IPL* 135 (2018), 41-46.
- [224] [225] A. Thomasian. 2021. *Storage Systems: Organization, Performance, Coding, Reliability, and Their Data Processing*, Elsevier 2021.
<https://www.elsevier.com/books/storage-systems/thomasian/978-0-323-90796-5>
<https://www.sciencedirect.com/book/9780323907965/storage-systems>
- [225] [226] A. Thomasian. 2022, Optimizing Apportionment of Redundancies in Hierarchical RAID. *CoRR abs/2205.06330* (2022).
<https://arxiv.org/abs/2205.06330>
- [226] [227] E. Thorp. 1973. Nonrandom shuffling with applications to the game of Faro. *J. American Statistical Association - JASA*, 68, 344 (Dec, 1973), 842-847.

- [227] [228] K. Treiber and J. Menon. 1995. Simulation study of cached RAID5 designs. In Proc. 1st IEEE Symp. on High-Performance Computer Architecture - HPCA 1995, 186-197.
- [228] [229] K. S. Trivedi. 2002. Probabilistic and Statistics with Reliability, Queuing and Computer Science Applications, 2nd ed. Wiley-Interscience 2002.
- [229] [230] K. S. Trivedi and A. Bobbio. 2017. Reliability and Availability Engineering: Modeling, Analysis, and Applications Cambridge Univ. Press 2017.
- [230] [231] E. Varki, A. Merchant, J. Xu, X. Qiu. 2004. Issues and challenges in the performance analysis of real disk arrays. IEEE Trans. Parallel Distributed Systems 15, 6 (2004), 559-574.
- [231] [232] D. Verma. 2004. Service level agreements on IP networks. Proc. IEEE, 92, 9 (Sept. 2004), 382–1388.
- [232] [233] Y. Wang, X. Dong, L. Wang, W. Chen, X. Zhang. 2022 Optimizing small-sample disk fault detection based on LSTM-GAN model, ACM Trans. Architecture and Code Optimization, 19, 1 (Jan. 2022), Article 13.
- [233] [234] W. W. Wilcke, R. B. Garner, C. Fleiner et al. 2006. IBM Intelligent Bricks Project - Petabytes and Beyond. IBM J. Research & Development 50, 2-3 (2006), 181-198.
- [234] [235] A. Wildani, T. J. E. Schwarz, E. L. Miller, D. D. E. Long. 2009. Protecting against rare event failures in archival systems. In Proc. 17th IEEE/ACM Int'l Symp. on MASCOTS 2009: 1-11
- [235] [236] J. Wilkes, R. A. Golding, C. Staelin, T. Sullivan. 1996. The HP AutoRAID hierarchical storage system. ACM Trans. Computer Systems 14, 1 (1996), 108-136.
- [236] [237] A. Wilner. 2001. Multiple drive failure tolerant RAID system. US Patent 6,327,672, December 2001
- [237] [238] R. W. Wolff. 1982. Poisson arrivals see time averages. Operations Research 30, 2 (1982), 223-231.
- [238] [239] B. L. Worthington, G. R. Ganger, Y. N. Patt. 1994 Scheduling Algorithms for Modern Disk Drives. In Proc. ACM SIGMETRICS Conf. on Measurement and Modeling of Computer Systems 1994: 241-252
- [239] [240] M. Xia, M. Saxena, M. Blaum, D. Pease. 2015. A tale of two erasure codes in HDFS. In Proc. 13th USENIX Conf. on File and Storage Technologies, FAST 2015, 213-226.
- [240] [241] Q. Xin, E. L. Miller, T. J. E. Schwarz, D. D. E. Long, S. A. Brandt, W. Litwin. 2003. Reliability mechanisms for very large storage systems. In Proc, IEEE Symp.on Mass Storage Systems, MSST 2003, 146-156
- [241] [242] L. Xiang, Y. Xu, J. C. S. Lui, Q. Chang. 2010. Optimal recovery of single disk failure in RDP code storage systems. In Proc. ACM SIGMETRICS Conf. on Measurement and Modeling of Computer Systems 2010, 119-130.

- [242] [243] L. Xiang, Y. Xu, J. C. S. Lui, Q. Chang, Y. Pan, R. Li. 2011. A hybrid approach to failed disk recovery using RAID-6 Codes: Algorithms and performance evaluation. *ACM Trans. Storage* 7, 3 (2011), 11:1-11:34.
- [243] [244] L. Xu and J. Bruck. 1999. X-Code: MDS Array codes with optimal encoding. *IEEE Trans. Information Theory* 45, 1 (1999), 272-276.
- [244] [245] S. Xu, R. Li, P. P. C. Lee, Y. Zhu, L. Xiang, Y. Xu, J. C. S. Lui. 2014. Single disk failure recovery for X-code-based parallel storage systems. *IEEE Trans. Computers* 63, 4 (2014), 995-1007.
- [245] [246] E. Yaakobi, S. Kayser, P. H. Siegel, A. Vardy, J. K. Wolf. Codes for Write-Once Memories *IEEE Trans. Information Theory*, 58, 9 (Sept. 2012), 5885-5999.
- [246] [247] K. Yu. 2012. Optimizing OLTP Oracle database performance using Dell Express Flash PCIe SSDs. White Paper, Dell Global Solutions Engineering, 2012.
https://downloads.dell.com/solutions/enterprise-solution-resources/PCIe_SSD_for_oracle_database_performance.pdf
- [247] [248] J. Zhang, Y. Wang; Y. Wang, K. Zhou, S. Sebastian, P. Huang, B. Cheng. Y. Ji. 2022. Tier-scrubbing: An adaptive and tiered disk scrubbing scheme with improved MTTD and reduced cost. In *Proc. 2020 57th ACM/IEEE Design Automation Conference - DAC, 2020*, 1-6.
- [248] [249] M. Zhang, S. Han, P. P. C. Lee. 2019. SIMedc: A simulator for the reliability analysis of erasure-coded data centers. *IEEE Trans. Parallel Distributed Systems* 30, 12 (Dec. 2019), 2836–2848.
- [249] [250] Y. Zhang, W. Hao, B. Niu, K. Liu, S. Wang, N. Liu, X. He, Y. Gwon, C. Koh. 2023. Multi-view feature-based SSD failure prediction: What, when, and why. In *Proc. 21st USENIX Conf. on File and Storage Technologies - FAST 2023*, 409-424.
- [250] [251] P. Zhou, V. Pandey, J. Sundaresan, A. Raghuraman, Y. Zhou, S. Kumar. 2004. Dynamic tracking of page miss ratio curve for memory management. In *Proc. 11th Int'l Conf. on Architectural Support for Programming Languages and OS, ASPLOS 2004*, 177-188.